J Bone Miner Metab (2005) 23:226–230
DOI 10.1007/s00774-004-0588-x

ORIGINAL ARTICLE

Tomohiko Urano · Masataka Shiraki · Masayo Fujita
Takayuki Hosoi · Hajime Orimo · Yasuyoshi Ouchi
Satoshi Inoue

Association of a single nucleotide polymorphism in the lipoxygenase *ALOX15* 5′-flanking region (−5229G/A) with bone mineral density

Received: October 22, 2004 / Accepted: November 16, 2004

Abstract The 12/15-lipoxygenase gene *Aloxl5* has been identified as a susceptibility gene for bone mineral density (BMD) in mice through combined genetic and genomic analyses. Here we studied the association between bone mineral density and an *ALOX15* gene single nucleotide polymorphism to assess the potential involvement of the human *ALOX15* gene in postmenopausal osteoporosis. Specifically, we examined the association between a single nucleotide polymorphism at −5299G/A in the *ALOX15* 5′-flanking region with BMD in 319 postmenopausal Japanese women (66.7 ± 8.9 years, mean ± SD). We found that subjects bearing at least one variant A allele (GA + AA; n = 273) had significantly lower Z scores for lumbar spine and total body bone mineral density than did subjects with no A allele (GG; n = 46) (lumbar spine, −0.25 ± 1.34 versus 0.48 ± 1.70; P = 0.0014; total body, 0.25 ± 1.01 vs 0.62 ± 1.11; P = 0.048). These findings suggest that the *ALOX15* gene is one of the genetic determinants of BMD in postmenopausal women. Accordingly, this polymorphism could be useful as a genetic marker for predicting the risk of osteoporosis.

Key words Adipogenesis · *ALOX15* · PPARγ · Osteoporosis · Bone mineral density · Polymorphism

T. Urano · M. Fujita · Y. Ouch · S. Inoue (✉)
Department of Geriatric Medicine, Graduate School of Medicine, University of Tokyo, 7-3-1 Hongo, Bunkyo-ku, Tokyo 113-8655, Japan
Tel. +81-3-3815-5411; Fax +81-3-5800-6530
e-mail: INOUE-GER@h.u-tokyo.ac.jp

M. Shiraki
Research Institute and Practice for Involutional Diseases, Nagano, Japan

M. Fujita · S. Inoue
Research Center for Genomic Medicine, Saitama Medical School, Saitama, Japan

T. Hosoi
Tokyo Metropolitan Geriatric Hospital, Tokyo, Japan

H. Orimo
Health Science University, Yamanashi, Japan

Introduction

Osteoporosis is characterized by low bone mineral density (BMD), increased bone fragility, and consequently increased risk of fracture [1]. Studies of twins and siblings have shown that BMD is under genetic control, with estimates of heritability ranging from 50% to 90% [2,3]. BMD is regulated by interaction of multiple environmental and genetic factors, each having modest effects on bone mass and bone turnover [4,5]. Polymorphisms of several genes have been investigated to clarify the determinants of BMD [6,7]. These genes of which polymorphisms were associated with BMD include those implicated in bone formation by regulation of osteoblast growth and function, such as *vitamin D receptor* gene [8], *transforming growth factor beta-1* (*TGFβ1*) gene, *collagen type Iα1* (*COLIA1*) gene [9], *peroxisome proliferator-activated receptor-γ* (*PPARγ*) gene [10], and *low-density lipoprotein receptor-related protein 5* (*LRP5*) gene [11]. Identification of candidate genes that affect bone mass will be useful for early detection of individuals who are at risk of osteoporosis for early institution of preventive measures.

The decrease in bone volume associated with osteoporosis is accompanied by an increase in marrow adipose tissues [12,13]. Indeed, an increase in marrow adipocytes is observed in several conditions that lead to bone loss, such as ovariectomy [14], immobilization [15], and treatment with glucocorticoids [16]. Recent studies have identified rodent quantitative trait locus associated with increased BMD in the mouse gene encoding 12/15-lipoxygenase [17], the enzyme that converts linoleic acid and arachidonic acid into endogenous ligands for the PPARγ [18–20]. Activation of this pathway in marrow-derived mesenchymal progenitors stimulates adipogenesis and inhibits osteoblastogenesis [21,22]. Mice that are deficient in this gene or have been treated with 12/15-lipoxygenase inhibitors demonstrate increased bone mass as compared with controls [17]. These findings suggest that genetic variants of the 12/15-lipoxygenase encoding gene may affect the BMD in humans as well as mice. The mouse 12/15-lipoxygenase enzyme corresponds to at least three lipoxygenases in humans. 15-Lipoxygenase has two isoenzymes: type 1 (human *ALOX15*, encoded by a gene at chromosome 17p13.3) and type 2 (human *ALOX15B*, encoded by a separate gene at 17p13.1). 12-Lipoxygenase (human *ALOX12*, encoded by a gene at chromosome 17p13.1) is predominantly expressed in platelets and macrophages and is distinct from 15-lipoxygenase [23]. In the present study, we examined the possibility that there is an association between a polymorphism in the human *ALOX15* gene and BMD in Japanese women to investigate the possible contribution of the lipoxygenase to bone metabolism.

Subjects and methods

Subjects

We analyzed genotypes in DNA samples from 319 healthy postmenopausal Japanese women (66.7 ± 8.9 years, mean ± SD). We excluded women having endocrine disorders such as hyperthyroidism, hyperparathyroidism, diabetes mellitus, liver disease, and renal disease; those who used medications known to affect bone metabolism (e.g., corticosteroids, anticonvulsants, and heparin); and those with an unusual gynecological history. All subjects were unrelated volunteers. Each subject provided informed consent before entering the study.

Measurement of bone mineral density and biochemical markers

We measured the lumbar spine BMD and total body BMD of participants by dual-energy X-ray absorptiometry using the fast-scan mode (DPX-L; Lunar, Madison, WI, USA). The BMD data were recorded as Z scores, as the deviation from the weight-adjusted average BMD for each year of age, based on data from 20000 Japanese women. We also measured each subject's serum concentrations of alkaline phosphatase (ALP), intact osteocalcin (I-OC), intact parathyroid hormone (PTH), calcitonin, 1,25-$(OH)_2D_3$, total cholesterol (TC), and triglyceride (TG). We also measured urinary ratios of deoxypyridinoline (DPD) to creatinine using the high pressure liquid chromatography (HPLC) method.

Determination of a single nucleotide polymorphism in the ALOX15 gene

We extracted a polymorphic variation of the putative *ALOX15* gene promoter/enhancer region from the Assays-on-Deman SNP Genotyping Products database (Applied Biosystems, Foster City, CA, USA) and, according to its localization on the gene, denoted it −5299 G>A. We determined the −5299G/A polymorphism of the *ALOX15* gene using the TaqMan (Applied Biosystems) polymerase chain reaction (PCR) method [24]. To determine the *ALOX15* SNP we used Assays-on-Demand SNP Genotyping Products C_926671_10 (Applied BioSystems), which contains sequence-specific forward and reverse primers and two TaqMan MGB probes for detecting alleles. During the PCR cycle, two TaqMan probes competitively hybridize to a specific sequence of the target DNA and the reporter dye is separated from the quencher dye, resulting in an increase in fluorescence of the reporter dye. The fluorescence levels of the PCR products were measured with the ABI PRISM 7000 (Applied Biosystems), resulting in clear identification of three genotypes of the single nucleotide polymorphism (SNP).

Statistical analysis

We divided subjects into those having one or two chromosomes of the major A allele and those with only the minor G allele encoded at the same locus. Comparisons of Z scores and biochemical markers between these two groups were subjected to statistical analysis (Student's t test; StatView-J 4.5). A P value of less than 0.05 was considered statistically significant.

Results

Association of ALOX15 gene polymorphism with bone mineral density

Among our 319 subjects, 46 were GG homozygotes, 155 were GA heterozygotes, and 118 were AA homozygotes. Allelic frequencies were 0.613 for the A allele and 0.387 for the G allele in this population. The allelic frequencies of this SNP in the present study were in Hardy–Weinberg equilibrium.

We compared the 273 subjects bearing at least one chromosome with the A allele (genotype GA + AA) and the 46 subjects having no A allele (GG) with respect to their Z scores for lumbar spine and total body BMD. Those with the A allele had significantly lower Z scores for lumbar spine BMD (−0.25 ± 1.34 vs 0.48 ± 1.70; P = 0.0014) (Fig. 1A) and total body BMD (0.25 ± 1.01 vs 0.62 ± 1.11; P = 0.048) (Fig. 1B). As shown in Table 1, the background and biochemical data did not significantly differ between these groups.

Discussion

Various regulating elements have been identified within the *ALOX15* 5′-flanking promoter/enhancer region, including a site for binding with Sp1 [25], AP1 [25], and GATA [26], as well as sites for methylation [27] and acetylation [28,29] and a Stat6 response element [29], suggesting that 15-lipoxygenase expression is directly regulated through transcription regulation. In the present study, we observed a significant association between BMD and a G/A SNP at the

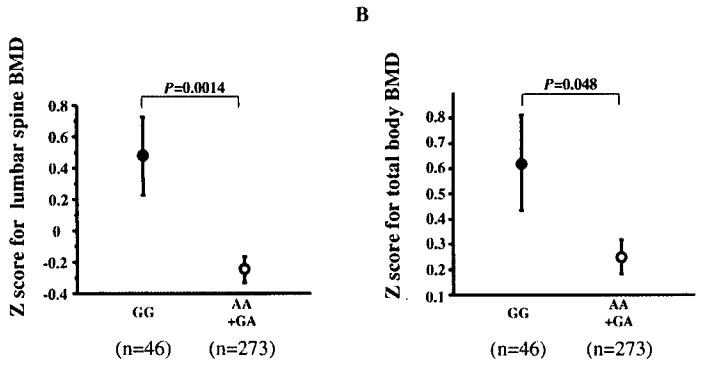

Fig. 1. *Z* scores of lumbar spine and total body bone mineral density (BMD) in subject groups with each genotype of *ALOX15* gene polymorphism in the 5′-flanking region (−5229G/A). **A** *Z* scores for lumbar spine BMD are shown for genotype AA + GA and genotype GG. Values are expressed as mean ± SE. Numbers of subjects are shown in *parentheses*. **B** *Z* scores for total body BMD are shown in the same manner as in **A**

Table 1. Comparison of background, BMD and biochemical data between subjects bearing at least one A allele (AA + GA) and subjects with no A allele (GG) in the *ALOX15* gene 5′-flanking region (−5299G/A)

Items	Genotype (mean ± SD)		*P* value*
	GG	GA + AA	
Number of subjects	46	273	
Age (years)	69.0 ± 8.9	66.3 ± 8.9	NS
Height (cm)	149.5 ± 6.9	150.3 ± 6.1	NS
Body weight (kg)	49.6 ± 8.6	50.3 ± 7.9	NS
Lumber spine BMD (Z score)	0.48 ± 1.70	−0.25 ± 1.37	0.0014
Total body BMD (Z score)	0.62 ± 1.12	0.25 ± 1.01	0.048
ALP (IU/l)	185.6 ± 63.9	193.4 ± 66.0	NS
I-OC (ng/ml)	8.2 ± 3.2	7.8 ± 3.6	NS
DPD (pmol/μmol Cr)	7.0 ± 3.0	7.6 ± 2.7	NS
Intact PTH (pg/ml)	38.6 ± 20.0	35.2 ± 15.1	NS
Calcitonin (pg/ml)	16.6 ± 4.5	23.1 ± 11.4	NS
1,25-$(OH)_2D_3$ (pg/ml)	33.0 ± 7.7	35.7 ± 11.8	NS
TC (mg/dl)	193.0 ± 45.0	199.4 ± 36.5	NS
TG (mg/dl)	142.5 ± 74.0	142.4 ± 81.8	NS
% Fat	32.1 ± 6.6	31.9 ± 7.7	NS
BMI	22.1 ± 3.0	22.1 ± 3.1	NS

BMD, bone mineral density; ALP, alkaline phosphatase; I-OC, intact-osteocalcin; DPD, deoxypyridinoline; Cr, creatinine; PTH, parathyroid hormone; TC, total cholesterol; TG, triglyceride; BMI, body mass index; NS, not significant

*Statistical analysis was performed according to the method described in the text

−5299 site in the *ALOX15* 5′-flanking region. This is the first report to our knowledge that a common SNP in the *ALOX15* gene affects BMD. One possible explanation for this effect is that this 5′-flanking region polymorphism may be involved in the newly defined transcriptional regulating element of the *ALOX15* promoter/enhancer. Alternatively, the 5′-flanking region polymorphism may have a linkage with another base of the *ALOX15* promoter/enhancer that may control transcription of the *ALOX15* gene. It is also possible that this SNP may be linked with mutation of the *ALOX15* exons or another unidentified gene adjacent to the *ALOX15* locus, which affect the bone mass.

Although there are three lipoxygenases in humans, *ALOX15*, *ALOX15B*, and *ALOX12*, that correspond to 12/15-lipoxygenase in mice [23], we know little of their roles in human bone metabolism. Our results suggest that the 15-lipoxygenase type 1, the *ALOX15*, may have a specific function in the regulation of bone mass in human. It should be required to determine how signals from 15-lipoxygenase can be transduced to the regulation of the bone metabolism.

Three major cellular events are involved in senile osteoporosis: declining levels of osteogenesis, increasing numbers of apoptotic osteoblasts and osteocytes, and increasing levels of bone marrow adipogenesis [30–32]. The bone marrow adipogenesis that occurs with aging may be due to alterations in cell differentiation, in part by PPARγ activation [33–35] and increasing lipid oxidation [36]. Previous

reports demonstrated that 12/15-lipoxygenases are involved in this system [17,18,37,38], suggesting that 12/15-lipoxygenase may increase with aging in progenitor cells and activate adipogenesis. It has been also shown that 12/15-lipoxygenase is increased in Alzheimer's disease, which is the most common neurodegenerative disorder of the elderly [39]. Therefore, it is tempting to speculate that 12/15-lipoxygenase is increased associated with aging and senile osteoporosis. To test this hypothesis, measurement of 12/15-lipoxygenase activity and association study between BMD and the *ALOX15* gene SNP in older subjects is desirable.

In conclusion, our finding suggests that the *ALOX15* gene may be a genetic determinant of BMD in postmenopausal women. Examining the variation in the *ALOX15* gene will hopefully enable us to elucidate one of the mechanisms of involutional osteoporosis. Furthermore, the variation may be a potential genetic susceptibility factor that need to be further evaluated with regard to the risk of other diseases in which 15-lipoxygenase have been clearly implicated, including atherosclerosis [40], asthma [41], cancer [42], and glomerulonephritis [43].

Acknowledgments This work was partly supported by grants from the Japanese Ministry of Health, Labor and Welfare and the Japanese Ministry of Education, Culture, Sports, Science and Technology. We thank Ms. E. Sekine, C. Onodera, and M. Kumasaka for expert technical assistance.

References

1. Kanis JA, Melton LJ III, Christiansen C, Johnston CC, Khaltaev N (1994) The diagnosis of osteoporosis. J Bone Miner Res 9:1137–1141
2. Flicker L, Hopper JL, Rodgers L, Kaymakci B, Green RM, Wark JD (1995) Bone density determinants in elderly women: a twin study. J Bone Miner Res 10:1607–1613
3. Young D, Hopper JL, Nowson CA, Green RM, Sherwin AJ, Kaymakci B, Smid M, Guest CS, Larkins RG, Wark JD (1995) Determinants of bone mass in 10 to 26 year old females: a twin study. J Bone Miner Res 10:558–567
4. Krall EA, Dawson-Hughes B (1993) Heritable and life-style determinants of bone mineral density. J Bone Miner Res 8:1–9
5. Gueguen R, Jouanny P, Guillemin F, Kuntz C, Pourel J, Siest G (1995) Segregation analysis and variance components analysis of bone mineral density in healthy families. J Bone Miner Res 10: 2017–2022
6. Nelson DA, Kleerekoper M (1997) The search for the osteoporosis gene. J Clin Endocrinol Metab 82:989–990
7. Liu YZ, Liu YJ, Recker RR, Deng HW (2002) Molecular studies of identification of genes for osteoporosis: the 2002 update. J Endocrinol 177:147–196
8. Morrison NA, Qi JC, Tokita A, Kelly PJ, Crofts L, Nguyen TV, Sambrook PN, Eisman JA (1994) Prediction of bone density from vitamin D receptor alleles. Nature (Lond) 367:284–287
9. Uitterlinden AG, Burger H, Huang Q, Yue F, McGuigan FE, Grant SF, Hofman A, van Leeuwen JP, Pols HA, Ralston SH (1998) Relation of alleles of the collagen type Ialpha1 gene to bone density and the risk of osteoporotic fractures in postmenopausal women. N Engl J Med 338:1016–1021
10. Ogawa S, Urano T, Hosoi T, Miyao M, Hoshino S, Fujita M, Shiraki M, Orimo H, Ouchi Y, Inoue S (1999) Association of bone mineral density with a polymorphism of the peroxisome proliferator-activated receptor gamma gene: PPARgamma expression in osteoblasts. Biochem Biophys Res Commun 260:122–126
11. Urano T, Shiraki M, Ezura Y, Fujita M, Sekine E, Hoshino S, Hosoi T, Orimo H, Emi M, Ouchi Y, Inoue S (2004) Association of a single-nucleotide polymorphism in low-density lipoprotein receptor-related protein 5 gene with bone mineral density. J Bone Miner Metab 22:341–345
12. Meunier P, Aaron J, Edouard C, Vignon G (1971) Osteoporosis and the replacement of cell populations of the marrow by adipose tissue. A quantitative study of 84 iliac bone biopsies. Clin Orthop 80:147–154
13. Burkhardt R, Kettner G, Bohm W, Schmidmeier M, Schlag R, Frisch B, Mallmann B, Eisenmenger W, Gilg T (1987) Changes in trabecular bone, hematopoiesis and bone marrow vessels in aplastic anemia, primary osteoporosis, and old age: a comparative histomorphometric study. Bone (NY) 8:157–164
14. Wronski TJ, Walsh CC, Ignaszewski LA (1986) Histologic evidence for osteopenia and increased bone turnover in ovariectomized rats. Bone (NY) 7:119–123
15. Miniare P, Meunier PJ, Edouard C, Bernard J, Courpron J, Bourret J (1974) Quantitative histological data on disuse osteoporosis. Calcif Tissue Res 17:57–73
16. Wang GW, Sweet D, Reger S, Thompson R (1977) Fat cell changes as a mechanism of avascular necrosis in the femoral head in cortisone-treated rabbits. J Bone Joint Surg 59A:729–735
17. Klein RF, Allard J, Avnur Z, Nikolcheva T, Rotstein D, Carlos AS, Shea M, Waters RV, Belknap JK, Peltz G, Orwoll ES (2004) Regulation of bone mass in mice by the lipoxygenase gene Alox15. Science 303:229–232
18. Huang JT, Welch JS, Ricote M, Binder CJ, Willson TM, Kelly C, Witztum JL, Funk CD, Conrad D, Glass CK (1999) Interleukin-4-dependent production of PPAR-gamma ligands in macrophages by 12/15-lipoxygenase. Nature (Lond) 400:378–382
19. Kuhn H, Walther M, Kuban RJ, Wiesner R, Rathmann J, Kuhn H (2002) Prostaglandins Other Lipid Mediat 68–69:263–290
20. Nosjean O, Boutin JA (2002) Natural ligands of PPARgamma: are prostaglandin J(2) derivatives really playing the part? Cell Signal 14:573–583
21. Lecka-Czernik B, Moerman EJ, Grant DF, Lehmann JM, Manolagas SC, Jilka RL (2002) Divergent effects of selective peroxisome proliferator-activated receptor-gamma 2 ligands on adipocyte versus osteoblast differentiation. Endocrinology 143: 2376–2384
22. Khan E, Abu-Amer Y (2003) Activation of peroxisome proliferator-activated receptor-gamma inhibits differentiation of preosteoblasts. J Lab Clin Med 142:29–34
23. Krieg P, Marks F, Furstenberger G (2001) A gene cluster encoding human epidermis-type lipoxygenases at chromosome 17p13.1: cloning, physical mapping, and expression. Genomics 73:323–330
24. Asai T, Ohkubo T, Katsuya T, Higaki J, Fu Y, Fukuda M, Hozawa A, Matsubara M, Kitaoka H, Tsuji I, Araki T, Satoh H, Hisamichi S, Imai Y, Ogihara T (2001) Endothelin-1 gene variant associates with blood pressure in obese Japanese subjects: the Ohasama Study. Hypertension 38:1321–1324
25. Kelavkar U, Wang S, Montero A, Murtagh J, Shah K, Badr K (1998) Human 15-lipoxygenase gene promoter: analysis and identification of DNA binding sites for IL-13-induced regulatory factors in monocytes. Mol Biol Rep 25:173–182
26. Kamitani H, Kameda H, Kelavkar UP, Eling T (2000) A GATA binding site is involved in the regulation of 15-lipoxygenase-1 expression in human colorectal carcinoma cell line, caco-2. FEBS Lett 467:341–734
27. Liu C, Xu D, Sjoberg J, Forsell P, Bjorkholm M, Claesson HE (2004) Transcriptional regulation of 15-lipoxygenase expression by promoter methylation. Exp Cell Res 297:61–67
28. Kamitani H, Taniura S, Ikawa H, Watanabe T, Kelavkar UP, Eling TE (2001) Expression of 15-lipoxygenase-1 is regulated by histone acetylation in human colorectal carcinoma. Carcinogenesis (Oxf) 22:187–191
29. Shankaranarayanan P, Chaitidis P, Kuhn H, Nigam S (2001) Acetylation by histone acetyltransferase CREB-binding protein/p300 of STAT6 is required for transcriptional activation of the 15-lipoxygenase-1 gene. J Biol Chem 276:42753–42760
30. Kirkland JL, Dobson DE (1997) Preadipocyte function and aging: links between age-related changes in cell dynamics and altered fat tissue function. J Am Geriatr Soc 45:959–967

31. Justesen J, Stenderup K, Ebbesen EN, Mosekilde, Steiniche T, Kassem M (2001) Adipocyte tissue volume in bone marrow is increased with aging and in patients with osteoporosis. Biogerontology 2:165–171
32. Chan GK, Duque G (2002) Age-related bone loss: old bone, new facts. Gerontology 48:62–71
33. Daiscro DD Jr, Vogel RL, Johnson TE, Witherup KM, Pitzenberger SM, Rutledge SJ, Prescott DJ, Rodan GA, Schmidt A (1998) High fatty acid content in rabbit serum is responsible for the differentiation of osteoblasts into adipocyte-like cells. J Bone Miner Res 13:96–106
34. Kirkland JL, Tchkonia T, Pirtskhalava T, Han J, Karagiannides I (2002) Adipogenesis and aging: does aging make fat go MAD? Exp Gerontol 37:757–767
35. Duque G, Macoritto M, Kremer R (2004) $1,25(OH)_2D_3$ inhibits bone marrow adipogenesis in senescence accelerated mice (SAM-P/6) by decreasing the expression of peroxisome proliferator-activated receptor gamma 2 (PPARgamma2). Exp Gerontol 39:333–338
36. Lecka-Czernik B, Moerman EJ, Grant DF, Lehmann JM, Manolagas SC, Jilka RL (2002) Divergent effects of selective peroxisome proliferator-activated receptor-gamma 2 ligands on adipocyte versus osteoblast differentiation. Endocrinology 143: 2376–2384
37. Kiefer CR, Snyder LM (2000) Oxidation and erythrocyte senescence. Curr Opin Hematol 7:113–116
38. Spiteller G (2001) Lipid peroxidation in aging and age-dependent diseases. Exp Gerontol 36:1425–1457
39. Pratico D, Zhukareva V, Yao Y, Uryu K, Funk CD, Lawson JA, Trojanowski JQ, Lee VM (2004) 12/15-Lipoxygenase is increased in Alzheimer's disease: possible involvement in brain oxidative stress. Am J Pathol 164:1655–1662
40. Harats D, Shaish A, George J, Mulkins M, Kurihara H, Levkovitz H, Sigal E (2000) Overexpression of 15-lipoxygenase in vascular endothelium accelerates early atherosclerosis in LDL receptor-deficient mice. Arterioscler Thromb Vasc Biol 20:2100–2105
41. Shannon VR, Chanez P, Bousquet J, Holtzman MJ (1993) Histochemical evidence for induction of arachidonate 15-lipoxygenase in airway disease. Am Rev Respir Dis 147:1024–1028
42. Shureiqi I, Chen D, Lee JJ, Yang P, Newman RA, Brenner DE, Lotan R, Fischer SM, Lippman SM (2000) 15-LOX-1: a novel molecular target of nonsteroidal anti-inflammatory drug-induced apoptosis in colorectal cancer cells. J Natl Cancer Inst 92:1136–1142
43. Montero A, Badr KF (2000) 15-Lipoxygenase in glomerular inflammation. Exp Nephrol 8:14–19

Estrogen Receptor–Binding Fragment–Associated Antigen 9 Is a Tumor-Promoting and Prognostic Factor for Renal Cell Carcinoma

Tetsuo Ogushi,[1] Satoru Takahashi,[1] Takumi Takeuchi,[1] Tomohiko Urano,[2] Kuniko Horie-Inoue,[3] Jinpei Kumagai,[1] Tadaichi Kitamura,[1] Yasuyoshi Ouchi,[2] Masami Muramatsu,[3] and Satoshi Inoue[2,3]

Departments of [1]Urology and [2]Geriatric Medicine, Faculty of Medicine, The University of Tokyo, Hongo, Bunkyo-ku, Tokyo, Japan and [3]Research Center for Genomic Medicine, Saitama Medical School, Yamane, Hidaka-shi, Saitama, Japan

Abstract

The estrogen receptor–binding fragment–associated antigen 9 (*EBAG9*) has been identified as a primary estrogen-responsive gene in human breast cancer MCF7 cells. A high expression of EBAG9 has been observed in invasive breast cancer and advanced prostate cancer, suggesting a tumor-promoting role of the protein in malignancies. Here we show that intratumoral (i.t.) administration of small interfering RNA against EBAG9 exerted overt regression of tumors following s.c. implantation of murine renal cell carcinoma (RCC) Renca cells. Overexpression of EBAG9 did not promote the proliferation of culture Renca cells; however, the inoculated Renca cells harboring EBAG9 (Renca-EBAG9) in BALB/c mice grew faster and developed larger tumors compared with Renca cells expressing vector alone (Renca-vector). After renal subcapsular implantation, Renca-EBAG9 tumors significantly enlarged compared with Renca-vector tumors in BALB/c mice, whereas both Renca-EBAG9 and Renca-vector tumors were developed with similar volumes in BALB/c nude mice. No apparent difference was observed in specific cytotoxic T-cell responses against Renca-EBAG9 and Renca-vector cells; nonetheless, the number of infiltrating $CD8^+$ T lymphocytes was decreased in Renca-EBAG9 subcapsular tumors. Furthermore, immunohistochemical study of EBAG9 in 78 human RCC specimens showed that intense and diffuse cytoplasmic immunostaining was observed in 87% of the cases and positive EBAG9 immunoreactivity was closely correlated with poor prognosis of the patients. Multivariate analysis revealed that high EBAG9 expression was an independent prognostic predictor for disease-specific survival ($P = 0.0485$). Our results suggest that EBAG9 is a crucial regulator of tumor progression and a potential prognostic marker for RCC. (Cancer Res 2005; 65(9): 3700-6)

Introduction

Estrogen receptor–binding fragment associated gene 9 (*EBAG9*) is an estrogen-responsive gene that we previously identified in MCF-7 human breast carcinoma cell line using a CpG-genomic binding site cloning method (1). EBAG9 protein, whose molecular size is 32 kDa by Western blot analysis, is expressed in estrogen target organs as well as several other tissues such as brain, liver, and kidney (2). The protein expression of EBAG9 is estrogen inducible, as it has been shown in ovariectomized mice treated with 17β-estradiol administration (2). The physiologic function of EBAG9 has not been well defined, yet the molecule may be implicated in cancer pathophysiology, with several lines of evidence of the protein expression in malignancies, including breast (3), ovarian (4), prostate (5), and hepatocellular carcinomas (6). In prostate cancer (5), EBAG9 expression significantly correlated with advanced pathologic stages and high Gleason score ($P = 0.0305$ and $P < 0.0001$, respectively), suggesting the abundance of EBAG9 may relate to the progression of malignant tumors.

In the present study, we investigated whether EBAG9 expression is critical in tumor development of renal cell carcinoma (RCC). RCC that comprises the majority of kidney cancer is one of the 10 most common malignancies in industrialized countries (7). The prognosis of patients with advanced RCC is poor, as 5-year survival rate is <5% (8), and the treatment of metastatic RCC remains a difficult clinical challenge. Development of new and alternative modalities of diagnosis and therapy for RCC is a clinical requisite. We used murine syngeneic renal adenocarcinoma model of Renca cells in this study and investigated whether gene silencing or overexpression of EBAG9 influences Renca cell growth and/or *in vivo* tumorigenesis. Administration of small interfering RNA (siRNA) against EBAG9 regressed s.c. Renca tumors. The proliferation of culture Renca cells constitutively expressing EBAG9 was not basically different from control Renca cells, whereas EBAG9-expressing cells grew faster in BALB/c mice and developed larger tumors. The tumor-promoting effect of EBAG9 in Renca tumors may relate to the suppression of antitumor immunity, as i.t. $CD8^+$ T lymphocytes were reduced in renal subcapsular Renca tumors. The tumorigenic relevance of EBAG9 in Renca models further extended to clinicopathologic significance of the molecule in human RCC. EBAG9 immunoreactivity was closely correlated with poor prognosis of the patients and it was an independent prognostic predictor for disease-specific survival. Our findings show that EBAG9 is a tumor-promoting factor and a potential prognostic marker in RCC.

Materials and Methods

Reagents. Rabbit anti-EBAG9 polyclonal antibody was generated against a fusion protein of glutathione *S*-transferase and EBAG9 (2). Rabbit polyclonal antihuman CD3 antibody (DakoCytomation, Carpinteria, CA), rat antimouse CD4 (L3T4; clone RM 4-5), rat antimouse CD8a (Ly-2; 53-6.7) monoclonal antibodies (BD PharMingen, San Diego, CA), and anti–β-actin monoclonal antibody (Sigma, St. Louis, MO) were commercially purchased. Human EBAG9 cDNA was cloned into a mammalian expression vector pcDNA3 (Invitrogen, Carlsbad, CA).

Note: Supplementary data for this article are available at Cancer Research Online (http://cancerres.aacrjournals.org/).

Requests for reprints: Satoshi Inoue, Department of Geriatric Medicine, Graduate School of Medicine, The University of Tokyo, 7-3-1 Hongo, Bunkyo-ku, Tokyo 113-8655, Japan. Phone: 81-3-5800-8652; Fax: 81-3-5800-6530; E-mail: INOUE-GER@h.u-tokyo.ac.jp.

Tumor cells. Renca is a spontaneously arising murine RCC and was prepared as previously described (9, 10). Tumor cells were maintained in RPMI 1640 containing 10% FCS and antibiotics.

Mice. BALB/c mice and BALB/c *nu/nu* mice (Nisseizai, Tokyo, Japan) that were syngeneic to Renca cells were kept under specific pathogen-free conditions and fed dry food and water. All mice used for experiments were male at the age of 5 weeks.

Patients and tissue preparation. We investigated 78 tissue samples of RCC obtained from patients (14 females and 64 males) who underwent radical or partial nephrectomy at Tokyo University Hospital between 1990 and 1995. Patient information was retrieved from the review of patient charts. Staging and grading of the tumors were done according to the 1997 International Union Against Cancer tumor-node-metastasis classification and WHO histopathologic typing, respectively (11). The mean age of this population was 54 years (26-76 years) and the mean follow-up period was 60 months (2-78 months). For 32 patients with advanced tumors (pT2 or greater), adjuvant therapy was done, including immune therapy (n = 30), radiation (n = 5), and surgery for metastatic diseases in lung, colon, and pancreas (n = 8). During the follow-up period, 55 patients (70.5%) survived without evidence of disease, eight cases (10.3%) presented with tumor recurrence, and 15 cases (19.2%) died of disease. None died of other diseases.

Western blot analysis. Cells were lysed in radioimmunoprecipitation assay buffer [50 mmol/L Tris-HCl (pH 8.0), 200 mmol/L NaCl, 20 mmol/L NaF_2, 2 mmol/L EGTA, 1 mmol/L DTT, 2 mmol/L sodium vanadate, 0.5% v/v NP40 supplemented with a protease inhibitor cocktail Complete (Boehringer Manheim GmbH, Mennheim, Germany)]. Proteins were resolved by 12.5% SDS-PAGE and transferred to polyvinylidene difluoride membranes. Membranes were probed with rabbit anti-EBAG9 antibody or anti–β-actin monoclonal antibody.

Tumor regression by EBAG9 small interfering RNA. Small interfering RNA (siRNA) duplex that targets EBAG9 was generated by Dharmacon (Lafayette, CO). The target sequence of EBAG9 siRNA was 5′-AAGAAGA-UGCAGCCUGGCAAG-3′. Scramble II Duplex (Dharmacon) was used as a nontargeting control siRNA that does not possess homology with known gene targets in mammalian cells. The GC content of Scramble II Duplex was 57.9%, which was identical to that of EBAG9 siRNA.

To investigate *in vivo* silencing effect of EBAG9 siRNA in Renca tumors, i.t. injection of siRNA duplexes was done twice every week. Briefly, Renca cells (1×10^4 cells) were implanted in the flank of BALB/c mice. Tumor size was measured weekly with a micrometer in two dimensions, and tumor volume was estimated according to the formula: (smallest diameter)^2 × (longest diameter). When the volumes of tumors reached 300 mm^3, siRNA duplexes (10 μg) were injected directly into tumors twice every week, along with 4 μL of GeneSilencer (Gene Therapy System, San Diego, CA) dissolved in 0.1 mL of Opti-MEM (Life Technologies, Gaithersburg, MD). Mice were sacrificed 4 weeks after treatment.

Generation of Renca cells stably expressing EBAG9. Renca cells were transfected with an expression vector pcDNA3, including human EBAG9 cDNA or vector alone using LipofectAMINE (Life Technologies). G418-resistant cells were selected and several independent clones were isolated.

Reverse transcription-PCR. Total cellular RNA of Renca cells was extracted using ISOGEN reagent (Nippon Gene, Tokyo, Japan) and first-stand cDNA was generated from 5 μg of total cellular RNA using a reverse transcriptase Omniscript RT (Qiagen, Tokyo, Japan) and random hexamers. To validate the expression of exogenous human EBAG9, reverse transcription-PCR (RT-PCR) was done using specific primers for human EBAG9 (sense 5′-GCTACACAAGATCTGCCTTT-3′ and antisense 5′-CTTCTTCATTAGCCGT-TGTG-3′). The amplification was done for 35 cycles at 62°C for annealing, using AmpliGold Taq polymerase (Perkin-Elmer, Boston, MA).

***In vivo* tumor challenge.** For s.c. implantation, transfected Renca cells (1×10^4 cells per mouse) suspended in 0.1 mL of complete medium were injected in the flank of BALB/c mice. Tumor volume was calculated weekly. In survival analyses, Renca-bearing mice were followed up for 14 weeks after implantation.

For renal subcapcular implantation, tumors cells (1×10^4 cells per mouse) suspended in 0.1 mL of complete medium were inoculated into the subcapsule of the left kidney of BALB/c wild-type and nude mice. Mice were sacrificed 25 days after implantation and tumors were excised.

Cell proliferation assay. Cells were seeded at a density of 1 to 3×10^5 cells per dish into 10-cm dishes and hemocytometer counting was done every 2 days. Doubling time during exponential growth was determined by a formula: [incubation time (h) × $\log_{10}2$] / [$\log_{10}$(cell number at sampling period) − $\log_{10}$(plating cell number)] (12).

Proliferation assays were done using the 2-(2-methoxy-4-nitrophenyl)-3-(4-nitrophenyl)-5-(2,4-disulfophenyl)-2*H* tetrazolium monosodium salt (WST-8) reagent (Nacalai, Kyoto, Japan; ref. 13). The assay is based on the conversion of the 3-(4,5-dimethylthiazol-2-yl)-2,5-diphenyltetrazolium bromide (MTT)-like tetrazolium salt WST-8 to a water-soluble formazan by metabolically active cells and provides a quantitative determination of viable cells. Cells were seeded in 96-well plates at an initial density of 625 to 5,000 cells per well. At 1 hour after inoculation, cells were transfected with either EBAG9 siRNA or Scramble II Duplex (100 ng per well) using GeneSilencer reagent (Gene Therapy Systems). Assays were done on days 0, 2, and 4. For cells cultured up to day 4, medium was once exchanged on day 2. Spectrophotometric absorbance at 450 nm (for formazan dye) was measured with absorbance at 620 nm for reference.

Cytotoxicity assay. Renca-EBAG9 or Renca-vector cells were used as target cells. Splenocytes of Renca-bearing BALB/c mice were stimulated for 5 days *in vitro* with irradiated Renca cells at a splenocyte/tumor cell ratio of 20:1 in the presence of 1,000 IU/mL interleukin-2 and used as effector CTLs. Target cells were incubated with effector CTLs at various E/T ratios in a final volume of 200 μL for 18 hours at 37°C. Lactate dehydrogenase release from cells with a damaged membrane was examined using CytoTox-ONE Reagent (Promega, Madison, WI) and fluorescence was measured with an excitation wavelength of 560 nm and an emission wavelength of 590 nm. Experiments were done in triplicate.

Immunohistochemistry. Immunohistochemical studies were done using the streptavidin-biotin amplification method with horseradish peroxidase detection. Paraffin sections of tumors were blocked in 0.3% H_2O_2 (30 minutes) and in 10% FCS (30 minutes), incubated overnight with specific antibodies against CD3, CD4, or CD8a for Renca tumors (1:20 dilution), or with purified rabbit anti-EBAG9 antibody for human RCC (1:40 dilution). Sections were incubated with biotinylated rabbit antirat immunoglobulin G or antirabbit EnVison$^+$ reagent (DakoCytomation), developed by diaminobenzidine (Sigma), and counterstained with hematoxylin (Sigma). Negative controls were done for each slide, using nonimmune immunoglobulin G.

In Renca experiments, numbers of tumor-infiltrating lymphocytes (TILs) positive for CD3, CD4, or CD8 expression were microscopically examined in the high-power field of view at a magnification of 400× (14). BALB/c mouse spleen specimen was used as a positive control.

In RCC examination, immunoreactivity scores of EBAG9 expression were determined by two pathologists according to percentages of positive cells. Human breast cancer section (DakoCytomation) was used as a positive control. Positivity was 0% to 4% for immunoreactivity score of 0 (negative), 5% to 24% for a score of 1+, 25% to 49% for a score of 2+, and 50% to 100% for a score of 3+. Sections that had ≥25% positive cells but apparent lower intensity compared with positive controls were scored as immunoreactivity score of 1+. Immunoreactivity scores of 1+, 2+, and 3+ were defined as positive staining. If immunoreactivity scores were different between two pathologists, the average immunoreactivity score was adopted. If several types of histology were included in one section, immunoreactivity score of predominant histology was used.

Statistical analyses. Comparisons between different groups of Renca samples were analyzed with nonparametrical Mann-Whitney U test. The associations between EBAG9 immunoreactivity and clinicopathologic characteristics were evaluated by Student's t test or Fisher's exact probability test. Disease-specific survival was computed by Kaplan-Meier method and the curves were compared by log-rank test. Multivariate analysis of prognostic factors was done using Cox proportional hazard regression model. Computations were done with the StatView 5.0J software (SAS Institute, Inc., Cary, NC). All Ps are two sided and evaluated as significant if $P < 0.05$.

Results

Gene silencing of EBAG9 suppressed *in vivo* tumor growth of Renca cells. To determine the role of EBAG9 in tumor growth of renal cancer cells, we investigated the effects of synthesized siRNA duplexes targeting EBAG9 on s.c. tumor models of Renca cells implanted in syngeneic BALB/c mice. Intratumoral injection of EBAG9 siRNA reduced the protein levels of endogenous EBAG9 compared with the levels of EBAG9 in parental Renca cells or in the Renca tumor treated with control scrambled siRNA duplexes (Fig. 1*A*). Under the treatment of scrambled siRNA, s.c. implanted Renca cells developed prominent tumors, whereas the injection of EBAG9 siRNA suppressed tumor growth of Renca cells (Fig. 1*B* and *C*). After 4-week treatments, the volume of tumors with EBAG9 siRNA treatment was significantly smaller than that with scrambled siRNA (3,854 ± 665 versus 6,315 ± 1,053 mm^3, n = 5; P = 0.0472). We infer that tumor growth is modulated by EBAG9 expression, implicating EBAG9 as a tumor-promoting factor in renal carcinoma.

Generation of Renca cells stably expressing EBAG9. To explore whether constitutive EBAG9 expression influences tumor growth, we generated Renca cells stably expressing human EBAG9. We selected two Renca-EBAG9 cell clones 3 and 4 that express human EBAG9 mRNA as confirmed by RT-PCR using human EBAG9–specific primers (Fig. 2*A*, *top*). The amounts of EBAG9 proteins in Renca-EBAG9 cells were ~2.0 fold increased compared with those in parental Renca cells and Renca-vector cell clones 1 and 2, which were transfected with pcDNA3 empty vector (Fig. 2*A*, *bottom*). In terms of cell growth rate, doubling time of culture Renca-EBAG9 cells was not significantly different from that of Renca-vector cells (Fig. 2*B*). Proliferation of Renca cells was further analyzed by a colorimetric MTT-like assay using a tetrazolium monosodium salt WST-8 that is converted to a water-soluble formazan by metabolically active cells (Fig. 2*C*). Neither EBAG9 overexpression nor RNA interference against EBAG9 did not significantly influence the growth of Renca cells. Moreover, EBAG9 overexpression did not influence the incorporation of bromodeoxyuridine in culture Renca cells (data not shown). The results suggest that stable expression of EBAG9 itself does not accelerate the proliferation of culture tumor cells.

EBAG9 promotes *in vivo* tumor growth of Renca cells. In spite of little difference of propagation abilities between Renca-EBAG9 cells and Renca-vector cells in culture, Renca-EBAG9 cells s.c. implanted into BALB/c mice developed >4-fold larger tumors compared with Renca-vector cells at 4 weeks after inoculation (Fig. 3*A* and *B*). Mean tumor volumes at 4 weeks were 1,712 ± 506 mm^3 for Renca-EBAG9 cell clones 3 and 4 versus 366 ± 110 mm^3 for Renca-vector cell clones 1 and 2 (P = 0.0055; Fig. 3*B*).

In terms of prognosis of mice harboring Renca tumors, 23.5% of mice with Renca-vector cells (n = 17) survived on day 100 after tumor challenge whereas only 5.6% of mice with Renca-EBAG9 cells (n = 18) survived at the same period (Fig. 3*C*; P = 0.0412 by log-rank test). Systemic metastases, including tumor dissemination into peritoneum and distant metastases of lung and liver, were reasons for death in all deceased cases.

EBAG9 suppresses host immune surveillance. To determine whether aberrant EBAG9 expression in Renca cells affects the local immune responses in tumors, we implanted Renca-EBAG9 cells or Renca-vector cells under the renal capsule of BALB/c mice and immunodeficient BALB/c nude mice. Both Renca cell lines formed macroscopic tumors in all of the cancer-bearing hosts by day 25 (Fig. 4*A*). In conventional BALB/c mice, Renca-EBAG9 tumors grew significantly larger compared with Renca-vector tumors (Fig. 4*A* and *B*). Mean volumes of tumors on day 25 in BALB/c mice were 856 ± 162 mm^3 (n = 19) for Renca-EBAG9 clones 3 and 4 versus 149 ± 59 mm^3 (n = 18) for Renca-vector clones 1 and 2 (Fig. 4*B*; $P < 0.0001$). In immunodeficient BALB/c nude mice, both Renca-vector cells and Renca-EBAG9 cells developed extensive tumors compared with tumors in BALB/c mice and there was no significant difference in tumor volumes between Renca-vector cells and Renca-EBAG9 cells (Fig. 4*A* and *B*). Mean volumes of tumors on day 25 in BALB/c nude mice were 2,215 ± 227 mm^3 (n = 18) for Renca-EBAG9 clones 3 and 4 versus 1,802 ± 240 mm^3 (n = 23) for Renca-vector clones 1 and 2 (Fig 4*B*; P = 0.118). These results may suggest that aberrant EBAG9 expression in Renca cells hampers a local primary immune response

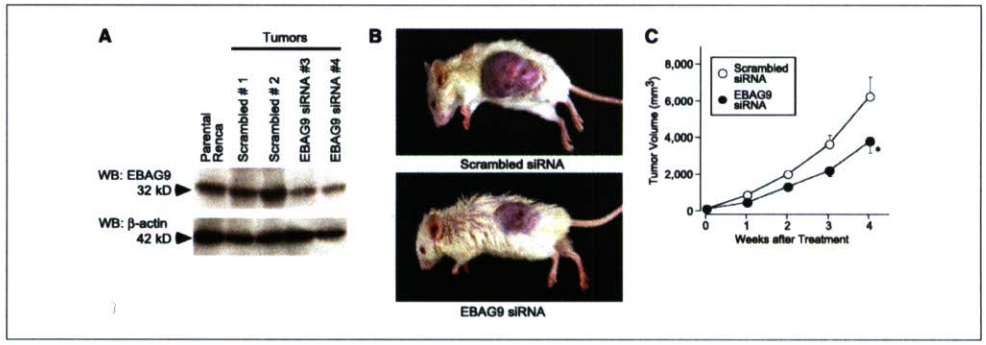

Figure 1. Expression of EBAG9 siRNA suppresses tumor growth derived from murine renal cell carcinoma Renca cells in BALB/c mice. S.c. primary Renca tumors were established by midflank injections of 10,000 tumor cells and i.t. injections of either control scrambled siRNA or EBAG9 siRNA duplexes together with a transfection reagent GeneSilencer were done twice a week in five mice per group when the initial tumor volumes reached 300 mm^3. Mice were sacrificed after 4 weeks of siRNA administration and tumors were homogenized for protein extraction. *A*, Western blot analysis of lysates from *in vitro* culture Renca cells and tumor samples expressing either control scrambled siRNA or EBAG9 siRNA. *B*, representative mice after 4 weeks of siRNA treatment. *Top*, mouse treated with control scrambled siRNA. *Bottom*, mouse treated with EBAG9 siRNA. *C*, tumor volume in EBAG9 siRNA–treated mice (n = 5) is reduced compared with control mice (n = 5). *, $P < 0.05$ at 4 weeks (EBAG9 siRNA versus scrambled siRNA).

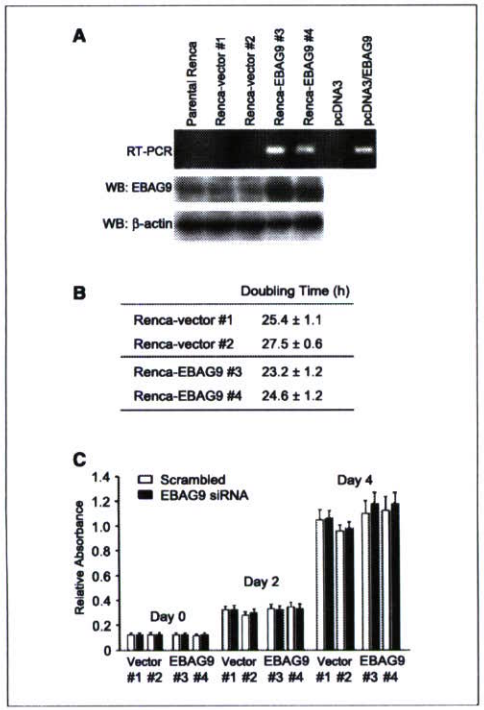

Figure 2. Overexpression of EBAG9 in Renca cells does not accelerate culture cell growth. *A*, RT-PCR analysis and Western blot analysis of Renca cells stably expressing human EBAG9 (Renca-EBAG9) or empty vector (Renca-vector). *Top*, human EBAG9 mRNA is expressed in clones 3 and 4 of Renca-EBAG9 cells. Empty pcDNA3 vector was used as a negative control and pcDNA3 including EBAG9 cDNA as a positive control. *Bottom*, EBAG9 protein is overexpressed in Renca-EBAG9 clones compared with Renca-vector clones or parental Renca cells. *B*, doubling time of culture Renca cells. The numbers of cells in the exponential growth were counted every 2 days and doubling time was calculated according to a formula as described in Materials and Methods ($n = 5$ for each). *C*, proliferative assay using WST-8 tetrazolium salt. Cells seeded into 96-well plates were transfected with control scrambled siRNA or EBAG9 siRNA duplexes (100 ng per well) and cell proliferation was evaluated on days 0, 2, and 4 ($n = 3$ for each). Absorbance at 450 nm (for formazan dye) was measured with absorbance at 620 nm for reference.

that retards the growth of tumors rather than potentiates the intrinsic tumorigenicity of the tumor cells.

To investigate whether the progression of Renca-EBAG9 tumors depends on a reduced sensitivity of the cells to tumor-specific CTLs, we did cytotoxicity assays. Effector CTLs were derived from splenocytes of Renca-bearing BALB/c mice, after a 5-day restimulation with Renca cells in the presence of interleukin-2. (Fig. 4*C*). Renca-EBAG9 cells and Renca-vector cells were equally lysed by tumor-specific CTLs, suggesting that EBAG9 expression itself does not affect the sensitivity of Renca cells to CTL lysis.

To assess whether EBAG9 modulates the subtype-specific reactivity of T lymphocytes against tumors, we examined the numbers of TILs in renal subcapsular Renca tumors developed in BALB/c mice (Fig. 4*D*). No significant differences in numbers of $CD3^+$ and $CD4^+$ T cells were observed between Renca-vector and Renca-EBAG9 tumors, whereas the number of $CD8^+$ T cells in Renca-EBAG9 tumors was significantly decreased compared with that in Renca-vector tumors ($P < 0.05$).

Expression of EBAG9 protein in human renal cell carcinoma tumors. The finding that EBAG9 modulated the growth of Renca tumors led us to the notion whether the molecule contributes to the progression of RCC in human tissues. EBAG9 expression was evaluated immunohistochemically in 78 RCC whole tissue specimens including normal lesions. In noncarcinomatous lesions, a weak and scattered immunostaining of EBAG9 was observed in the cytoplasm of the mesangial cells (Fig. 5*A*) as well as on the luminal surface of the renal tubular

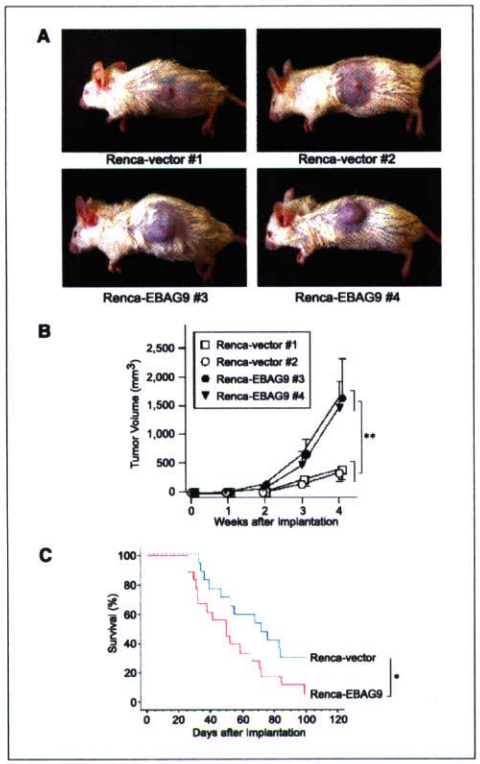

Figure 3. Renca cells stably expressing EBAG9 develop large tumors in BALB/c mice. *A*, representative mice 4 weeks after the inoculation of tumor cells. *B*, volumes of tumors derived from Renca-EBAG9 cells are significantly larger compared with Renca-vector cells in BALB/c mice. S.c. primary tumors were established by midflank injections of 10,000 tumor cells. **, $P < 0.01$ at 4 weeks (Renca-EBAG9 versus Renca-vector). Renca-vector 1, $n = 16$; Renca-vector 2, $n = 6$; Renca-EBAG9 3, $n = 6$; Renca-EBAG9 4, $n = 8$. *C*, poorer prognosis of mice inoculated with Renca-EBAG9 cells compared with mice with Renca-vector cells. Disease-specific survival on day 100: $P = 0.0412$ (Renca-EBAG9 versus Renca-vector). Renca-vector 1, $n = 9$; Renca-vector 2, $n = 8$; Renca-EBAG9 3, $n = 8$; Renca-EBAG9 4, $n = 10$.

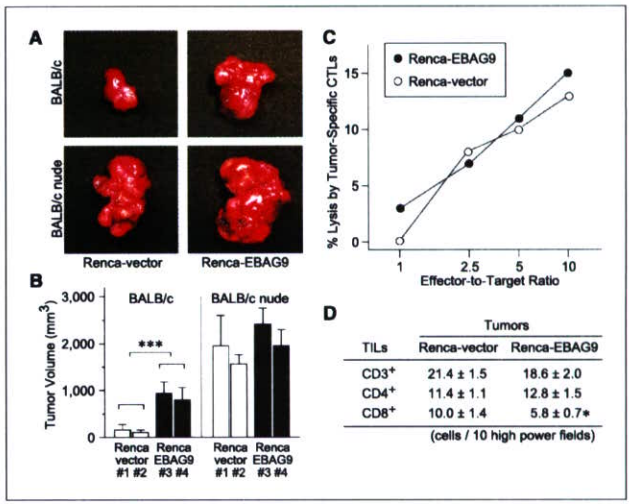

Figure 4. EBAG9 overexpression promotes renal subcapsular tumor growth by Renca cells in wild-type BALB/c mice. *A*, representative tumors 25 days after the inoculation of tumor cells (10,000 cells). *B*, volumes of Renca-EBAG9 tumors are larger than Renca-vector tumors in BALB/c mice, whereas no significant difference of tumor volumes between Renca-vector and Renca-EBAG9 in BALB/c nude mice. **, $P < 0.0001$ on day 25 (Renca-EBAG9 versus Renca-vector). Renca-vector 1, $n = 12$; Renca-vector 2, $n = 11$; Renca-EBAG9 3, $n = 9$; Renca-EBAG9 4, $n = 9$. *C*, lysis of Renca-EBAG9 and Renca-vector cells by tumor-specific CTLs. Splenocytes from Renca-bearing mice were cultured with Renca cells at a ratio of 20:1 pulsed with interleukin-2 (1,000 units/mL) for 5 days. Lactate dehydrogenase release from cells with a damaged membrane was examined using CytoTox-ONE Reagent and fluorescence was measured with an excitation wavelength of 560 nm and an emission wavelength of 590 nm. *D*, numbers of tumor infiltrating-lymphocytes positive for CD3, CD4, or CD8 immunostaining were microscopically examined in the high-power field of view at a magnification of 400×. BALB/c mouse spleen specimen was used as a positive control. *, $P < 0.05$ (Renca-EBAG9 versus Renca-vector).

cells (data not shown). The levels of EBAG9 expression in normal renal tissues corresponded to immunoreactivity score of 0. In RCC tumors, 10 of 78 cases (13%) had negative immunoreactivity of EBAG9, whereas 68 of cases (87%) showed EBAG9 positivity. With regard to EBAG9-positive RCC tumors, the cancer cells generally retain intense and diffuse staining patterns in the cytoplasm or on the membrane (Fig. 5*B*, *C*, and *D*). The levels of EBAG9 positivity were immunoreactivity score of 1+ for 18 RCC tumors (23%), 2+ for 31 tumors (40%), and 3+ for 19 tumors (24%). With respect to RCC histology, clear cell tumors displayed an intense membrane staining as well as a diffuse cytoplasmic staining of EBAG9 (Fig. 5*B*; immunoreactivity score, 2+). Sarcomatoid tumors showed an intense and frequent cytoplasmic immunoreactivity (Fig. 5*C*; immunoreactivity score, 3+). Lung metastatic tumors showed the highest EBAG9 staining, predominantly in the cytoplasm (Fig. 5*D*; immunoreactivity score, 3+).

A significant association between EBAG9 immunoreactivity and clinicopathologic variables was observed in RCC patients (Supplementary Table 1). EBAG9 positivity (immunoreactivity score, >1+) was significantly correlated with advanced pathologic tumor stages, positivity of vascular infiltration, and nonclear cell histology ($P = 0.0017$, $P = 0.0109$, and $P = 0.0126$, respectively).

In Kaplan-Meier analysis of the RCC patients, those in which the tumor had high EBAG9 immunoreactivity (immunoreactivity score, 3+) showed a shorter disease-specific survival (Fig. 6) compared with patients showing low or negative EBAG9 immunoreactivity (immunoreactivity score, 0-2+). The 5-year disease-specific survival in cases with EBAG9 immunoreactivity score of 3+ was 55%, whereas 91.2% of patients with low or negative EBAG9 immunoreactivity were alive during the same period.

In univariate Cox proportional hazards analysis for a 5-year disease-specific survival, established prognostic factors including infiltration, pathologic stage, and metastatic status are the most significant univariate variables of survival (Supplementary Table 2; $P < 0.0001$ for all). Lower EBAG9 immunoreactivity as well as negativity of lymph node status or vascular infiltration are also involved in significant univariate survival predictors ($P = 0.0007$, 0.0002, and 0.0003, respectively). In multivariate Cox proportional hazards analysis, negative metastatic status is the most significant predictor of survival (Supplementary Table 3; $P < 0.001$; relative risk, 42.53). Notably, high EBAG9 immunoreactivity is associated with disease-specific death in multivariate analysis ($P = 0.0485$; relative risk, 5.09). These results indicate that high immunoreactivity of EBAG9 is a potential poor prognostic variable in RCC patients.

Discussion

The present study shows the first evidence regarding a tumor-promoting role of EBAG9 *in vivo*. We showed that Renca tumors overexpressing EBAG9 had a much aggressive phenotype with poorer prognosis compared with Renca tumors expressing empty vector, although the effects of EBAG9 on culture cell proliferation was relatively minimal. EBAG9 immunoreactivity was detected in most of human RCC samples and high amounts of EBAG9 protein may associate with poor prognosis of the patients. Our findings suggest that EBAG9 is a tumor-promoting factor in RCC yet does not function as an essential oncogene by itself. The present results lead us to the notion that EBAG9 potentiates tumor growth by altering tumor microenvironment.

Decreased local immune responses may be one of the critical mechanisms that change tumor microenvironment. In antitumor immunity, T lymphocyte–mediated immune surveillance is thought a principal host defense mechanism (15). Although tumors such as RCC are immunogenic and could be targeted by tumor-specific CTL or natural killer cells, antitumor immune

reactions are not completely effective to reject tumor cells so that tumors continue to grow progressively (16). In our cytotoxicity assay, there was no significant difference of CTL lysis between Renca-EBAG9 and Renca-vector cells, suggesting that overexpression of EBAG9 may not particularly alter the presentation of tumor-associated antigens or the levels of MHC class I molecule expression. In TIL assay, however, $CD8^+$ T cells seemed specifically reduced by aberrant EBAG9 expression. We suspect that generation of immunosuppressive factors or apoptosis activation may result in the reduction of $CD8^+$ TIL, leading to hamper antitumor immunity.

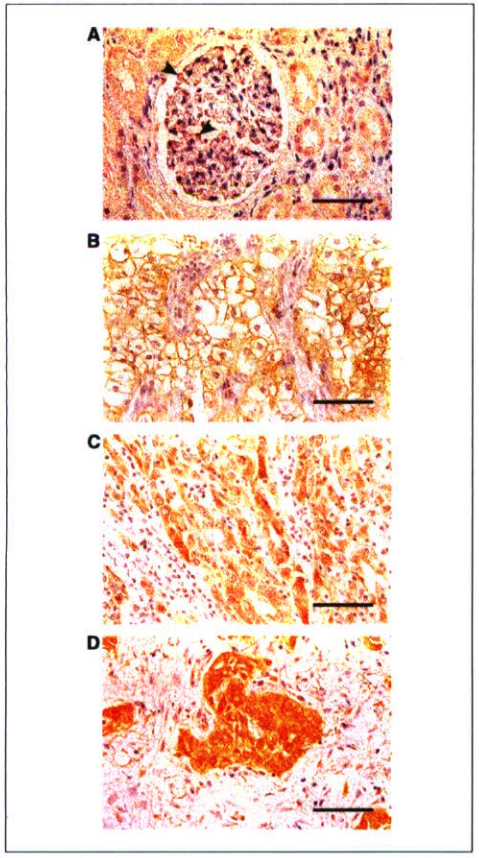

Figure 5. EBAG9 immunostaining in human kidney and renal cell carcinoma specimens. *A*, normal kidney (immunoreactivity score, 0). EBAG9 is weakly expressed in the mesangial cells (*arrowheads*). *B*, clear cell carcinoma (immunoreactivity score, 1+). EBAG9 is immunostained predominantly on the cell membrane in cancerous regions. *C*, spindle cell carcinoma (immunoreactivity score, 3+). Intense immunostaining of EBAG9 is observed in the cytoplasm of sarcomatoid cancerous regions. *D*, lung metastatic tumors (immunoreactivity score, 3+). Intense immunoreactivity of EBAG9 is observed in metastatic tumors with high immunoreactivity scores. *Bars*, 50 μm.

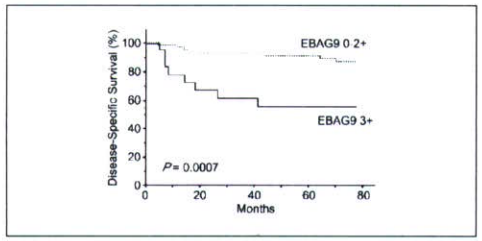

Figure 6. Association of immunocytochemical staining for EBAG9 with disease-specific survival of 78 RCC patients. Five-year disease-specific survival of the patients with high EBAG9 immunoreactivity (immunoreactivity score, 3+; $n = 19$) was significantly worse than the patients with immunoreactivity scores of 0-2+ ($n = 59$; 55% versus 91%, $P = 0.0007$, by log-rank test).

The alteration in cell surface glycosylation could be implicated in the modulation of tumor microenvironments (17, 18). It has been recently shown that tumor-associated ganglioside expression in human RCC cells suppresses nuclear factor-κB activation in T cells and mediates T-cell apoptosis (19, 20). RCC display increased levels of gangliosides including GM2, GM1, and GD1a (21) as well as several disialogangliosides (22), which may inhibit the function of antigen-presenting cells (23) or modulate tumor vascularization (24). It has been recently shown that tumor-associated *O*-linked glycan antigens Tn and TF were expressed in transfected cells expressing RCAS1 (receptor-binding cancer antigen expressed on SiSo cells; ref. 25), whose cDNA has been found to be a homologue of EBAG9 (26).

Another possible explanation is that EBAG9 may stimulate angiogenesis by up-regulating growth factors or cytokines. There are literatures that suggest that vascular endothelial growth factor (VEGF) could be involved in RCC tumor progression. Mutations of the von Hippel-Lindau tumor suppressor gene, which are often observed in hereditary RCC and sporadic clear cell RCC, result in overproduction of VEGF through a mechanism involving hypoxia-inducible factor α (27, 28). It has been recently shown that VEGF interferes with the development of T cells at pathologically relevant concentrations *in vivo* (29); thus, the growth factor may contribute to tumor-associated immune deficiencies.

It has been generally accepted that tumor cells may escape from immune surveillance by expressing the EBAG9 homologue RCAS1, which targets RCAS1 receptor–expressing immune cells and induces apoptosis (26). Nakashima et al. identified the RCAS1 cDNA through expression cloning using the 22-1-1 monoclonal antibody that they originally generated (30). Engelsberg et al. recently showed, however, that the 22-1-1 epitope was distinct from the products encoded by RCAS1 cDNA, because the RCAS1 protein was not recognized by the 22-1-1 antibody, whereas the 22-1-1 antibody recognized the tumor-associated *O*-linked glycan antigens (25). They showed that their raised polyclonal antibody recognized a ~35-kDa protein, consistent with the immunoblotting results using our polyclonal antibody. On the contrary, the putative RCAS1 protein recognized by the 22-1-1 antibody was identified as an ~80-kDa membrane molecule expressed on human uterine cancer cells (26, 30). Although there are a number of publications concerning RCAS1 in cancers from the point of view as the 22-1-1 antigen, we consider that a pathophysiologic role of EBAG9 in tumor immunology needs to be properly evaluated. The present article may provide new insights into an EBAG9-mediated *in vivo* function in cancer progression.

We have previously reported that the immunoreactivity of EBAG9 was mainly observed in the cytoplasm of normal epithelial cells with a granular staining pattern, or particularly in perinuclear regions (3, 5). In carcinoma tissues, an intense staining of the cell surface could be also observed such as in prostate cancer or hepatocellular carcinoma. The expression of RCAS1 immunoreactivity recognized by antibodies against recombinant RCAS1 was localized to perinuclear structures, suggesting that the protein is predominantly distributed in the Golgi system (25). Given that EBAG9 is a Golgi-predominant protein that could be trafficking from the perinuclear regions to the cell surface membrane, it is likely that EBAG9 immunoreactivity could be observed in both cytoplasm and cell surface of cancerous tissues with the abundant expression of EBAG9. Notably, EBAG9 immunoreactivity in RCC with advanced stages such as sarcomatoid or metastatic tumors was cytoplasmic predominant (Fig. 5*C* and *D*). Further studies using confocal or electron microscopic examination may elucidate the dynamic distribution of EBAG9.

As we showed that there are several types of cancer that intensely express EBAG9 and the expression levels of EBAG9 may relate to advanced tumor grades (3–6), it is likely that the tumor-promoting effect of EBAG9 is a general event in malignancies regardless of their estrogen dependency. We also observed the lack of association between sex and EBAG9 expression in human RCC in our clinicopathologic study (Supplementary Table 1). Thus, EBAG9 could be a therapeutic target for various tumors constitutively expressing the molecule.

In summary, we show that EBAG9 is a tumor-promoting factor in both murine Renca RCC and human RCC. We propose that EBAG9 immunoreactivity is a new potential biomarker for prognosis of RCC and a treatment modality targeting EBAG9 will provide a novel therapeutic option for advanced RCC.

Acknowledgments

Received 9/28/2004; revised 2/15/2005; accepted 2/25/2005.

Grant support: Ministry of Health, Labor and Welfare Japan, the Ministry of Education, Culture, Sports, Science and Technology Japan.

The costs of publication of this article were defrayed in part by the payment of page charges. This article must therefore be hereby marked *advertisement* in accordance with 18 U.S.C. Section 1734 solely to indicate this fact.

We thank T. Suzuki for her technical assistance.

References

1. Watanabe T, Inoue S, Hiroi H, Orimo A, Kawashima H, Muramatsu M. Isolation of estrogen-responsive genes with a CpG island library. Mol Cell Biol 1998;18:442–9.
2. Tsuchiya F, Ikeda K, Tsutsumi O, et al. Molecular cloning and characterization of mouse EBAG9, homolog of a human cancer associated surface antigen: expression and regulation by estrogen. Biochem Biophys Res Commun 2001;284:2–10.
3. Suzuki T, Inoue S, Kawabata W, et al. EBAG9/RCAS1 in human breast carcinoma: a possible factor in endocrine-immune interactions. Br J Cancer 2001;85:1731–7.
4. Akahira JI, Aoki M, Suzuki T, et al. Expression of EBAG9/RCAS1 is associated with advanced disease in human epithelial ovarian cancer. Br J Cancer 2004;90:2197–202.
5. Takahashi S, Urano T, Tsuchiya F, et al. EBAG9/RCAS1 expression and its prognostic significance in prostatic cancer. Int J Cancer 2003;106:310–5.
6. Aoki T, Inoue S, Imamura H, et al. EBAG9/RCAS1 expression in hepatocellular carcinoma: correlation with tumour dedifferentiation and proliferation. Eur J Cancer 2003;39:1552–61.
7. Landis SH, Murray T, Bolden S, Wingo PA. Cancer statistics. CA Cancer J Clin 1999;49:8–31.
8. Moch H, Gasser T, Amin MB, Torhorst J, Sauter G, Mihatsch MJ. Prognostic utility of the recently recommended histologic classification and revised TNM staging system of renal cell carcinoma: a Swiss experience with 588 tumors. Cancer 2000;89:604–14.
9. Takeuchi T, Ueki T, Sasaki Y, et al. Th2-like response and antitumor effect of anti-interleukin-4 mAb in mice bearing renal cell carcinoma. Cancer Immunol Immunother 1997;43:375–81.
10. Nishimatsu H, Takeuchi T, Ueki T, et al. CD95 ligand expression enhances growth of murine renal cell carcinoma *in vivo*. Cancer Immunol Immunother 1999;48:56–61.
11. Gelb AB. Renal cell carcinoma: current prognostic factors. Union Internationale Contre le Cancer (UICC) and the American Joint Committee on Cancer (AJCC). Cancer 1997;80:981–6.
12. Dawson M. Initiation and maintenance of cultures. In: Bulter M, Dawson M, editors. Cell culture labfax. Oxford: BIOS Scientific; 1992. p. 25–42.
13. Miyamoto T, Min W, Lillehoj HS. Lymphocyte proliferation response during *Eimeria tenella* infection assessed by a new, reliable, nonradioactive colorimetric assay. Avian Dis 2002;46:10–6.
14. Schumacher K, Haensch W, Roefzaad C, Schlag PM. Prognostic significance of activated CD8(+) T cell infiltrations within esophageal carcinomas. Cancer Res 2001;61:3932–6.
15. Shankaran V, Ikeda H, Bruce AT, et al. IFNγ and lymphocytes prevent primary tumour development and shape tumour immunogenicity. Nature 2001;410:1107–11.
16. Pawelec G. Immunotherapy and immunoselection: tumour escape as the final hurdle. FEBS Lett 2004;567:63–6.
17. Springer GF. Immunoreactive T and Tn epitopes in cancer diagnosis, prognosis, and immunotherapy. J Mol Med 1997;75:594–602.
18. Hakomori S. Glycosylation defining cancer malignancy: new wine in an old bottle. Proc Natl Acad Sci U S A 2002;99:10231–3.
19. Kudo D, Rayman P, Horton C, et al. Gangliosides expressed by the renal cell carcinoma cell line SK-RC-45 are involved in tumor-induced apoptosis of T cells. Cancer Res 2003;63:1676–83.
20. Thornton MV, Kudo D, Rayman P, et al. Degradation of NF-κ B in T cells by gangliosides expressed on renal cell carcinomas. J Immunol 2004;172:3480–90.
21. Ritter G, Livingston PO. Ganglioside antigens expressed by human cancer cells. Semin Cancer Biol 1991;2:401–9.
22. Ito A, Levery SB, Saito S, Satoh M, Hakomori S. A novel ganglioside isolated from renal cell carcinoma. J Biol Chem 2001;276:16695–703.
23. Caldwell S, Heitger A, Shen W, Liu Y, Taylor B, Ladisch S. Mechanisms of ganglioside inhibition of APC function. J Immunol 2003;171:1676–83.
24. Manfredi MG, Lim S, Claffey KP, Seyfried TN. Gangliosides influence angiogenesis in an experimental mouse brain tumor. Cancer Res 1999;59:5392–7.
25. Engelsberg A, Hermosilla R, Karsten U, Schulein R, Dorken B, Rehm A. The Golgi protein RCAS1 controls cell surface expression of tumor-associated O-linked glycan antigens. J Biol Chem 2003;278:22998–3007.
26. Nakashima M, Sonoda K, Watanabe T. Inhibition of cell growth and induction of apoptotic cell death by the human tumor-associated antigen RCAS1. Nat Med 1999;5:938–42.
27. Gnarra JR, Zhou S, Merrill MJ, et al. Post-transcriptional regulation of vascular endothelial growth factor mRNA by the product of the VHL tumor suppressor gene. Proc Natl Acad Sci U S A 1996;93:10589–94.
28. Turner KJ, Moore JW, Jones A, et al. Expression of hypoxia-inducible factors in human renal cancer: relationship to angiogenesis and to the von Hippel-Lindau gene mutation. Cancer Res 2002;62:2957–61.
29. Ohm JE, Gabrilovich DI, Sempowski GD, et al. VEGF inhibits T-cell development and may contribute to tumor-induced immune suppression. Blood 2003;101:4878–86.
30. Sonoda K, Nakashima M, Kaku T, Kamura T, Nakano H, Watanabe T. A novel tumor-associated antigen expressed in human uterine and ovarian carcinomas. Cancer 1996;77:1501–9.

Estrogen-Responsive Finger Protein as a New Potential Biomarker for Breast Cancer

Takashi Suzuki,[1] Tomohiko Urano,[3] Tohru Tsukui,[4] Kuniko Horie-Inoue,[4] Takuya Moriya,[1] Takanori Ishida,[2] Masami Muramatsu,[4] Yasuyoshi Ouchi,[3] Hironobu Sasano,[1] and Satoshi Inoue[3,4]

Abstract **Purpose:** Estrogen-responsive finger protein (Efp) is a member of RING finger-B box-Coiled Coil family and is also a downstream target of estrogen receptor α. Previously, Efp was shown to mediate estrogen-induced cell growth, which suggests possible involvement in the development of human breast carcinomas. In this study, we examined expression of Efp in breast carcinoma tissues and correlated these findings with various clinicopathologic variables.

Experimental Design: Thirty frozen specimens of breast carcinomas were used for immunohistochemistry and laser capture microdissection/real-time PCR of Efp. Immunohistochemistry for Efp was also done in 151 breast carcinoma specimens fixed with formalin and embedded in paraffin wax.

Results: Efp immunoreactivity was detected in breast carcinoma cells and was significantly associated with the mRNA level ($n = 30$). Efp immunoreactivity was positively associated with lymph node status or estrogen receptor α status and negatively correlated with histologic grade or 14-3-3σ immunoreactivity ($n = 151$). Moreover, Efp immunoreactivity was significantly correlated with poor prognosis of breast cancer patients, and multivariate analyses of disease-free survival and overall survival for 151 breast cancer patients showed that Efp immunoreactivity was the independent marker.

Conclusions: Our data suggest that Efp immunoreactivity is a significant prognostic factor in breast cancer patients. These findings may account for an oncogenic role of Efp in the tumor progression of breast carcinoma.

Breast cancer is the most common type of cancer and continues to be the most frequent cause of cancer-related deaths in women in the Western world. Whether or not human primary breast cancers are estrogen dependent is a critical factor that determines patient prognosis and availability of antiestrogenic endocrine therapy (1). Two thirds of breast carcinomas are positive for estrogen receptor α (ERα) and a great majority of these tumors initially respond to antiestrogens such as tamoxifen and aromatase inhibitors. However, it is also true that these ERα-positive breast carcinomas frequently acquire resistance to endocrine therapy, although ERα remains to be expressed (1, 2). The molecular mechanisms through which breast carcinomas become hormone-refractory are still largely unclear.

Identification and functional studies of ERα target molecules may provide a clue for understanding the mechanism that alters tumor phenotypes. We have previously isolated estrogen-responsive finger protein (Efp), which is a member of RING finger-B box-Coiled Coil family (3). Efp also is one of the downstream targets of ERα (3–6). Efp-deficient mice displayed underdeveloped uteri and reduced estrogen responsiveness (7), and therefore, Efp is considered to be essential for estrogen-dependent proliferation. It has also been shown that Efp promotes the growth of breast tumor by functioning as a ubiquitin ligase (E3) that targets the negative cell cycle checkpoint 14-3-3σ (8).

Expression of Efp was previously reported in breast carcinoma tissues at mRNA (5) and protein levels (9). However, information on the expression of Efp in human breast carcinoma tissues is still very limited, and the biological significance of Efp remains unclear at this juncture. Therefore, in this study, we examined expression of Efp in 30 cases of breast carcinoma tissues using immunohistochemistry and laser capture microdissection/real-time PCR. We subsequently examined immunolocalization of Efp in 151 cases of human breast carcinoma tissues and correlated these findings with various clinicopathologic factors including clinical outcome of the patients.

Authors' Affiliations: Departments of [1]Pathology and [2]Surgery, Tohoku University School of Medicine, Aoba-ku, Sendai, Miyagi-ken, Japan; [3]Department of Geriatric Medicine, Graduate School of Medicine, The University of Tokyo, Hongo, Bunkyo-ku, Tokyo, Japan; and [4]Research Center for Genomic Medicine and Department of Molecular Biology, Saitama Medical School, Yamane, Hidaka-shi, Saitama, Japan
Received 1/6/05; revised 6/9/05; accepted 6/28/05.

Grant support: Ministry of Health, Labor, and Welfare Japan, the Ministry of Education, Culture, Sports, Science and Technology Japan, the Core Research for Evolutional Science and Technology, and the Princess Takamatsu Cancer Research Fund (02-23402).

The costs of publication of this article were defrayed in part by the payment of page charges. This article must therefore be hereby marked *advertisement* in accordance with 18 U.S.C. Section 1734 solely to indicate this fact.

Requests for reprints: Takashi Suzuki, Department of Pathology, Tohoku University School of Medicine, 2-1 Seiryo-machi, Aoba-ku, Sendai, 980-8575, Japan. Phone: 81-22-717-8050; Fax: 81-22-717-8051; E-mail: t-suzuki@patholo2.med.tohoku.ac.jp.

doi:10.1158/1078-0432.CCR-05-0040

Materials and Methods

Patients and tissues. Thirty specimens of invasive ductal carcinoma were obtained from patients who underwent mastectomy in 2001 in the Department of Surgery at Tohoku University Hospital, Sendai, Japan. Specimens for RNA isolation were snap-frozen and stored at −80°C, and those for immunohistochemistry were fixed with 10% formalin and embedded in paraffin wax. Informed consent was obtained from all patients before their surgery and examination of specimens used in this study.

One hundred fifty-one specimens of invasive ductal carcinoma of the breast were obtained from female patients who underwent mastectomy from 1982 to 1989 in the Department of Surgery, Tohoku University Hospital, Sendai, Japan. All specimens were fixed with 10% formalin and embedded in paraffin wax, and snap-frozen tissues were not available for examination in these cases. These patients did not receive any preoperative radiotherapy and chemotherapy as well as any postoperative hormone therapy. Information on patient age, menopausal status, stage, tumor size at operation, lymph node status, histologic grade, and relapse and survival times was retrieved from the review of patient charts. The mean follow-up period was 105 months (3-157 months).

Research protocols for this study were approved by the Ethics Committee at Tohoku University School of Medicine.

Immunohistochemistry. Anti-human Efp antibody was generated as previously described (3). Polyclonal antibody for 14-3-3σ (N-14) and monoclonal antibodies for ERα (1D5), progesterone receptor (MAB429), Ki-67 (MIB-1), and p53 (DO7) were purchased from Santa Cruz Biotechnology (Santa Cruz, CA), Immunotech (Marseille, France), Chemicon (Temecula, CA), DAKO (Tokyo, Japan), and Novocastra Laboratories (Newcastle, United Kingdom), respectively. A Histofine Kit (Nichirei, Tokyo, Japan), which employs the streptavidin-biotin amplification method, was used for immunohistochemistry, and the antigen-antibody complex was visualized with 3.3′-diaminobenzidine solution [1 mmol/L 3,3′-diaminobenzidine, 50 mmol/L Tris-HCl buffer (pH 7.6), and 0.006% H_2O_2]. For a negative control for Efp immunohistochemistry, an immunohistochemical preabsorption test was done.

Efp immunoreactivity was classified into three groups: ++, >50% positive carcinoma cells; +, 1% to 50% positive cells; and −, no immunoreactivity, according to a previous report (10). Immunoreactivity of ERα, progesterone receptor, and Ki-67 was scored in more than 1,000 carcinoma cells for each case, and the percentage of immunoreactivity [i.e., labeling index (LI)] was determined. Cases that were found to have ERα LI of more than 10% were considered ERα-positive breast carcinomas (11).

Laser capture microdissection/real-time PCR. Laser capture microdissection was conducted using the Laser Scissors CRI-337 (Cell Robotics, Inc., Albuquerque, NM). A detailed procedure has been described previously (12, 13). Briefly, ~1,000 carcinoma or intratumoral stromal cells were separately collected under the microscope from breast carcinoma frozen tissue sections embedded in Tissue-Tek O.T.C. The Light Cycler System (Roche Diagnostics GmbH, Mannheim, Germany) was used to semiquantify the level of Efp mRNA expression in this study. The primers used for real-time PCR were the following: Efp sense, 5′-CGTGGAGTGGTTCAACAC-3′, and Efp antisense, 5′-GAGCAGATGGAGAGTGTGG-3′; glyceraldehyde-3-phosphate dehydrogenase sense, 5′-TGAACGGGAAGCTCACTGG-3′, and glyceraldehyde-3-phosphate dehydrogenase antisense, 5′-TCCACCACCCTGTTGCTGTA-3′. To verify amplification of the correct sequences, PCR products were purified and subjected to direct sequencing. Efp mRNA levels were normalized to those of glyceraldehyde-3-phosphate dehydrogenase, and subsequently, the fold change of Efp mRNA level in each sample was evaluated using the mRNA level in MCF7 cells as a positive control. Negative control experiments lacked cDNA substrate to check for the possibility of exogenous contaminant DNA, and no amplified products were detected under these conditions.

Statistical analyses. Statistical analyses were done using one-way ANOVA and Bonferroni test or a cross-table using χ^2 test. Overall and disease-free survival curves were generated according to the Kaplan-Meier method, and statistical significance was calculated using log-rank test. Univariate and multivariate analyses were evaluated by a proportional hazard model (Cox) using PROC PHREG in our SAS software. Differences with $P < 0.05$ were considered significant.

Results

Expression of Efp in 30 breast cancer tissues: Immunohistochemistry. Efp immunoreactivity was detected in the cytoplasm of breast carcinoma cells, but not in intratumoral

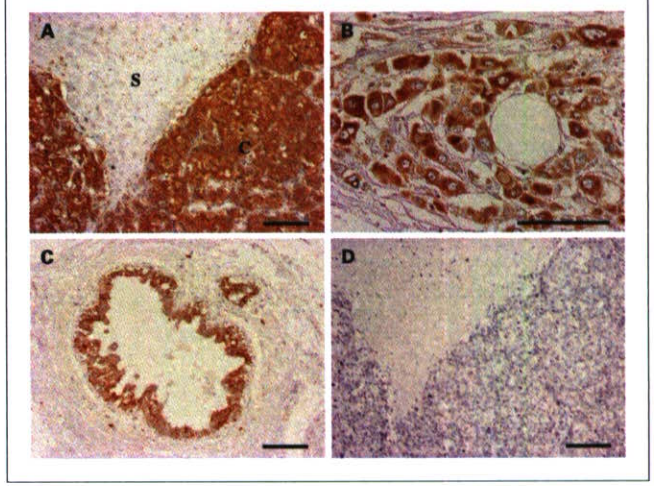

Fig. 1. Immunohistochemistry for Efp in breast carcinoma (invasive ductal carcinoma). *A* and *B*, Efp immunoreactivity was detected in the cytoplasm of the carcinoma cells (*C*), but not in intratumoral stromal cells (*S*). *C*, in morphologically normal mammary glands, Efp immunoreactivity was also detected in the epithelial cells. *D*, no significant immunoreactivity of Efp was detected in a section analyzed by immunohistochemical preabsorption test as a negative control. Same area as *A*. *Bar*, 100 μm.

stromal cells (Fig. 1A and B). The number of cases expressing immunoreactive Efp in each group of 30 breast carcinoma tissues is summarized as follows: ++, n = 9 (30.0%); +, n = 13 (43.3%); and −, 17 (56.7%). Efp immunoreactivity was also positive in epithelial cells of morphologically normal mammary glands (Fig. 1C). Immunohistochemical preabsorption test for Efp showed no specific immunoreactivity in a negative control (Fig. 1D).

Laser capture microdissection/real-time PCR. To examine the localization of Efp mRNA in breast carcinoma tissues, we did laser capture microdissection/real-time PCR analyses. Expression of Efp mRNA was detected in carcinoma cells, but not in intratumoral stromal cells (Fig. 2A). As shown in Fig. 2B, a significant association was detected between Efp immunoreactivity and Efp mRNA level (P = 0.0012, ++ versus − and ++ versus +, respectively) in 30 cases of breast cancer tissues examined.

Correlation between Efp immunoreactivity and clinicopathologic variables in 151 breast carcinomas. Results of associations between Efp immunoreactivity and clinicopathologic variables in 151 breast carcinomas were summarized in Table 1. The number of cases expressing immunoreactive Efp in each group is summarized as follows: ++, n = 46 (30.5%); +, n = 64 (42.4%); and −, n = 41 (27.2%). Efp immunoreactivity was significantly associated with lymph node status (P = 0.0027), ERα status (P = 0.0013), or ERα LI (P = 0.0023, ++ versus −; P = 0.0045, + versus −). On the other hand, negative correlation was detected between Efp immunoreactivity and histologic grade (P = 0.0064) or 14-3-3σ immunoreactivity (P < 0.0001). There was, however, no significant relationship between Efp immunoreactivity and other clinicopathologic variables, including patient age, menopausal status, stage, tumor size, progesterone receptor LI, Ki-67 LI, and 53 status, in this study. Similar tendencies described above were confirmed in increased rankings of positivity for Efp immunoreactivity into five groups (0%, 1-25%, 26-50%, 51-75%, and 76-100% positive cells; data not shown).

Correlation between Efp immunoreactivity and clinical outcome of the 151 breast cancer patients. Efp immunoreactivity was significantly associated with an increased risk of recurrence (P < 0.0001; Fig. 3A). A similar tendency was also detected when Efp immunoreactivity was further categorized into five groups (0%, 1-25%, 26-50%, 51-5%, and 76-100% positive cells; Fig. 3B). Following univariate analysis by Cox (Table 2), lymph node status (P < 0.0001), Efp immunoreactivity (P < 0.0001), tumor size (P = 0.0019), and 14-3-3σ immunoreactivity (P = 0.0314) were shown as significant prognostic variables for disease-free survival in 151 breast carcinoma patients examined. A multivariate analysis revealed that lymph node status (P < 0.0001), Efp immunoreactivity (P = 0.0011), and tumor size (P = 0.0349) were independent prognostic factors with relative risks over 1.0, whereas 14-3-3σ immunoreactivity was not significant (P = 0.0681; Table 2).

Overall survival curve was shown in Fig. 3C. A significant correlation was detected between Efp immunoreactivity and adverse clinical outcome of the patients (P < 0.0001), and a similar tendency was also detected when Efp immunoreactivity was categorized into five groups (Fig. 3D). Using a univariate analysis (Table 3), Efp immunoreactivity (P < 0.0001), lymph node status (P < 0.0001), tumor size (P = 0.0084), and p53 status (P = 0.0230) turned out to be

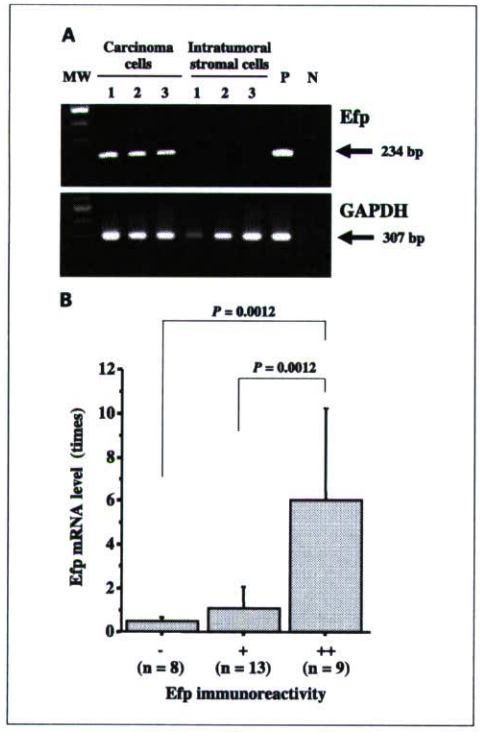

Fig. 2. Laser capture microdissection/real-time PCR analysis for Efp in breast carcinoma tissues. *A*, expression for Efp mRNA (234 bp) was detected only in the component of breast carcinoma cells, whereas that of glyceraldehyde-3-phosphate dehydrogenase (*GAPDH*) mRNA (307 bp) was detected in both components of carcinoma cells and intratumoral stromal cells. Three cases are represented in this agarose gel photo. PCR was done for 40 cycles. *P*, positive control (MCF7 cells); *N*, negative control (no cDNA substrate). *B*, association between Efp immunoreactivity and Efp mRNA level in the carcinoma cell component in 30 breast carcinoma tissues. A significant positive correlation was detected (P = 0.0012, ++ versus + and ++ versus −, respectively). Expression level of Efp mRNA in the carcinoma cell component of each case was represented as a ratio of that of glyceraldehyde-3-phosphate dehydrogenase, and was subsequently evaluated as the ratio (%) compared with that of MCF7 cells.

significant prognostic factors for overall survival in this study. However, multivariate analysis revealed that only Efp immunoreactivity (P = 0.0030) and lymph node status (P = 0.0065) were independent prognostic factors with a relative risk over 1.0; other factors were not significant in this study (Table 3).

The significant association between Efp immunoreactivity and clinical outcome of the patients was detected regardless of ERα status in this study (Fig. 4A-D).

Discussion

In this study, Efp immunoreactivity was significantly associated with Efp mRNA level, and was detected in carcinoma cells in 110 of 151 human breast carcinomas (72.8%).

Table 1. Association between Efp immunoreactivity and clinicopathologic variables in 151 human breast carcinomas

	Efp immunoreactivity			P
	++ (n = 46)	+ (n = 64)	− (n = 41)	
Age* (y)	52.8 ± 1.9	53.5 ± 1.6	52.4 ± 1.3	>0.05
Menopausal status				
Premenopausal	23 (15.2%)	33 (21.9%)	15 (9.9%)	
Postmenopausal	23 (15.2%)	31 (20.5%)	26 (17.2%)	>0.05
Stage				
I	11 (7.3%)	16 (10.6%)	11 (7.3%)	
II	26 (17.2%)	42 (27.8%)	26 (17.2%)	
III	9 (6.0%)	6 (31.6%)	4 (21.0%)	>0.05
Tumor size* (mm)	29.5 ± 2.5	24.1 ± 1.3	26.9 ± 3.0	>0.05
Lymph node status				
Positive	29 (19.2%)	20 (13.2%)	15 (9.9%)	
Negative	17 (11.3%)	44 (29.1%)	26 (17.2%)	0.0027
Histologic grade				
1	17 (11.3%)	17 (11.3%)	3 (2.0%)	
2	16 (10.6%)	22 (14.6%)	14 (9.3%)	
3	13 (8.6%)	25 (16.6%)	24 (15.9%)	0.0064
ERα status				
Positive	39 (25.8%)	49 (32.5%)	21 (13.9%)	
Negative	7 (4.6%)	15 (9.9%)	20 (13.2%)	0.0013
ERα LI*	48.9 ± 4.8	46.0 ± 4.2	27.0 ± 4.9	− vs ++; 0.0023 − vs +; 0.0045
Progesterone receptor LI*	46.8 ± 11.5	47.6 ± 4.3	34.6 ± 5.6	>0.05
14-3-3α immunoreactivity				
Positive	9 (6.0%)	20 (13.2%)	29 (19.2%)	
Negative	37 (24.5%)	44 (29.1%)	12 (7.9%)	<0.0001
Ki-67 LI*	23.9 ± 2.2	25.8 ± 2.2	27.2 ± 2.9	>0.05
P53 status				
Positive	13 (8.6%)	13 (8.6%)	17 (11.3%)	
Negative	33 (21.9%)	51 (33.8%)	24 (15.9%)	>0.05

*Data are presented as mean ± 95% confidence interval (95% CI). All other values represent the number of cases and percentage.

Previously, Ikeda et al. (5) reported Efp mRNA expression in 9 of 15 (60.0%) breast carcinoma tissues using RNase protection assay, and Thomson et al. (9) reported Efp immunoreactivity in breast carcinoma cells in 64 of 91 (70.3%) cases. The frequency and cellular localization of Efp in our present study were in good agreement with these reports (5, 9), and widespread distribution of Efp may suggest an important role of Efp in breast carcinomas. Efp immunoreactivity was also detected in normal glandular epithelia in our study. It is also consistent with previous studies (5, 9) and Thomson et al. (9) suggested the involvement of Efp in mammary gland differentiation.

Efp is known as a downstream product of ERα (3-7). *Efp* gene has an estrogen-responsive element at the 3′-untranslated region (3). The estrogen-responsive element of *Efp* responded to ERα in transfected estrogen receptors in 293T cells (5), and Efp mRNA was rapidly induced by estrogen treatment within 0.5 hour in MCF7 cells (5). In this study, Efp immunoreactivity was significantly associated with ERα status and ERα LI in 151 breast carcinoma tissues. Therefore, it is suggestive that Efp is mainly produced in carcinoma cells through ERα as a result of estrogenic action in breast carcinoma. On the other hand, we also found Efp immunoreactivity in 22 of 42 ERα-negative breast carcinomas. It may be partly explained that Efp expression was induced by a low or undetectable level of ERα in these cases. However, Ikeda et al. (14) analyzed human 5′-flanking region of human Efp gene, and reported the possible regulation of Efp promoter by multiple elements and/or interacting factors. Therefore, other factors rather than ERα may be also involved in the expression of Efp in some breast carcinomas.

In our study, Efp immunoreactivity was significantly associated with an increased risk of recurrence or worse prognosis (P < 0.0001, respectively). Both univariate and multivariate analyses have shown that Efp immunoreactivity was a potent prognostic factor for both recurrence and overall survival in breast carcinomas, and that the effect is similar to that of lymph node status, a well-established diagnostic modality (15). Efp knockout mice showed a smaller increase in uterine weight and a lower cell cycle progression from G_0/G_1 to S phase compared with the wild-type (7), suggesting a pivotal role of Efp in ERα-induced cell growth in the uterus. In addition, Urano et al. (8) showed that overexpression of Efp caused tumor cell growth in MCF7 breast cancer cells. Therefore, taken together with these previous reports and our present results, it is suggested that Efp

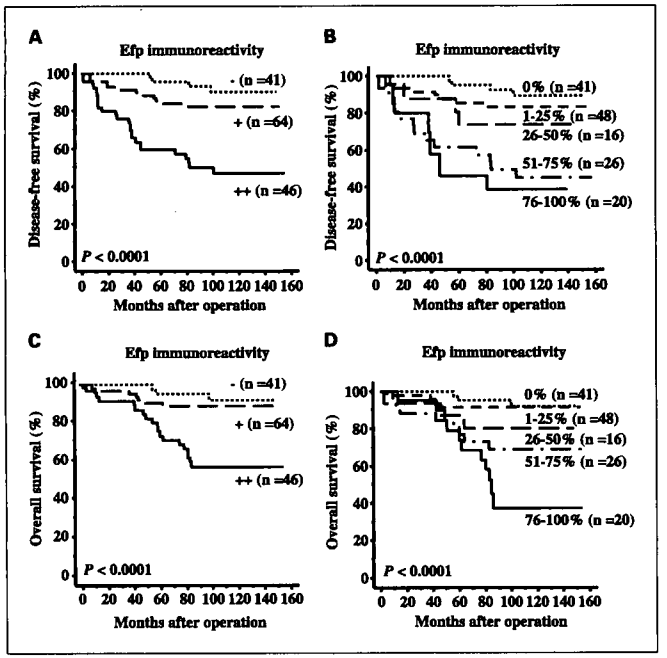

Fig. 3. Disease-free (*A* and *B*) and overall (*C* and *D*) survival of 151 patients with breast carcinoma according to Efp immunoreactivity (Kaplan-Meier method). *A*, Efp immunoreactivity was significantly ($P < 0.0001$, log-rank test) associated with an increased risk of recurrence. *B*, association between Efp immunoreactivity and increased risk of recurrence was also detected in increased rankings of positivity for Efp immunoreactivity into five groups (0%, 1-25%, 26-50%, 51-75%, and 76-100% positive cells). *C* and *D*, Efp immunoreactivity was significantly ($P < 0.0001$, log-rank test) associated with worse overall survival when Efp immunoreactivity was classified into three (*C*) or five (*D*) groups.

plays an important role in the proliferation of breast carcinoma cells. It is well known that biologically active estrogen, estradiol, is locally produced in breast carcinoma tissues from circulating inactive steroids, and acts on these cells via ERα (16). Therefore, residual cancer cells following surgical treatment in Efp-positive breast carcinomas may grow rapidly in the presence of local estrogens, thereby resulting in an increased recurrence and poor prognosis in these patients.

14-3-3σ induces G_2 arrest and inhibits the progression of cell cycle (17) by sequestering the mitotic initiation complex Cdc2-cyclin B1 in the cytoplasm, blocking nuclear entry (18). Expression of 14-3-3σ was examined by several groups in breast carcinoma tissues. However, results of these studies seem to be inconsistent. Ferguson et al. (19) reported that 14-3-3σ mRNA was detected only in 3 of 48 (6.3%) breast carcinoma tissues by Northern blot analysis. Ferguson et al. (19) and Umbricht et al. (20) showed hypermethylation of CpG islands in the 14-3-3σ gene in more than 90% of breast carcinomas, and postulated that loss of 14-3-3σ expression was an early event in neoplastic transformation of the breast. Simooka et al.

Table 2. Univariate and multivariate analyses of disease-free survival in 151 breast cancer patients examined

Variable	Univariate	Multivariate	
	P	*P*	Relative risk (95% CI)
Lymph node status (positive/negative)	<0.0001*	<0.0001	6.053 (2.549-14.379)
Efp immunoreactivity (++/+, –)	<0.0001*	0.0011	3.090 (1.572-6.073)
Tumor size (≥20 mm/<20 mm)	0.0019*	0.0349	3.157 (1.085-9.184)
14-3-3α immunoreactivity (negative/positive)	0.0314*	0.0681	
Ki-67 LI (≤10/<10)	0.1149		
ERα status (positive/negative)	0.1392		
Histologic grade (3/1, 2)	0.2362		
p53 status (positive/negative)	0.4094		

*Data were considered significant in the univariate analyses and were examined in the multivariate analyses.

Table 3. Univariate and multivariate analyses of overall survival in 151 breast cancer patients examined

Variable	Univariate	Multivariate	
	P	*P*	Relative risk (95% CI)
Efp immunoreactivity (++/+, –)	<0.0001*	0.0030	5.343 (1.725-16.175)
Lymph node status (positive/negative)	<0.0001*	0.0065	7.783 (1.773-34.166)
Tumor size (≥20 mm/<20 mm)	0.0084*	0.1514	
p53 status (positive/negative)	0.0230*	0.0832	
ERα status (positive/negative)	0.2890		
Ki-67 LI (≥10/<10)	0.3562		
Histologic grade (3/1, 2)	0.3827		
14-3-3α immunoreactivity (negative/positive)	0.6286		

*Data were considered significant in the univariate analysis and were examined in the multivariate analyses.

(21) detected 14-3-3σ immunoreactivity in 23% of invasive ductal carcinomas and reported that loss of 14-3-3σ expression was relatively low compared with the methylation status of 14-3-3σ gene in breast carcinoma previously reported. On the other hand, Urano et al. (8) showed that 14-3-3σ is a primary target for proteolysis by Efp, and 14-3-3σ protein was regulated by Efp-mediated posttranslational modification. However, Moreira et al. (22) recently reported that expression level of 14-3-3σ was similar in nonmalignant breast epithelial tissue and matched malignant tissue with only sporadic loss of expression observed in 3 of the 68 (4.4%) tumors examined. The lack of expression of 14-3-3σ in the three breast carcinomas was not associated with increased expression of Efp, and they suggested that loss of expression of 14-3-3σ protein was a sporadic event in the breast carcinoma (22). In our present study, immunoreactivity of 14-3-3σ was detected in 58 of 151 (38.4%) breast carcinomas, and was inversely associated with Efp immunoreactivity. These results seem to support the down-regulation of

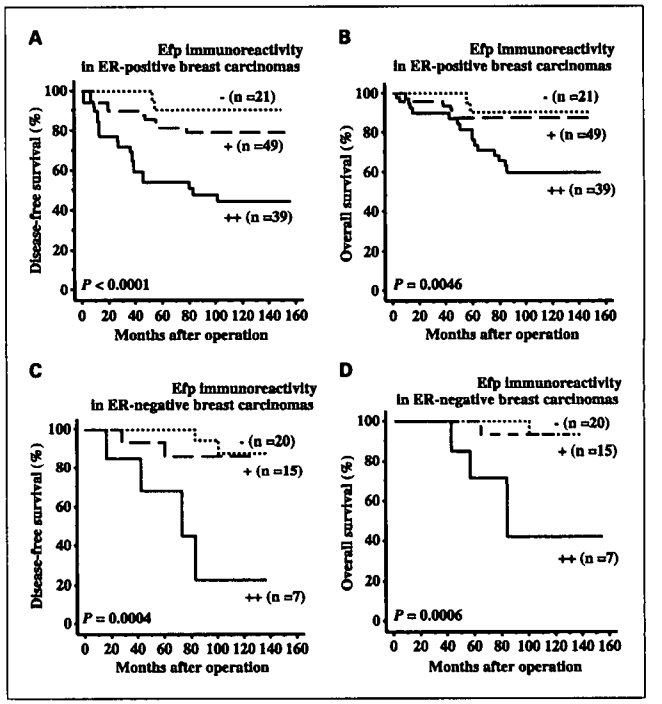

Fig. 4. Association between Efp immunoreactivity and disease-free (*A* and *C*) or overall (*B* and *D*) survival of 151 patients according to ERα status (Kaplan-Meier method). Efp immunoreactivity was significantly associated with poor clinical outcome of 151 breast cancer patients regardless of ERα status. Statistical association was evaluated by log-rank test.

14-3-3σ by methylation of the gene and/or proteolysis by Efp in breast carcinoma tissues; however, these are not necessarily consistent with the findings by Moreira et al. (22). Further examinations, including validation of the immunohistochemical results by another laboratories, are required to clarify the expression of 14-3-3σ in breast carcinoma tissues.

In summary, Efp immunoreactivity was detected in carcinoma cells in 72.8% of breast cancer tissues, and it was associated with the mRNA level. Efp immunoreactivity was significantly associated with lymph node status or ERα status, and was inversely correlated with histologic grade or 14-3-3σ immunoreactivity. Moreover, Efp immunoreactivity was significantly associated with poor clinical outcome of the patients. These present results suggest that Efp is mainly involved in the estrogen-dependent growth of breast carcinomas, and Efp immunoreactivity is a potent prognostic factor in breast carcinoma patients.

Acknowledgments

We appreciate the skillful technical assistance of Dr. Yasuhiro Miki (Department of Pathology, Tohoku University School of Medicine, Sendai, Japan) and Toshiki Hishinuma (Saitama Medical School, Hidaka, Japan). We thank Dr. Bruce Blumberg (Department of Developmental and Cell Biology, University of California, Irvine, CA) for critical reading and comments on the manuscript.

References

1. Ali S, Coombes RC. Endocrine-responsive breast cancer and strategies for combating resistance. Nat Rev Cancer 2002;2:101–12.
2. Jordan VC. Fourteenth Gaddum Memorial Lecture. A current view of tamoxifen for the treatment and prevention of breast cancer. Br J Pharmacol 1993;110: 507–17.
3. Inoue S, Orimo A, Hosoi T, et al. Genomic binding-site cloning reveals an estrogen-responsive gene that encodes a RING finger protein. Proc Natl Acad Sci U S A 1993;90:11117–21.
4. Orimo A, Inoue S, Ikeda K, Noji S, Muramatsu M. Molecular cloning, structure, and expression of mouse estrogen-responsive finger protein Efp. Co-localization with estrogen receptor mRNA in target organs. J Biol Chem 1995;270:24406–13.
5. Ikeda K, Orimo A, Higashi Y, Muramatsu M, Inoue S. Efp as a primary estrogen-responsive gene in human breast cancer. FEBS Lett 2000;472:9–13.
6. Muramatsu M, Inoue S. Estrogen receptors: how do they control reproductive and nonreproductive functions? Biochem Biophys Res Commun 2000; 270:1–10.
7. Orimo A, Inoue S, Minowa O, et al. Underdeveloped uterus and reduced estrogen responsiveness in mice with disruption of the estrogen-responsive finger protein gene, which is a direct target of estrogen receptor α. Proc Natl Acad Sci U S A 1999;96:12027–32.
8. Urano T, Saito T, Tsukui T, et al. Efp targets 14-3-3σ for proteolysis and promotes breast tumour growth. Nature 2002;417:871–5.
9. Thomson SD, Ali S, Pickles L, et al. Analysis of estrogen-responsive finger protein expression in benign and malignant human breast. Int J Cancer 2001;91: 152–8.
10. Suzuki T, Nakata T, Miki Y, et al. Estrogen sulfotransferase and steroid sulfatase in human breast carcinoma. Cancer Res 2003;63:2762–70.
11. Allred DC, Harvey JM, Berardo M, Clark GM. Prognostic and predictive factors in breast cancer by immunohistochemical analysis. Mod Pathol 1998;11:155–68.
12. Emmert-Buck MR, Bonner RF, Smith PD, et al. Laser capture microdissection. Science 1996;274: 998–1001.
13. Niino YS, Irie T, Takaishi M, et al. PKCθ II, a new isoform of protein kinase C specifically expressed in the seminiferous tubules of mouse testis. J Biol Chem 2001;276:36711–7.
14. Ikeda K, Inoue S, Orimo A, et al. Multiple regulatory elements and binding proteins of the 5′-flanking region of the human estrogen-responsive finger protein (efp) gene. Biochem Biophys Res Commun 1997;236: 765–71.
15. Dowlatshahi K, Fan M, Snider HC, Habib FA. Lymph node micrometastases from breast carcinoma: reviewing the dilemma. Cancer 1997;80:1188–97.
16. Suzuki T, Moriya T, Ishida T, Ohuchi N, Sasano H. Intracrine mechanism of estrogen synthesis in breast cancer. Biomed Pharmacother 2003;57: 460–2.
17. Hermeking H, Lengauer C, Polyak K, et al. 14-3-3σ is a p53-regulated inhibitor of G_2/M progression. Mol Cell 1997;1:3–11.
18. Chan TA, Hermeking H, Lengauer C, Kinzler KW, Vogelstein B. 14-3-3σ is required to prevent mitotic catastrophe after DNA damage. Nature 1999;401: 616–20.
19. Ferguson AT, Evron E, Umbricht CB, et al. High frequency of hypermethylation at the 14-3-3σ locus leads to gene silencing in breast cancer. Proc Natl Acad Sci U S A 2000;97:6049–54.
20. Umbricht CB, Evron E, Gabrielson E, Ferguson A, Marks J, Sukumar S. Hypermethylation of 14-3-3σ (stratifin) is an early event in breast cancer. Oncogene 2001;20:3348–53.
21. Simooka H, Oyama T, Sano T, Horiguchi J, Nakajima T. Immunohistochemical analysis of 14-3-3σ and related proteins in hyperplastic and neoplastic breast lesions, with particular reference to early carcinogenesis. Pathol Int 2004;54:595–602.
22. Moreira JM, Ohlsson G, Rank FE, Celis JE. Down-regulation of the tumor suppressor protein 14-3-3σ is a sporadic event in cancer of the breast. Mol Cell Proteomics 2005;4:555–69.

J Hum Genet (2005) 50:235–240
DOI 10.1007/s10038-005-0244-x

ORIGINAL ARTICLE

Yoshihiro Sudo · Yoichi Ezura · Mitsuko Kajita
Hideyo Yoshida · Takao Suzuki · Takayuki Hosoi
Satoshi Inoue · Masataka Shiraki · Hiromoto Ito
Mitsuru Emi

Association of single nucleotide polymorphisms in the promoter region of the pro-opiomelanocortin gene (*POMC*) with low bone mineral density in adult women

Received: 10 December 2004 / Accepted: 23 February 2005 / Published online: 29 April 2005

Abstract Among multiple factors influencing osteoporosis, genetic variations involved in bone-mineral metabolism can affect risks predisposing to the disease onset. Here, we studied single-nucleotide polymorphisms (SNPs) in the pro-opiomelanocortin (*POMC*) gene for possible association with bone mineral density (BMD) among 384 adult Japanese women and observed significant correlation between adjusted BMD and three SNPs in the promoter region ($r > 0.14$, $p < 0.01$). The most significant correlation was observed for −2353G/A ($r = -0.16$, $p = 0.002$); homozygous carriers of the major (G) allele had the highest BMD (0.405 ± 0.054 g/cm^2) while heterozygous carriers were intermediate (0.390 ± 0.053 g/cm^2) and homozygous A-allele carriers had the lowest BMDs (0.369 ± 0.048 g/cm^2). Although no association was detected between these SNPs and body weight or body mass index (BMI), significant association was detected between the −2313A/C genotype and plasma total cholesterol level ($r = -0.12$, $p = 0.019$). We propose that *POMC* is among the likely susceptibility genes for osteoporosis and may also be involved in dyslipidemia.

Keywords Single nucleotide polymorphism · Pro-opiomelanocortin (POMC) · Bone mineral density · Association study · Osteoporosis

Y. Sudo · Y. Ezura · M. Kajita · M. Emi
Department of Molecular Biology,
Institute of Gerontology,
Nippon Medical School Kawasaki,
Kanagawa, Japan

Y. Sudo · H. Ito
Department of Orthopaedics,
Nippon Medical School,
Tokyo, Japan

H. Yoshida · T. Suzuki
Epidemiology and Health Promotion Research Group,
Tokyo Metropolitan Institute of Gerontology,
Tokyo, Japan

T. Hosoi
Department of Endocrinology,
Tokyo Metropolitan Geriatric Hospital,
Tokyo, Japan

S. Inoue
Department of Geriatric Medicine,
Faculty of Medicine,
University of Tokyo,
Tokyo, Japan

M. Shiraki
Research Institute and Practice for Involutional Diseases,
Nagano, Japan

Present address: Y. Ezura (✉)
Department of Molecular Pharmacology
Institute of Medical Research,
Tokyo Medical and Dental University,
2-3-10 Kanda-Surugadai,
Chiyoda-ku, Tokyo 101-0062, Japan
E-mail: ezura.mph@mri.tmd.ac.jp
Tel.: +81-3-52808067
Fax: +81-3-52808067

Introduction

Osteoporosis, one of the most prevalent disease conditions in older age groups, is pathologically defined by low bone mineral density (BMD) and deterioration of bone structure (Riggs and Melton 1986; Kanis et al. 1994). Like many other common diseases, multiple factors, including genetic variations, determine predisposition for onset or progression of osteoporosis, as has been indicated by genetic-epidemiological studies (Peacock et al. 2002; Albagha and Ralston 2003). Numerous studies on genetic risks for osteoporosis have been investigated to date, mainly by association studies and linkage analysis for quantitative trait BMD (Liu et al. 2003).

Among those studies, a quantitative trait locus (QTL) for spinal BMD has been identified in the chromosomal region 2p23–24 in large Caucasian pedigrees (Devote

et al. 1998). An independent study for distal forearm BMD in Chinese (Niu et al. 1999) detected contribution of similar locus (2p23.3) expanding about 18-Mbp, which completely overlaps the formerly detected locus (about 5-Mbp; markers from D2S149 to D2S387). In the later study, several candidates, including the pro-opiomelanocortin gene (*POMC*), were proposed; however, no responsible variations have been identified as yet.

An important aspect of BMD regulation is conducted through immunological responses to inflammatory events, presumably through activation of osteoclastogenesis (Manolagas 1995; Rodan and Martin 2000). In addition to complex cytokine pathways for which the most attention have been paid, regulation through endocrine systems, notably hormonal regulation of adrenal corticoids, is important, as indicated by clinical knowledge of glucocorticoid-induced osteoporosis (Patschan et al. 2001). Moreover, higher hierarchical regulation of systemic corticoid levels, i.e., hypothalamus–pituitary–adrenal axis (HPA-axis), may have critical effects on homeostatic regulation of the immune system. Thus, genes involved in this system, such as *POMC*, should be considered for the association study.

POMC is a large precursor protein for multiple functional peptide hormones, including adrenocorticotrophic hormone (ACTH), melanocyte-stimulating hormones (alpha-MSH, beta-MSH, and gamma-MSH), and beta-endorphin. In addition to classical knowledge of influences on serum corticoid levels or on metabolic control of energy expenditure and body mass (Pritchard et al. 2002; Appleyard et al. 2003), direct and indirect effects of these peptides on the immune system have been clarified recently (Luger et al. 2003). Here, in this study, we investigated the eight single nucleotide polymorphisms (SNPs) of the *POMC* as good candidates for testing association between the genotypes and bone phenotype. In addition, to evaluate the effects on other metabolic systems, we investigated the association of body mass index (BMI) and serum cholesterol levels to the genotypes among 384 adult Japanese women.

Materials and methods

Subjects

DNA samples were obtained from peripheral blood of 384 adult Japanese women (Ishida et al. 2003; Iwasaki et al. 2003). All were nonrelated volunteers who gave informed consent prior to the study. No participant had medical complications or was undergoing treatment for conditions known to affect bone and lipid metabolism, such as pituitary diseases, hyperthyroidism, primary hyperparathyroidism, liver disease, renal failure, adrenal diseases, or rheumatic diseases, and none was receiving estrogen replacement therapy. Physical and clinical profiles of the subjects, including age, body weight, height, BMD, plasma total cholesterol (T-chol), triglycerides, and high-density lipoprotein cholesterol (HDL-C) levels were obtained from the records of a health-check screening program. Mean values and standard deviations (SD) were 58.4 ± 8.6 (range 32–69) years for age, and 23.7 ± 3.61 kg/m^2 (range 14.7–38.5) for BMI. The areal BMD (expressed in grams per centimeter squared) of the distal radius, measured by dual energy X-ray absorptiometry (DXA) using DTX-200 (Osteometer Meditech Inc., Hawthorne, CA, USA) showed normal distribution (0.399 ± 0.054 g/cm^2; range 0.225–0.554). Among 384 subjects, we regarded 64 individuals as low-bone-mass subjects whose adjusted BMD distributed below 0.38 (mean adjusted BMD − 1SD) and 55 individuals as high-bone-mass subjects whose adjusted BMD was above 0.48 (mean adjusted BMD + 1SD). Plasma lipid and lipoprotein concentrations were measured from peripheral blood collected after 12–16 h of fasting by procedures described previously (Hattori et al. 2002). All measured values were within the normal range (T-chol: 187.0 ± 32.2 mg/dl, triglycerides: 85.5 ± 59.8 mg/dl, HDL-C: 59.1 ± 12.2 mg/dl).

Genotyping for molecular variants in the *POMC* gene

Eight SNPs (Table 1) from the NCBI database (dbSNP) or the Celera database (Celera Diagnostics, Rockville, MD, USA) were selected and denoted as −2353G/A, −2345G/A, −2313A/C, −1845C/T, IVS1 + 267C/G, IVS2 + 276C/G, A132P (c.396G/C), and c.585T/C (195-Ala) according to their positions in a contig-sequence (NT_022184.13; NCBI RefSeq database) (Fig. 1a). All were confirmed to be polymorphic in our test population ($n = 24$), and thus, the 384 subjects were genotyped either by cycle sequencing, TaqMan Assay (Livak 1999), or Invader assay (Mein et al. 2000) (Table 1).

For five SNPs (−2353G/A, −2313A/C, −2345G/A, −1845C/T, and A132P), cycle sequencing was carried out using the BigDye terminator v1.1 Cycle Sequencing Kit (Applied Biosystems, Foster City, CA, USA) and the ABI PRISM 377 DNA Sequencing System (Applied Biosystems). The following primers were used: F-1, 5′-ACTCTTTCAAGCAGATGGTGGT-3′ and R-1, 5′-AGCAGGTTCTGCTGCATTAAA-3′ (for SNP −1845C/T); F-2, 5′-AAGGCCATTGAACTGCATTTAG-3′ and R-2, 5′-GTCTATGTCAGACGCCTGTGGT-3′ (for −2353G/A, −2313A/C and −2345G/A); and F-3, 5′-AACCCCCGGAAGTACGTCAT-3′ and R-3, 5′-GAAGTGCTCCATCCTGTAGGG-3′ (for A132P). TaqMan assay was carried out for IVS2 + 4229C/G and c.585T/C, according to the manufacturers' protocol (TaqMan Assays-on-Demand; Applied Biosystems). Invader assay was carried out for IVS1 + 352C/G according to the manufacturers' protocol (Invader Assay: Third Wave Technologies, inc, Madison City, WI, USA) and the methods described previously (Ezura et al. 2003).

Table 1 Summary of polymorphisms examined at the *POMC* locus

SNP name[a]	dbSNP-ID[b]	Celera-ID[c]	Allele frequency	% heterozygosity
−2353G/A	rs3754863		0.81:0.19	32
−2345G/A	rs3754862		0.81:0.19	32
−2313A/C	rs3754861		0.79:0.21	28
−1845C/T	rs3754860		0.74:0.26	38
IVS1 + 267C/G	rs1009388		0.98:0.02	5
IVS2 + 276C/G	–	hCV3227244	0.68:0.32	39
A132P	rs8192606		0.99:0.01	1
c.585T/G	rs2071345		0.72:0.28	40

[a] Location of the SNP was defined by NT_023195.12 from the NCBI RefSeq database
[b] Identity number for NCBI dbSNP database
[c] Identity number for Celera database

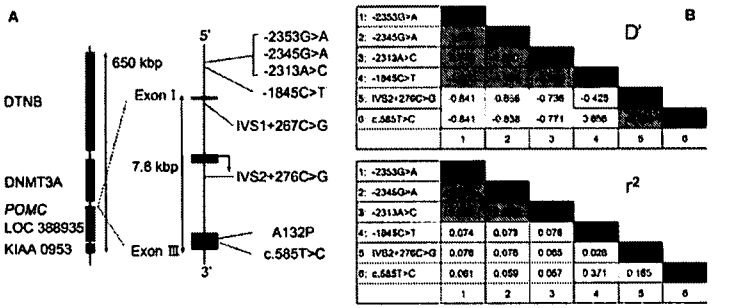

Fig. 1 Analysis of the linkage disequilibrium within the *POMC* locus. **a** Schematic diagram of the *POMC* gene showing positions of the eight examined SNPs. **b** Indices of LD, D' and r^2 were calculated on the basis of 17 estimated haplotypes (covering 100% of the chromosomes) constructed with six SNPs. Cells are highlighted with *gray* halftone when the D' values are greater than 0.4 or the r^2 values are greater than 0.1

Statistical analysis

Adjusted values of BMD were obtained after normalizing the measured data with age and BMI by means of multiple regression analysis, as described previously (Iwasaki et al. 2003). Plasma lipids and lipoprotein concentrations were adjusted by reference to an age group (40–49 years) among standard data from 11,994 individuals in a 2001 cohort study for the Japanese population, using a *Z*-score calculation (Fujita et al. 2003).

The three genotypic categories of each SNP were converted into incremental values 0, 1, and 2, corresponding to the number of chromosomes possessing a minor allele, and quantitative association with several physical and clinical values was analyzed via one-way analysis of variance (ANOVA) with linear regression analysis as a post hoc test. The statistical significance of any correlation was accepted when the given p values of the ANOVA F test were less than 5% ($p < 0.05$). To test the existence of dominant or recessive effects of minor allele of each SNP, Student's t test was applied to compare two divided subject groups by possession of minor allele or major allele ($p < 0.05$). Distribution analysis of contingency tables were applied for low-bone-mass ($n = 64$) or high-bone-mass individuals ($n = 55$). Chi-square test for trend was applied ($p < 0.05$). Hardy–Weinberg equilibrium among genotypes was ascertained by the chi-square test. A maximum-likelihood haplotype was estimated by the EM algorithm using Arlequin software (Genetics and Biometry Laboratory, Geneva, Switzerland) (Schneider et al. 2000), and indices of linkage disequilibrium (LD) were calculated.

Results

Eight SNPs in the *POMC* gene, one of the likely candidates for osteoporosis susceptibility, were examined in all 384 subjects. Allelic frequencies and genotypic frequencies were clarified and showed no deviation from Hardy–Weinberg equilibrium (Table 1). By excluding the data from two rare SNPs (IVS1 + 352C/G and A132P), we estimated haplotype frequencies from available genotypic data for the other six SNPs. The LD analysis, evaluated by D' and r^2 for every combination of SNPs, indicated apparent LD within the locus (Fig. 1b). Especially strong LD was detected among −2353G/A, −2345G/A, and −2313A/C ($D' > 0.97$, $r^2 > 0.85$).

By examining a correlation between SNP genotype and adjusted BMD for each of the eight SNPs (Table 2), significant correlation was evident with three promoter SNPs (−2353G/A, −2345G/A, and −2313A/C). For the most significant −2353G/A ($r = -0.16$, $p = 0.0020$), codominant BMD lowering effect of the minor A-allele was indicated where homozygous carriers of G-alleles had the highest values (0.405 ± 0.054 g/cm^2), heterozygous individuals were intermediate (0.390 ± 0.053 g/cm^2), and homozygous A-allele carriers had the lowest adjusted BMDs (0.369 ± 0.048 g/cm^2) (Fig. 2a). Dominant or codominant effect was supported by analyzing the differences between two genotypically divided groups based on dominant model (A-allele carriers: $n = 132$, adj-BMD = 0.388 ± 0.053; and noncarriers: $n = 242$, adj-BMD = 0.405 ± 0.054, $p = 0.004$, Student's t test) and recessive model (G-allele carriers: $n = 365$, adj-BMD = 0.400 ± 0.054; and noncarriers: $n = 9$,

Table 2 Summary of the regression analysis of *POMC* variations among 384 subjects. *BMD* bone mineral density

SNP name	Number[a]	Major homo (*n*)	Hetero (*n*)	Minor homo (*n*)	Correlation coefficient	*p* value
		Adjusted BMD (g/cm^2)				
−2353G/A	374	0.405 ± 0.054 (242)	0.390 ± 0.053 (123)	0.369 ± 0.048 (9)	−0.16	0.002
−2345G/A	374	0.404 ± 0.055 (244)	0.391 ± 0.052 (121)	0.369 ± 0.048 (9)	−0.14	0.005
−2313A/C	374	0.404 ± 0.055 (244)	0.392 ± 0.052 (106)	0.376 ± 0.051 (24)	−0.15	0.004
−1845C/T	375	0.397 ± 0.052 (206)	0.402 ± 0.057 (143)	0.403 ± 0.055 (26)	0.05	0.35
IVS1 + 267C/G	329	0.401 ± 0.056 (314)	0.376 ± 0.050 (15)	(−)	0.09	0.09
IVS2 + 276C/G	376	0.401 ± 0.057 (184)	0.398 ± 0.051 (145)	0.401 ± 0.056 (47)	−0.02	0.76
A132P	373	0.399 ± 0.055 (367)	0.425 ± 0.038 (4)	(−)	0.05	0.35
c.585T/G	377	0.397 ± 0.054 (195)	0.401 ± 0.054 (151)	0.409 ± 0.063 (31)	0.06	0.28
		Adjusted total cholesterol (mg/dl)				
−2353G/A	374	189.4 ± 34.0 (242)	183.2 ± 27.9 (123)	174.9 ± 16.7 (9)	−0.11	0.036
−2345G/A	374	189.6 ± 34.0 (244)	182.7 ± 27.8 (121)	174.9 ± 16.7 (9)	−0.12	0.024
−2313A/C	374	189.6 ± 34.0 (244)	183.4 ± 27.1 (106)	176.7 ± 27.3 (24)	−0.12	0.019
−1845C/T	375	186.9 ± 32.1 (206)	186.2 ± 29.8 (143)	195.1 ± 42.7 (26)	0.04	0.479
IVS1 + 267C/G	329	187.3 ± 32.0 (314)	185.7 ± 27.1 (15)	(−)	−0.01	0.848
IVS2 + 276C/G	376	185.0 ± 29.7 (184)	185.1 ± 32.9 (145)	195.8 ± 32.2 (47)	0.08	0.100
A132P	373	186.8 ± 32.2 (367)	192.3 ± 58.1 (4)	(−)	0.02	0.737
c.585T/G	377	186.0 ± 30.2 (195)	187.3 ± 33.4 (151)	187.8 ± 35.3 (31)	0.02	0.683

[a] represents the number of genotyped subjects
[b] *p* values are calculated for the regression analysis with ANOVA *F* test

adj-BMD = 0.369 ± 0.048, $p = 0.09$, Student's *t* test). The other two promoter SNPs also demonstrated allelic-dosage effects (data not shown). By comparing the distribution of genotypically divided subjects among low-bone-mass individuals ($n = 64$; 36, 25, and three individuals for G/G, A/G, and A/A genotypes, respectively) and high-bone-mass individuals ($n = 55$; 43 and 12 individuals for G/G and A/G: no individual for A/A), significant difference with trend was detected ($p = 0.006$), indicating minor A-allele of −2353G/A could be a genetic risk for low-bone-mass trait.

We examined whether these variations correlated with other clinical features (Table 2). The same three promoter SNPs (−2353G/A, −2345G/A, and −2313A/C) demonstrated significant correlation to adjusted T-chol levels (ex; −2313A/C; $r = -0.12$, $p = 0.019$) (Fig. 2b). No significant correlations were detected between other covariates (age, body weight, height, BMI or adjusted plasma HDL-C and triglyceride levels) and any SNPs.

Fig. 2 Effects of *POMC* variations on adjusted bone mineral density (BMD) and total cholesterol (T-chol) in plasma. Adjusted BMD levels were plotted against three genotypically classified subgroups at the −2353G/A SNP site. Adjusted T-chol levels were plotted against genotypically classified subgroups at −2313A/C site. The allelic-dosage effects of these variants on BMD or T-chol were analyzed by linear regression as a post-hoc test of ANOVA. Calculations of *p* values were based on *F* tests. *Open circles* indicate mean values, *error bars* indicate standard deviations

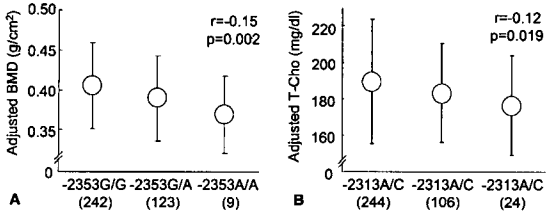

Discussion

In the work reported here, we detected significant association between genotypes of three *POMC* variations (−2353G/A, −2345G/A, and −2313A/C) and adjusted levels of radial BMD among adult Japanese women. In addition, the same promoter SNPs showed an association with plasma T-chol level but not with body mass. These data indicated possible influences of POMC polymorphism(s) on bone-mineral status for the first time, as well as on lipoprotein metabolism.

Association of promoter SNP genotype to low-bone-mass phenotype indicates that the altered level of POMC peptide might affect the bone metabolism. Lowered BMD can result from accelerated bone loss and/or deficient acquisition of bone mass (Riggs and Melton 1986). However, because bone loss caused by systemic corticoid use is thought to occur mainly through resorption (Weinstein et al. 2002, 2004), *POMC* variations would also affect resorptive mechanisms. In addition, anabolic aspect of corticoid function should be considered on the skeletal system through multiple pathways (Patschan et al. 2001). In the feedback system of HPA-axis, multiple cross-talks between the corticotropin releasing hormone, somatostatin growth hormone system, gonadotropin system, and thyroid hormone are known. Longitudinal studies in large cohorts, as well as functional studies, may clarify the molecular events by which SNPs in the *POMC* promoter bring about alterations in bone metabolism. Presumably, these variation(s) affect transcription of the ACTH-precursor peptide, which should affect secretion of ACTH from the anterior pituitary and/or the regulation of other POMC-derived peptide hormones. The consequent effects on bone metabolism might, in turn, introduce variation in BMD in an adult woman. Those assumptions should be validated by additional studies.

As mentioned, *POMC* was selected as a candidate because it is a precursor of ACTH. Although its function on the skeletal system may mainly depend on the catabolic aspect of corticoids, alternative pathways would also contribute, as described. In addition, other POMC-derived peptides, such as MSHs, could be responsible for alterations in bone metabolism. Anti-inflammatory function of alpha-MSH through effects on macrophages has been reported (Star et al. 1995). Also, alpha-MSH and beta-endorphin functioning in body-mass maintenance and in energy expenditure may contribute to bone-mass regulation because a close relationship between these two regulatory systems has been assumed (Reid 2002).

Interrelationship between these clinical phenotypes has been documented: Individuals carrying *POMC* mutations that impair synthesis of ACTH and alpha-MSH were reported to become obese (Krude et al. 1998). In addition, linkage and association of the *POMC* locus were reported for the serum leptin level (Hixson et al. 1999), fasting insulin level (Santoro et al. 2004), and obesity (Delplanque et al. 2000). However, in our test subjects, we detected no significant correlation between the SNP genotype and the indices of obesity; thus, the correlation we observed between BMD and the SNP genotypes was not secondary to altered body mass. Instead, we found an association between variant −2313A/C and adjusted T-chol. Although the detected correlation was weak and reproducibility of this finding or the correlation between the low-density lipoprotein cholesterol (LDL-C) and the genotype was no investigated in our study, the possibility has to be examined in a future study as to whether POMC-derived peptides regulate lipoprotein metabolism through a distinctive mechanism.

Another of our findings, the existence of strong LD among the three significantly BMD-correlated promoter SNPs, may imply an important promoter/enhancer function of the region they share up-stream of the *POMC* coding sequence. In fact, a computer algorithm, MatInspector program v2.2 (Quandt et al. 1995), predicted that two of these three SNPs were part of presumed consensus binding sequences of known transcription factors; i.e., −2345G/A in the acute myeloid leukemia (AML) −1a binding sequence (TGCGGT; underlined "G" is a variant nucleotide) and −2353G/A in the GATA-1 or GATA-2 sequence (CGAGATCGCG; underlined "G" is a variant nucleotide). The functional significance of these *cis* elements and *trans* factors remains to be clarified. Of course, our study does not stipulate specific SNP(s) that functionally regulate BMD. Thus, we cannot rule out the possibility that these polymorphic markers at chromosome 2 (2p23) may themselves be in linkage disequilibrium with other, unmeasured functional variants (see Fig. 1). Functional studies as well as longitudinal studies will be required to find a true mechanistic basis for the associations reported here.

In summary, we have shown a significant association of three variations in the promoter region of the *POMC* gene (−2353G/A, −2345G/A, and −2313A/C) with radial BMD levels among adult Japanese women. An association was also detected between these SNPs and plasma cholesterol levels. Structural inspection proposed that transcription factors AML-1a and GATA-1 or −2 might bind to sequences containing these SNP sites. Detailed investigations involving molecules of the HPA axis may clarify the true mechanism of BMD regulation by *POMC* SNPs.

Acknowledgements We thank Mina Kodaira, Miho Kawagoe, and Naoko Tsuruta for their expert technical assistance. This work was supported by a grant for Strategic Research from the Ministry of Education, Science, Sports and Culture of Japan; by a Research Grant for Research from the Ministry of Health and Welfare of Japan; and by a Research for the Future Program Grant of The Japan Society for the Promotion of Science.

References

Albagha OM, Ralston SH (2003) Genetic determinants of susceptibility to osteoporosis. Endocrinol Metab Clin North Am 32:65–81

Appleyard SM, Hayward M, Young JI, Butler AA, Cone RD, Rubinstein M, Low MJ (2003) A role for the endogenous opioid beta-endorphin in energy homeostasis. Endocrinology 144:1753–1760

Delplanque J, Barat-Houari M, Dina C, Gallina P, Clement K, Guy-Grand B, Vasseur F, Boutin P, Froguel P (2000) Linkage and association studies between the proopiomelanocortin (POMC) gene and obesity in caucasian families. Diabetologia 43:1554–1557

Devote M, Shimoya K, Caminis J, Ott J, Tenenhouse A, Whyte MP, Sereda L, Hall S, Considine E, Williams CJ, Tromp G, Kuivaniemi H, Ala-Kokko L, Proskop DJ, Spotila LD (1998) First-stage autosomal genome screen in extended pedigrees suggests genes predisposing to low bone mineral density on chromosomes 1p, 2p and 4p. Eur J Hum Genet 6:151–157

Ezura Y, Kajita M, Ishida R, Yoshida S, Yoshida H, Suzuki T, Hosoi T, Inoue S, Shiraki M, Orimo H, Emi M (2003) Association of multiple nucleotide variations in the pituitary glutaminyl cyclase gene (QPCT) with low radial BMD in adult women. J Bone Miner Res 19:1296–1301

Fujita Y, Ezura Y, Emi M, Sato K, Takada D, Iino Y, Katayama Y, Takahashi K, Kamimura K, Bujo H, Saito Y (2003) Hypercholesterolemia associated with splice-junction variation of inter-alpha-trypsin inhibitor heavy chain 4 (ITIH4) gene. J Hum Genet 49:24–28

Hattori H, Hirayama T, Nobe Y, Nagano M, Kujiraoka T, Egashira T, Ishii J, Thuji M, Emi M (2002) Eight novel mutations and functional impairments of the LDL receptor. J Hum Genet 47:80–87
Hixson JE, Almasy L, Cole S, Birnbaum S, Mitchell BD, Mahaney MC, Stern MP, MacCluer JW, Blangero J, Comuzzie AG (1999) Normal variation in leptin levels is associated with polymorphisms in the proopiomelanocortin gene, POMC. J Clin Endocrinol Metab 84:3187–3191
Ishida R, Ezura Y, Emi M, Kajita M, Yoshida H, Suzuki T, Hosoi T, Inoue S, Shiraki M, Ito H, Orimo H (2003) Association of a promoter haplotype (−1542G/−525C) in the tumor necrosis factor receptor associated factor-interacting protein gene with low bone mineral density in Japanese women. Bone 33:237–241
Iwasaki H, Emi M, Ezura Y, Ishida R, Suzuki T, Hosoi T, Inoue S, Shiraki M, Swensen J, Orimo H (2003) Association of a Trp16Ser variation in the gonadotropin releasing hormone signal peptide with bone mineral density, revealed by SNP-dependent PCR typing. Bone 32:185–190
Kanis JA, Melton LJ, Christiansen C, Johnston CC, Khaltaev N (1994) The diagnosis of osteoporosis. J Bone Miner Res 9:1137–1141
Krude H, Biebermann H, Luck W, Horn R, Brabant G, Gruters A (1998) Severe early-onset obesity, adrenal insufficiency and red hair pigmentation caused by POMC mutations in humans. Nat Genet 19:155–157
Liu YZ, Liu YJ, Robert RR, Deng HW (2003) Molecular studies of identification of genes for osteoporosis: the 2002 update. Endocrinology 177:147–196
Livak KJ (1999) Allelic discrimination using fluorogenic probes and the 5′ nuclease assay. Genet Anal 14:143–149
Luger TA, Scholzen TE, Brzoska T, Bohm M (2003) New insights into the functions of alpha-MSH and related peptides in the immune system. Ann NY Acad Sci 994:133–140
Manolagas SC (1995) Role of cytokines in bone resorption. Bone 17:63–67
Mein CA, Barratt BJ, Dunn MG, Siegmund T, Smith AN, Esposito L, Nutland S, Stevens HE, Wilson AJ, Phillips MS, Jarvis N, Law S, de Arruda M, Todd JA (2000) Evaluation of single nucleotide polymorphism typing with invader on PCR amplicons and its automation. Genome Res 10:330–343
Niu T, Chen C, Cordell H, Yang J, Wang B, Wang Z, Fang Z, Nicholas JS, Clifford JR, Xu X (1999) A genome-wide scan for loci linked to forearm bone mineral density. Hum Genet 104:226–233
Patschan D, Loddenkemper K, Buttgereit F (2001) Molecular mechanisms of glucocorticoid-induced osteoporosis. Bone 29:498–505
Peacock M, Turner CH, Econs MJ, Foroud T (2002) Genetics of osteoporosis. Endocrinol Rev 23:303–326
Pritchard LE, Turnbull AV, White A (2002) Pro-opiomelanocortin processing in the hypothalamus: impact on melanocortin signaling and obesity. J Endocrinol 172:411–421
Quandt K, Frech K, Karas H, Wingender E, Werner T (1995) MatInd and MatInspector: new fast and versatile tools for detection of consensus matches in nucleotide sequence data. Nucleic Acids Res 23:4878–4884
Reid IR (2002) Relationships among body mass, its components, and bone. Bone 31:547–555
Riggs BL, Melton LJ III (1986) Involutional osteoporosis. N Engl J Med 314:1676–1686
Rodan GA, Martin TJ (2000) Therapeutic approaches to bone diseases. Science 289:1508–1514
Santoro N, del Giudice EM, Cirillo G, Raimondo P, Corsi I, Amato A, Grandone A, Perrone L (2004) An insertional polymorphism of the proopiomelanocortin gene is associated with fasting insulin levels in childhood obesity. J Clin Endocrinol Metab 89:4846–4849
Schneider S, Roessli D, Excoffier L (2000) Arlequin ver. 2.000: a software for population genetics data analysis. Genetics and Biometry Laboratory, University of Geneva, Geneva, Switzerland
Star RA, Rajora N, Huang J, Stock RC, Catania A, Lipton JM (1995) Evidence of autocrine modulation of macrophage nitric oxide synthase by alpha-melanocyte-stimulating hormone. Proc Natl Acad Sci USA 92:8016–8020
Weinstein RS, Chen JR, Powers CC (2002) Inhibition of osteoblastogenesis and promotion of apoptosis of osteoblasts and osteocytes by glucocorticoids. J Clin Invest 109:1041–1048
Weinstein RS, Jia D, Powers CC, Stewart SA, Jilka RL, Parfitt AM, Manolagas SC (2004) The skeletal effects of glucocorticoid excess override those of orchidectomy in mice. Endocrinology 145:1980–1987

Available online at www.sciencedirect.com
SCIENCE DIRECT
Gynecologic Oncology 99 (2005) 664 – 670
Gynecologic Oncology
www.elsevier.com/locate/ygyno

Expression of estrogen-responsive finger protein (Efp) is associated with advanced disease in human epithelial ovarian cancer

Michiko Sakuma[a,*], Jun-ichi Akahira[a,b], Takashi Suzuki[b], Satoshi Inoue[c], Kiyoshi Ito[a], Takuya Moriya[b], Hironobu Sasano[b], Kunihiro Okamura[a], Nobuo Yaegashi[a]

[a]*Department of Obstetrics and Gynecology, Tohoku University Graduate School of Medicine, 1-1 Seiryo-machi, Aoba-ku, Sendai 980-8574, Japan*
[b]*Department of Pathology, Tohoku University Graduate, School of Medicine, Sendai, Japan*
[c]*Division of Gene Regulation and Signal Transduction, Research Center for Genomic Medicine, Saitama Medical School, Saitama, Japan*

Received 28 March 2005
Available online 2 September 2005

Abstract

Objective. The estrogen-responsive ring finger protein (Efp) gene, one of estrogen receptor (ER) target genes, is considered to be essential for estrogen-dependent cell proliferation. To understand the estrogenic action on ovarian cancer, we studied the relationships between Efp and ERs expressions and the correlations of Efp expression with clinicopathological parameters in epithelial ovarian cancer.

Methods. The protein expressions for Efp, ERα and ERβ were examined by immunoblotting in 12 ovarian cancer cell lines. Efp mRNA expressions were evaluated by quantitative RT-PCR in 12 ovarian cancer cell lines. A total of 100 surgical specimens diagnosed as epithelial ovarian cancer were examined immunohistochemically using antibodies for Efp, ERα and ERβ.

Results. Efp protein was detected in 8 out of 12 cell lines. In Efp protein-positive cell lines, Efp mRNA was expressed higher than that in negative ($P = 0.021$). All of the Efp protein-positive cell lines simultaneously expressed either ERα or ERβ protein. By immunohistochemical staining, Efp immunoreactivity was detected in 63 out of 100 ovarian cancer specimens and positive signals were in the cytoplasm of carcinoma cells. There were significant correlations between Efp and ERα, ERβ immunoreactivity (Efp and ERα, $P = 0.022$; Efp and ERβ, $P = 0.032$). Efp expression was significantly higher in a subgroup with serous adenocarcinoma ($P = 0.010$) and with advanced disease ($P = 0.026$). No significant relationship was detected between Efp immunoreactivity and overall survival.

Conclusion. The expression of Efp was detected in human epithelial ovarian cancer and high expression of Efp was correlated with advanced disease and serous adenocarcinoma, and ERs status.

Keywords: Efp; Ovarian cancer; Immunohistochemistry; Estrogen receptor

Introduction

Estrogen and progesterone are sex steroid hormones that are secreted from the ovary and cause the development of the female sex organs. They are also recognized as a significant modifier of the growth, development, invasion and metastasis of gynecological cancers. The actions of estrogen are mediated through specific ligand receptors. There are two receptor subtypes for estrogen, estrogen receptor-α (ERα) and estrogen receptor-β (ERβ) [1,2]. It is assumed that these receptors, members of the steroid/thyroid hormone receptor superfamily mediate these actions by binding ligand dependently to the estrogen-responsive element (ERE) that is located in the promoter region of target genes, thus directly regulating their transcription [3,4]. A variety of estrogenic functions are characterized by the expression of the estrogen-responsive genes following the binding of receptor protein to EREs [5,6].

Estrogen-responsive finger protein (Efp) is a member of the Ring-finger B-box Coiled-Coil family that is thought to be involved in the regulation of various celluer functions, including cell-cycle regulation and gene transcription [5,7].

* Corresponding author. Fax: +81 22 717 7258.
E-mail address: msakuma@mail.tains.tohoku.ac.jp (M. Sakuma).

0090-8258/$ - see front matter © 2005 Elsevier Inc. All rights reserved.
doi:10.1016/j.ygyno.2005.07.103

Efp has been isolated from human genomic DNA binding-site cloning using a recombinant ER protein [5]. Efp gene has an estrogen-responsive element (ERE) in an exon corresponding with the 3′-untranslated region of mRNA [5,8]. Efp is widely expressed in various organs and structures such as the genital tracts, thyroid gland, aorta, spleen, kidney and brain [9]. Estrogen-induced Efp expression is found in the uterus, brain and mammary gland cells [5,8], and its expression is co-localized with ER [9]. A study of knock-out mice has revealed that Efp is essential for cell growth mediated by estrogen in the uterus [6], suggesting that Efp is essential for estrogen mediated cell growth.

Efp expression in the context of cancer has been studied predominantly in breast cancer. Efp mRNA was detected in the MCF-7 human breast carcinoma cell line, where it was induced by estrogen treatment within 0.5 h [10], suggesting that Efp can mediate estrogen actions such as cell growth as a primary responsive gene in breast cancer [10,11]. Recently, it has been suggested that negative cell-cycle regulators, such as 14-3-3 sigma are reduced in Efp-positive breast cancer cells because Efp targets 14-3-3 sigma for proteolysis as an ubiquitin ligase [11]. Thus, Efp may play roles not only as an estrogen target gene but also as a cell-cycle regulator.

Epithelial ovarian cancer is the leading cause of death due to a gynecological malignancy in the great majority of developed countries [12,13]. Sex steroid hormones have been implicated in the etiology and/or progression of some epithelial ovarian cancers, but the possible biological significance of steroid hormone actions in these cancers remains controversial [14–17]. The expression of Efp has not been examined in human epithelial ovarian cancer tissues, and thus the biological significance of Efp expression and correlation between the expression of Efp and ERs expression in this cancer have not yet been studied. We need to understand the new molecular targets or biological makers related to estrogenic actions for ovarian cancer as well as for those associated with breast cancer. In the current study, we examined the expression of Efp in human ovarian cancer tissues and cell lines.

Materials and methods

Cell lines

We used 12 ovarian carcinoma cell lines, two normal ovarian surface epithelial cell lines and one breast cancer cell line as follows. The seven cell lines OVCAR3, Caov3, SKOV3, TOV112D, TOV21G, OV90 and ES2 (adenocarcinoma OVCAR3, SKOV3; serous adenocarcinoma Caov3, OV90; clear cell adenocarcinoma TOV21G, ES2; endometrioid adenocarcinoma TOV112D) were purchased from American Type Culture Collection. The five cell lines JHOS2, JHOS3, HTOA, OMC3 and JHOC5 (serous adenocarcinoma JHOS2, JHOS3, HTOA; mucinous adenocarcinoma OMC3; clear cell adenocarcinoma JHOC5) were purchased from Riken cell bank (Tsukuba, Japan). Two cell lines OSE2 and OSE4 established from normal ovarian epithelial cells were kindly provided by the Department of Obstetrics and Gynecology, Kumamoto University School of Medicine, Kumamoto, Japan [18]. MCF-7 (the human breast cancer cell line) was provided by the Institute of Department, Aging and Cancer, Tohoku University, Sendai, Japan. Cell lines were maintained in DMEM/F12 medium (Invitrogen, CA, USA), supplemented with 10% fetal bovine serum and 1% penicillin/streptomycin (Invitrogen) and incubated in a 5% CO_2 atmosphere at 37°C.

Surgical specimens and clinical data

We examined surgical specimens from a total of 100 cases of common epithelial ovarian carcinoma obtained from patients treated between 1988 and 2000 at Tohoku University Hospital, Sendai, Japan. Information regarding age, performance status on admission, histology, stage, grade, residual tumor after primary surgery and overall survival was retrieved from the review of patient charts. Median follow-up time for patients was 59 months (range, 4–120 months). Of the 100 patients, 77 (77%) received optimal cytoreduction at time of surgery, 84 (84%) patients received platinum-based chemotherapy postoperatively. Patients with stage Ia disease, low grade-disease (G1, G2) or poor performance status did not receive platinum-based chemotherapy. Performance status was defined according to WHO criteria (World Health Organization, 1979). Histology, stage and grade were according to FIGO criteria (International Federation of Gynecology and Obstetrics; [19]). Residual tumor was determined by the amount of unresectable tumor left following primary cytoreductive surgery. Optimal cytoreduction was defined as no gross residual tumor or less than 2 cm in diameter, whereas suboptimal cytoreduction was defined as any gross residual tumor remaining 2 cm or residual tumor greater than 2 cm in diameter. Overall survival was calculated from the time of initial surgery to death or the date of the last contact. Survival times of patients still alive or lost to follow-up were censored as of December 2002. All of these archival specimens were retrieved from the surgical pathology files at Tohoku University Hospital, Sendai, Japan. The informed consent was obtained from each patient. These specimens were all fixed in 10% formalin and embedded in paraffin. The research protocol was approved by the Ethics Committee of Tohoku University Graduate School of Medicine, Sendai, Japan.

Quantitative reverse transcription-PCR

Total RNA was isolated from cells by phenol-chloroform extraction using Isogen (Nippon gene, Tokyo, Japan). RNA was treated with RNase-free DNase (Roche Diagnostics; 1 μg/μl) for 2 h at 37°C, followed by heat inactivation at 65°C for 10 min. A reverse transcription (RT)-PCR kit (SUPERSCRIPT II First-strand synthesis system, Invitrogen) was used and cDNA synthesis was carried out according to the manufacturer's instructions. cDNAs were synthesized from 5 μg of total RNA using random hexamer and RT was carried out for 50 min at 42°C with SUPERSCRIPT II reverse transcriptase. Quantitative PCR was performed using an iCycler system (Bio-Rad, Tokyo, Japan). For the determination of Efp cDNA content, a 25 μl-reaction mixture consisting of 23 μl iQ™SYBR Green MasterMix, 1 μl each primer and 1 μl of template cDNA was prepared. PCR conditions were as follows: 2-min denaturation at 90°C, 30-s annealing at 60°C (for Efp), 62°C (for β-actin) and 1.5-min extension at 72°C. Primers for PCR reactions were as follows: Efp-F, 5′-CGTGGAGTGGTTCAACAC-3′ and Efp-R, 5′-GAGCAGATGGAGATGGTG-3′ (1689–1923, 234 base pairs, bp); β-actin-F, 5′-CCAACCGCGAG-AAGATGAC-3′ and β-actin-R, 5′-GGAAGGAAGGCTG-GAAGAGT-3′ (382–841, 459 bp). In initial experiments, following amplification, PCR products were purified and subjected to direct sequencing to verify amplification of correct sequences (ABI prism 310 Genetic Analyzer, Applied Biosystems, CA, USA). β-Actin primers were utilized as a positive control and Efp expression level was calculated as value of Efp RT-PCR divided by value of β-actin RT-PCR. Negative controls without RNA and without reverse transcriptase were also performed.

Immunoblotting

Cells were grown to 70% confluence in 10-cm plates and after removal of culture medium with Phosphate-buffered saline (PBS). Whole-cell protein concentration was measured by Model 680 microplate reader (Biorad, USA) using BradFord reagent (Biorad). A rabbit polyclonal antibody against Efp protein was made by one of the authors (SI). Mouse monoclonal antibody for ERα was purchased from NOVOCASTRA (Newcastle, UK). Mouse monoclonal antibody for ERβ was purchased from GeneTex, Inc. (TX, USA). In all, 20 μg of protein of each sample was mixed with an equal volume of 2× concentrated sodium dodecyl sulfate (SDS)-polyacrylamide gel electrophoresis (SDS-PAGE) sample buffer, boiled and then electrophoresed on 7% ready-made gels containing SDS (Mini Protein II Western blotting system, Biorad). Proteins were then transferred to nitrocellulose membrane (Hybond PDVF, Biorad). The membranes were incubated in blocking solution (PBS containing 5% nonfat milk and 0.05% Tween-20), then incubated in 1:4000 dilution of Efp antibody (1:100 for ERα, 1:1500 for ERβ and 1:1000 for β-actin) in blocking solution overnight at 4°C. After incubation with horseradish peroxidase (HRP)-labeled anti-rabbit IgG (anti-mouse IgM for ERα and ERβ) (Vector Laboratories, USA), the antigen–antibody complex was visualized with ECL system (Amersham, Germany). The MCF-7 breast cancer cell line was used as positive control. Actin (Ab-1, Oncogene) was used as an internal positive control.

Immunohistochemistry and scoring of immunostaining

Immunohistochemical analysis was performed using a streptavidin–biotin amplification method using the Histofine Kit (Nichirei, Tokyo, Japan). For antigen retrieval, slides were heated in an autoclave at 120°C for 5 min in citric acid buffer (2 mM citric acid and 9 mM trisodium citrate gyhydrate, pH 6.0). The dilutions of primary antibodies for Efp, ERα and ERβ were 1:2000, 1:50 and 1:1500, respectively. The antigen–antibody complex was visualized with 3,3′-diaminobenzidine (DAB) solution (1mM DAB, 50mM Tris–HCl buffer (pH 7.6) and 0.006% H_2O_2), and counterstained with hematoxylin. The ER positive normal breast tissue was used as a positive control. For statistical analysis of Efp immunoreactivity, we classified carcinomas into two groups: +, positive carcinoma cells; and −, no immunoreactivity. For evaluation of ERα and ERβ immunoreactivity, we used the H score system to count carcinoma cells as described previously [20,21]. Scores were generated as follows: (3 × [percentage of strongly staining cells]) + (2 × [percentage of moderately staining cells]) + (1 × [percentage of weakly staining cells]). This scoring system yielded results ranging from 0 to 300. Evaluation was carried out independently by two of the authors (MS and JA) for at least 500 cells.

Statistical analysis

Statistical analysis was performed using Stat View 5.0 (SAS Institute Inc., NC, USA) software. The correlation between expression of Efp mRNA and protein was also assessed using the Mann–Whitney U test. The statistical significance between Efp immunoreactivity and clinicopathological parameters was evaluated using Friedman's χ_2-test. The correlation between Efp and ERα, ERβ immunoreactivity was assessed using the Mann–Whitney U test. The univariate analysis of prognostic significance was performed using the log-rank test after each survival curve was obtained by the Kaplan–Meier method. All patients who could be assessed were included in the intention-to-treat analysis. A result was considered significant when the P value was less than 0.05.

Results

First, we examined Efp expression in ovarian cancer cells. By immunoblotting with anti-Efp antibody, immunoreactive bands corresponding to Efp, sized at approximately 70 kDa, were detected in 8 out of 12 ovarian cancer cell lines (Fig. 1). Efp expression in cell lines was supported with data obtained by quantitative RT-PCR study. Of the 12 ovarian cancer cell lines, 8 were positive for Efp protein expression by immunoblotting showing relatively higher levels of Efp-mRNA than seen in the 4 cell lines negative for Efp protein expression (Fig. 2) ($P = 0.021$). From these

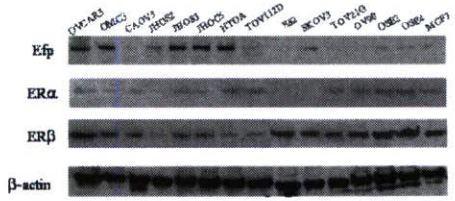

Fig. 1. Immunoblotting with variable cell lines, the top panel with anti-Efp antibody, the second panel with anti anti-ERα antibody, the third panel with anti-ERβ antibody and the bottom panel with anti β-actin antibody. OVCAR3, OMC3, CAOV3, JHOS2, JHOS3, JHOC5, HTOA, TOV112D, ES2, SKOV3, TOV21G and OV90 were derived from ovarian cancer. OSE2 and OSE4 were derived from normal ovarian surface epithelium. MCF-7 was a cell line derived from breast cancer and used as a positive control of Efp and ERs expressions. β-Actin was used as an internal positive control of antibody.

results, we were convinced that cell lines established from not only normal ovarian epithelium but also ovarian cancers expressed Efp genes at various levels similar to results seen with breast cancer cell lines.

Because the Efp gene was expressed by estrones through estrogen receptors, we next examined ERs protein expression in these cell lines (Fig. 2). By immunoblotting with anti-ERα antibody, 10 out of 12 ovarian cancer lines and the 2 cell lines from normal ovarian epithelium showed positive bands. All cell lines positive for Efp protein expression, except SKOV3, were simultaneously positive to ERα. Similarly, all cell lines showed positive bands for ERβ by immunoblotting with anti-ERβ antibody. From these results, we knew that all of the Efp-immunoreactive cell lines simultaneously expressed either ERα or ERβ protein.

Then, we performed immunohistochemical staining with anti-human Efp antibody for the 100 surgical specimens diagnosed as ovarian cancer to confirm Efp expression in ovarian cancer tissues. Efp protein expression was detected in 63 out of 100 specimens (63%). Positive staining was observed in the cytoplasm of ovarian cancer cells (Figs. 3A, D).

We then compared Efp expression and various clinicopathological parameters; results are summarized in Table 1. Differences by histological types were detected in Efp expression, i.e., the subgroup of serous adenocarcinomas showed significantly higher incidence of Efp positivity than other subgroups ($P = 0.010$). Similarly, the subgroup of advanced-stage disease showed a significantly higher incidence of Efp positivity than the subgroup consisting of early-stage disease ($P = 0.026$). There were no significant relationships between Efp immunoreactivity and patient age, performance status, histological grade or residual tumor (Table 1).

We decided to examine simultaneous ER and Efp expression in cancer tissues because Efp is mainly transactivated by ERs. Immunohistochemical studies showed that all ovarian cancer tissues were positive for both ERα and ERβ to a greater or lesser extent, and immunopositive signals were confined exclusively to the nuclei of tumor cells (Figs. 3B, C, E, F). The median H scores for ERα in Efp-immunopositive and Efp-immunonegative tumors were 80.1 ± 70.3 and 39.5 ± 59.4 (mean ± SD), respectively, indicating that Efp-positive cancers expressed significantly higher levels of ERα than Efp-negative cancers ($P = 0.022$). In the same way, the median H score for ERβ in Efp-immunopositive and Efp-immunonegative tumors was 67.7 ± 56.2 and 43.0 ± 43.7 (mean ± SD), respectively, indicating that Efp-positive cancers expressed significantly higher levels of ERβ than Efp-negative cancers ($P = 0.032$). Interestingly, the subgroup of serous adenocarcinomas showed significantly higher H scores (112.1 ± 60.7) than those of the other subgroups (29.7 ± 51.8) ($P < 0.0001$). In contrast, this tendency was not observed in immunoreactivity of ERβ among each histologic subgroup (data not shown).

Finally, we examined the possibility of Efp as a clinical prognostic factor by univariate analysis. As shown in Table 2, clinical variables including histologic type, grade, stage and residual tumor size were all significantly related with overall survival. These results seem to be consistent with data described previously [13,22,23]. With regard to analysis of Efp expression, we did not find any significant correlation between Efp immunoreactivity and overall survival ($P = 0.78$).

Discussion

In this study, we found strong correlations between Efp and ERα and between Efp and ERβ in ovarian cancer tissues; we also found that both ERα and ERβ proteins were expressed in most cancer cell lines with positive for Efp protein. Efp mRNA and protein are up-regulated by

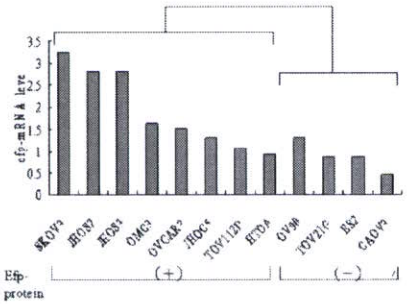

Fig. 2. Quantitative RT-PCR for expression of Efp mRNA in ovarian cancer cell lines. RT-PCR reactions were performed for each samples, and the ratio of Efp; β-actin was calculated and normalized. The left 8 cell lines were positive for Efp protein by immunoblotting, as determined from results of Fig. 1. Efp mRNA expression among cell lines positive for Efp protein was significantly higher than those among cell lines that are negative.

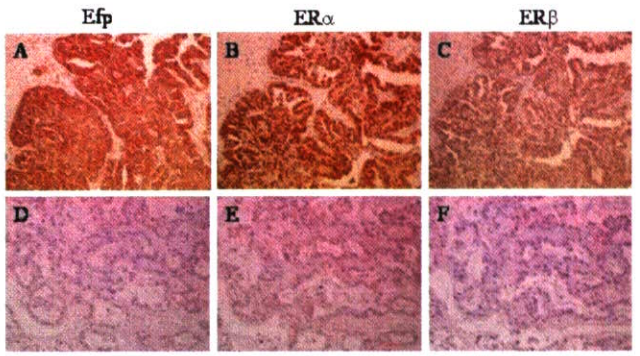

Fig. 3. Immunohistochemistry for Efp, EPα and ERβ in ovarian cancer tissues. Serial sections of each surgical specimens were stained with anti-Efp (A and D), anti-ERα (B and E) and anti-ERβ (C and F) antibodies, respectively. Representative data positive for each antibody (A–C) and negative (D–F) were shown. Positive signals for Efp were detected on the cytoplasm of cancer cells and positive signals for both ERα and ERβ were confined to the nuclei of cancer cells.

estrogen treatment in vivo [5,8]. Estrogen-responsive proliferation of uterine cells which express abundant ERα was impaired in Efp knock-out mice, suggesting that Efp is a mediator of cell proliferation as one of the direct targets of ERα [6]. In breast cancer, which is considered one of the sex steroid hormone-related malignant neoplasms, the Efp promoter could be enhanced by both ERα and ERβ in the setting of estrogen treatment. It has been suggested that Efp responds to estrogen as a common downstream gene of ERα and ERβ and that Efp mediates estrogen action in both ERα- and ERβ-positive breast cancer [10]. Results from our present study are consistent with these previous reports focusing on breast cancer [6,10], and suggest that Efp may mediate estrogen action through ERα and ERβ in some human epithelial ovarian cancer tissues and cell lines.

However, responsiveness and prognosis impact of steroid hormone in ovarian cancer may be different from those in breast cancer. Responsiveness to hormonal manipulation clearly results in favorable feature of breast cancer. It is known that most of the ER-positive breast cancers are primarily responsive to endocrine therapy, but breast cancer lacking any ER expression often reveals more aggressive phenotypes and is resistant to endocrine therapy [24]. Human epithelial ovarian cancer is believed to be a sex steroid hormone-related neoplasm, although the biological significance and the prognostic impact of hormone receptors are still controversial [14–17]. Previous studies have suggested a relation between progesterone receptor expression and favorable prognosis of epithelial ovarian cancer; especially, tumors of ER-negative/PR-positive showed a significantly superior prognosis when compared with the other combinations [14,25,26]. These evidences suggest that

Table 1
Association between Efp immunoreactivity and clinicopathological parameters in human epithelial ovarian cancer

	Total	Efp immunoreactivity		P value
		+	−	
		63	37	
Age				
≦50	50	33	17	
>50	50	30	20	NS
Performance status				
0, 1	70	44	26	
2, 3, 4	30	19	11	NS
Histological type				
Serous	43	34	9	
Mucinous	14	10	4	
Endometrioid	15	7	8	
Clear cell	27	11	16	
Squamous cell	1	1	0	0.01
Histological grade				
Grade 1	41	23	18	
Grade 2	35	22	13	
Grade 3	24	18	6	NS
Stage				
I, II	55	23	22	
III, IV	45	40	15	0.026
Residual tumor				
≦2cm	59	34	25	
>2cm	41	29	12	NS
ERα H score		80.1 ± 70.3	39.6 ± 59.4	0.022
ERβ H score		67.7 ± 56.2	43.0 ± 43.7	0.032

Histological type: serous, serous adenocarcinoma; mucinous, mucinous adenocarcinoma; endometrioid, endometrioid adenocarcinoma; clear cell, clear cell adenocarcinoma; squamous, squamous cell carcinoma.

Table 2
Univariate analysis of overall survival

Variable	P value
Efp immunoreactivity (+ vs. −)	0.78
Histological type	0.018
Histological grade	0.0085
Stage	<0.0001
Residual tumor	<0.0001

estrogen function in ovarian cancer has some differences from that in breast cancer, and this may be a reason why Efp expression was unrelated to survival in this study.

Efp immunoreactivity was associated in the current study with the histologic type, serous adenocarcinoma. Ovarian cancer is a morphologically, histologically and biologically heterogeneous disease, which has likely contributed to difficulties in defining the molecular alterations associated with development and progression. On the basis of morphological and histologic criteria, there are four major types of primary ovarian carcinomas: serous adenocarcinoma, mucinous adenocarcinoma, endometrioid adenocarcinoma and clear cell adenocarcinoma. Some molecular studies have offered support for the hypothesis that different histologic types of ovarian carcinoma likely represent distinct disease entities. For example, serous adenocarcinomas demonstrate frequent *p53* mutations and more than 85% of mucinous ovarian adenocarcinomas show *K-ras* mutations [27,28]. Endometrioid adenocarcinomas preferentially exhibit microsatellite instability and mutations of *CTNNB1* (β-catenin) [29,30]. Considering estrogenic action on ovarian cancer, which still remains controversial, it has been thought that ERs expression and its transcriptional gene expression differ in each histologic type. A higher expression of ERα relative to expression of ERβ has been observed in surface epithelial ovarian cancer compared with normal ovarian surface epithelium [2,31]. As for histologic type, there is a relative paucity of ERα expression in clear cell adenocarcinoma compared with the level of expression in serous, endometrioid and mucinous adenocarcinoma [32]. In epithelial ovarian cancer, especially in serous adenocarcinoma, the germ line mutations of BRCA1 have been observed as frequently as seen in breast cancer. The BRCA1 gene has been found to inhibit signaling by ligand-activated ERα through the estrogen-responsive enhancer element and to block the transcriptional activation domain of ERα, AF-2 [33,34]. Our results, together with those of previous reports, suggest that the expression of Efp might be one of the different characteristics of each histologic type and that Efp overexpression especially correlates with serous histology, as the result of estrogen actions through ERs.

Early stages of ovarian cancer are generally asymptomatic and difficult to detect, thus, by the time clinical diagnosis made, most of patients have widespread tumor dissemination beyond the ovaries. Despite a high response rate to first-line chemotherapy, the prognosis of these women is poor, with the 5-year overall survival only 10–20% [13,22]. We need some markers of ovarian cancer to identify subpopulations of patients whose disease is progressive and behaves differently from those in the majority of patients, and which might therefore benefit from adapted therapeutic options. To our knowledge, this current report is the first to evaluated the relationships between Efp and clinicopathological parameters in epithelial ovarian cancer. In our study, the expression of Efp had no prognostic value but was related to advanced-stage disease. Our results suggest that overexpression of Efp might cause invasive and progressive characteristics of epithelial ovarian cancer, if so Efp might have the potential to be useful as a biological marker.

The benefit of optimal surgery for patients with advanced ovarian cancer is well established [35]. Recently, Levine et al. reported that genetic differences failed to predict for outcome of surgical cytoreduction [36]. Our result that the expression of Efp did not correlate with residual tumor size after primary cytoreductive surgery is consistent with this previous report. With regard to tumor dissemination in the abdominal cavity, intrapelvic location of ovaries and their mobility in relation to adjacent structures might be in more relation to ability of optimal surgery than the genetic changes. These evidences suggest that some genetic differences including Efp expression could clarify a character of tumors but would not predict clinical outcome in epithelial ovarian cancer.

From our experimental data, the expression of Efp was detected in human epithelial ovarian cancer and correlated with ERs status, advanced-stage disease and serous adenocarcinoma histologic type. It has been suggested that the expression of Efp in human epithelial ovarian cancer relates to regulation of cell proliferation and carcinogenesis through ERs and that Efp could be a biological marker of this cancer. Further investigations are required to reveal the roles of Efp related to estrogenic action and cell-cycle regulation in epithelial ovarian cancer.

Acknowledgments

This work was supported in part by a grant-in-aid for Scientific Research from the Ministry of Health and Welfare, a grant-in-aid from the Ministry of Education, Science and Culture, a grant-in-aid from Kurokawa Cancer Research Foundation, a grant-in-aid from Japan Gynecologic Oncology Group (JGOG) and the 21st Century Center of Excellence (COE) Program Special Research Grant from the Ministry of Education Science, Sports and Culture.

References

[1] Enmark E, Gustafsson JA. Oestrogen receptors—An overview. J Int Med 1999;246:133–8.
[2] Li AJ, Baldwin RL, Karlan BY. Estrogen and progesterone receptor subtype expression in normal and malignant ovarian epithelial cell cultures. Am J Obstet Gynecol 2003;189:22–7.
[3] Evans RM. The steroid and thyroid hormone receptor family. Science 1988;240:889–95.
[4] Green S, Chambon P. Nuclear receptors enhance our understanding of transcription regulation. Trends Genet 1988;11:309–14.
[5] Inoue S, Orimo A, Hosoi T, et al. Genomic binding-site cloning reveals an estrogen-responsive gene that encodes a RING finger protein. Proc Natl Acad Sci U S A 1993;99:11117–21.
[6] Orimo A, Inoue S, Minowa O, et al. Underdeveloped uterus and reduced estrogen responsiveness in mice with disruption of the estrogen responsive finger protein gene, which is a direct target of estrogen receptor α. Proc Natl Acad Sci U S A 1999;96:12027–32.
[7] Ikeda K, Inoue S, Orimo A, et al. Multiple regulatory elements and binding protein of the 5′-flanking region of the human estrogen-responsive finger protein (efp) gene. Biochem Biophys Res Commun 1997;236(3):765–71.
[8] Orimo A, Inoue S, Ikeda K, Noji S, Muramatsu M. Molecular cloning, structure, and expression of mouse estrogen-responsive finger protein Efp. J Biol Chem 1995;270(41):24406–13.
[9] Shimada N, Suzuki T, Inoue S, et al. Systemic distribution of estrogen-responsive finger protein (Efp) in human tissues. Mol Cell Endocr 2004;218:147–53.
[10] Ikeda K, Orimo A, Higashi Y, Muramatsu M, Inoue S. Efp as a primary estrogen-responsive gene in human breast cancer. FEBS 2000;472:9–13.
[11] Horie K, Urano T, Ikeda K, Inoue S. Estrogen-responsive RING finger protein controls breast cancer growth. J Steroid Biochem Mol Biol 2003;85:101–4.
[12] Akahira JI, Aoki M, Suzuki T, et al. Expression of EBAG9/RCAS1 is associated with advanced disease in human epithelial ovarian cancer. Br J Cancer 2004;90:2197–202.
[13] Akahira JI, Yoshikawa H, Shimizu Y, et al. Prognostic factors of stage IV epithelial ovarian cancer: a multicenter retrospective study. Gynecol Oncol 2001;81:398–403.
[14] Akahira J, Inoue T, Suzuki T, et al. Progesterone receptor isoforms A and B in human epithelial ovarian carcinoma: immunohistochemical and RT-PCR studies. Br J Cancer 2000;83(11):1488–94.
[15] Bizzi A, Codegoni AM, Landoni F, et al. Steroid receptors in epithelial ovarian carcinoma: relation to clinical parameters and survival. Cancer Res 1988;48:6222–6.
[16] Masood S, Heitmann J, Nuss RC, Benrubi GI. Clinical correlation of hormone receptor status in epithelial ovarian cancer. Gynecol Oncol 1989;34:57–60.
[17] Rao BR, Slotman BJ. Endocrine factors in common epithelial ovarian cancer. Endocr Rev 1991;12:14–26.
[18] Nitta M, Katabuchi H, Ohtake H, et al. Characterization and tumorigenicity of human ovarian surface epithelial cells immortalized by SV40 large T antigen. Gynecol Oncol 2001;81:10–7.
[19] Shimizu Y, Kamoi S, Amada S, et al. Toward the development of a universal grading system for ovarian epithelial carcinoma: I. Prognostic significance of histopathologic features-problems involved in the architectural grading system. Gynecol Oncol 1998; 70:2–12.
[20] Akahira J, Suzuki T, Ito K, et al. Differential expression of progesterone receptor isoforms A and B in the normal ovary, and in benign, borderline, and malignant ovarian tumors. Jpn J Cancer Res 2002;93:807–15.
[21] McCarty KS Jr, Miller LS, Cox EB, Konrath J, McCarty KS Sr.. Estrogen receptor analysis. Arch Pathol Lab Med 1985;109:716–21.
[22] Bonnefoi H, A'Hern RP, Fisher C, et al. Natural history of stage IV epithelial ovarian cancer. J Clin Oncol 1999;17(3):767–75.
[23] Munkarah AK, Hallum III AV, Morris M, et al. Prognostic significance of residual disease in patients with stage IV epithelial ovarian cancer. Gynecol Oncol 1997;64(1):13–7.
[24] Clarke R, Skaar T, Baumann K, et al. Hormonal carcinogenesis in breast cancer: cellular and molecular studies of malignant progression. Breast Cancer Res Treat 1994;31:237–48.
[25] Lindgren P, Backstrom T, Mahlck CG, et al. Steroid receptors and hormones in relation to cell proliferation and apoptosis in poorly differentiated epithelial ovarian tumors. Int J Oncol 2001;19(1):31–8.
[26] Munstedt K, Steen J, Knauf AG, et al. Steroid hormone receptors and long term survival in invasive ovarian cancer. Cancer 2000;89(8): 1783–91.
[27] Anttila M, Kosma VM, Ji H, et al. Clinical significance of alpha-catenin, collagen IV, and Ki-67 expression in epithelial ovarian cancer. J Clin Oncol 1998;16(8):2591–600.
[28] van der Zee AG, Hollema H, Suurmeijer AJ, et al. Value of P-glycoprotein, glutathione *S*-transferase pi, c-erbB-2, and p53 as prognostic factors in ovarian carcinomas. J Clin Oncol 1995;13(1): 70–8.
[29] Aunoble B, Sanches R, Didier E, Bignon YJ. Major oncogenes and tumor suppressor genes involved in epithelial ovarian cancer [review]. Int J Oncol 2000;16:567–76.
[30] Feeley KM, Wells M. Precursor lesions of ovarian epithelial malignancy. Histopathology 2001;38:87–95.
[31] Pujol P, Rey JM, Nirde P, et al. Differential expression of estrogen receptor-α and β messenger RNAs as a potential maker of ovarian carcinogenesis. Cancer Res 1998;58:5367–73.
[32] Fujimura M, Hidaka T, Kataoka K, et al. Absence of estrogen receptor-α expression in human ovarian clear cell adenocarcinoma compared with ovarian serous, endometrioid, and mucinous adenocarcinoma. Am J Surg Pathol 2001;25(5):667–72.
[33] Aida H, Takakuwa K, Nagata H, et al. Clinical futures of ovarian cancer in Japanese woman with germ-line mutations of BRCA1. Clin Cancer Res 1998;4(1):235–40.
[34] Fan S, Wang JA, Yuan R, et al. BRCA1 inhibition of estrogen receptor signaling in transfected cells. Science 1999;284:1354–6.
[35] Chi DS, Franklin CC, Levine DA, et al. Improved optimal cytoreduction rares for stage IIIc and IV epithelial ovarian, fallopian tube, and primary peritoneal cancer: a change in surgical approach. Gynecol Oncol 2004;94:650–4.
[36] Levine D.A., Bonome T., Olshen A.B., et al. Gene expression profiling of advanced ovarian cancers to predict the outcome of primary surgical cytoreduction. ASCO 2004:448 [abstr 5000].

Survival Versus Apoptotic 17β-Estradiol Effect: Role of ERα and ERβ Activated Non-genomic Signaling

FILIPPO ACCONCIA,[1] PIERANGELA TOTTA,[1] SUMITO OGAWA,[2] IRENE CARDILLO,[1] SATOSHI INOUE,[2] STEFANO LEONE,[1] ANNA TRENTALANCE,[1] MASAMI MURAMATSU,[2] AND MARIA MARINO[1]*

[1]*Department of Biology, University "Roma Tre," Rome, Italy*

[2]*Research Center for Genomic Medicine, Saitama Medical School, Saitama, Japan*

The capability of 17β-estradiol (E2) to induce the non-genomic activities of its receptors (ERα and ERβ) and to evoke different signaling pathways committed to the regulation of cell proliferation has been analyzed in different cell cancer lines containing transfected (HeLa) or endogenous (HepG2, DLD1) ERα or ERβ. In these cell lines, E2 induced different effects on cell growth/apoptosis in dependence of ER isoforms present. The E2–ERα complex rapidly activated multiple signal transduction pathways (i.e., ERK/MAPK, PI3K/AKT) committed to both cell cycle progression and apoptotic cascade prevention. On the other hand, the E2–ERβ complex induced the rapid and persistent phosphorylation of p38/MAPK which, in turn, was involved in caspase-3 activation and cleavage of poly(ADP-ribose)polymerase, driving cells into the apoptotic cycle. In addition, the E2–ERβ complex did not activate any of the E2–ERα-activated signal molecules involved in cell growth. Taken together, these results demonstrate the ability of ERβ isoform to activate specific signal transduction pathways starting from plasma membrane that may justify the effect of E2 in inducing cell proliferation or apoptosis in cancer cells. In particular this hormone promotes cell survival through ERα non-genomic signaling and cell death through ERβ non-genomic signaling. J. Cell. Physiol. 203: 193–201, 2005.

Knowledge of the molecular mechanism by which estrogens exert pleiotropic functions in different tissues and organs has evolved rapidly during the past two decades. In particular, the mechanism by which 17β-estradiol (E2) induces cell proliferation has been the object of extensive studies in several tissues (Sutherland et al., 1983; Marino et al., 1998, 2001; Castoria et al., 1999, 2001; Razandi et al., 1999). However, recent reports demonstrated that E2 could even decrease cell growth by significantly increasing apoptosis in breast cancer MCF-7 cell variants, prostate cells, and several other cell types (see Song and Santen, 2003 for review). Whether the E2 apoptotic effects can be explained by the expression of different estrogen receptor (ER) isoforms (i.e., ERα and ERβ) is presently unknown.

It has been assumed that E2 exerts survival proliferative effects mainly by rapid non-genomic mechanisms originating from the hormone binding to ERα (Marino et al., 1998, 2002; Castoria et al., 1999, 2001; Lobenhofer et al., 2000; Fernando and Wimalasena, 2004). In line with this assumption, E2 treatment of MCF-7 cells triggers association of ERα with Src kinase and p85, the regulatory subunit of PI3K, leading to DNA synthesis (Castoria et al., 2001). Moreover, E2 induces rapid non-genomic pathways and DNA synthesis even in ERα transiently transfected cell lines (e.g., Chinese hamster ovary, CHO; cervix epitheloid carcinoma cell line, HeLa) (Razandi et al., 1999; Marino et al., 2002). In addition, multiple and parallel signal transduction pathways are rapidly activated by the E2–ERα complex in hepatoma, HepG2, cells (e.g., ERK/MAPK, PI3K/AKT) (Marino et al., 2003). The disruption of such membrane starting pathways completely prevents the E2-induced DNA synthesis and the cyclin D_1 expression at the specific response elements, activator protein-1 (AP-1) and stimulating protein-1 (SP-1) (Marino et al., 2002, 2003). All these results point to the concept that ERα is the primary endogenous mediator of rapid E2 actions committed to cell proliferation.

Less information is available on the role played by ERβ in E2 proliferative effects. Data from cell cultures, gene expression, and knockout mice clearly indicate that E2-activated ERβ may function as a tumor suppressor by modulating the proliferative effects of ERα (Couse and Korach, 1999; Weihua et al., 2003; Cheng et al., 2004; Paruthiyil et al., 2004, Strom et al., 2004). These studies support a functional antagonism between ERα and ERβ with respect to the E2-induced cell proliferation, but do not clarify either the putative role of ERβ in E2-induced apoptosis or the signal transduction pathways involved. However, the ability of E2–ERβ complex to activate rapid non-genomic mechanisms has been reported. A subpopulation of ERβ transfected into CHO cells is membrane bound and capable of activating IP_3 production, ERK/MAPK and c-Jun kinase phosphorylation (Razandi et al., 1999). Recently, Geraldes and coworkers (Geraldes et al., 2003) reported that E2 reduces ERK/MAPK activity through ERβ stimulation in porcine smooth muscle cells. Moreover, conflicting

Abbreviations: E2, 17β-estradiol; E2-BSA, β-estradiol 6-(o-carboxy-methyl)oxime:BSA; ER, estrogen receptor; ERE, estrogen responsive element; ERK, extracellular regulated kinase; MAPK, mitogen-activated protein kinase; PI3K, phosphoinositide-3-kinase; PKC, protein kinase C; PARP, poly(ADP-ribose) polymerase.

Contract grant sponsor: MURST; Contract grant sponsor: University "Roma Tre"; Contract grant number: RBAU01TXN3_001; Contract grant sponsor: FIRB 2001 and 2004 University "Roma Tre".

*Correspondence to: Maria Marino, Department of Biology, University "Roma Tre," Viale G. Marconi, 446, I-00146 Rome, Italy. E-mail: m.marino@uniroma3.it

Received 4 June 2004; Accepted 29 July 2004

DOI: 10.1002/jcp.20219

evidences on the ability of ERβ to activate or inactivate Src and p38 kinases (Castoria et al., 2001; Kousteni et al., 2001; Geraldes et al., 2003; Mori-Abe et al., 2003) has been also reported. In particular, the existence of non-genomic mechanism(s) underling the antiproliferative effects of E2–ERβ complex is to date completely unknown.

Here, the ability of E2 to induce ERs activities has been studied in the HeLa cells devoid of any ERs and rendered E2-sensitive by transient transfection with human ERα or ERβ expression vectors. We report that E2 induced different effects on cell growth/apoptosis decision in the presence of the two different isoforms of receptor. The E2–ERα complex activated multiple signal transduction pathways (i.e., ERK/MAPK, PI3K/AKT, p38/MAPK) involved in cell cycle progression, whereas the E2–ERβ complex activated only p38/MAPK, which in turn, drives cells to apoptosis. A role of E2-induced ERK/MAPK activation in regulating some steps of the pro-apoptotic pathways is also demonstrated. These results were confirmed also in cancer cell lines expressing endogenous level of ERα or ERβ. Altogether our findings indicate a new action mechanism for the E2–ERβ complex pointing to the role of E2-induced rapid non-genomic signals in driving cell proliferation or apoptosis in cancer cells.

MATERIALS AND METHODS

Reagents

17β-estradiol, 17α-estradiol, L-glutamine, gentamicin, penicillin, RPMI-1640 and DMEM (without phenol red), charcoal-stripped fetal calf serum, and estradiol-BSA conjugate (β-estradiol 6-(o-carboxy-methyl)oxime:BSA, E2-BSA) were purchased from Sigma Chemical Co. (St. Louis, MO). The estrogen receptor inhibitor ICI 182,780 was obtained from Tocris (Ballwin, MO). The ERK/MAPK cascade inhibitor, U 0126, the PI3K inhibitor, Ly 294002, and the p38/MAPK inhibitor, SB 203580, were obtained from Calbiochem (San Diego, CA). Lipofectamine reagent was obtained from GIBCO-BRL Life-technology (Gaithersburg, MD). The luciferase kit was obtained from Promega (Madison, WI). GenElute plasmid maxiprep kit was obtained from Sigma Chemical Co. Bradford Protein Assay was obtained from BIO-RAD Laboratories (Hercules, CA). The policlonal anti-phospho-AKT, anti-phospho-p38, and anti-p38 antibodies were obtained by New England Biolabs (Beverly, MA); the policlonal anti-ERα, anti-ERβ, and anti-ERK and the monoclonal anti-phospho-ERK, anti-AKT, anti-Bcl-2, anti-caspase-3, anti-poly(ADP-ribose) polymerase (PARP), and anti-actin antibodies were obtained from Santa Cruz Biotechnology (Santa Cruz, CA). CDP-Star, chemiluminescence reagent for Western blot was obtained from NEN (Boston, MA).

All the other products were from Sigma Chemical Co. Analytical or reagent grade products, without further purification, were used.

Cell culture

The ER devoid human cervix epitheloid carcinoma cell line (HeLa) (Marino et al., 2002), the ERα containing hepatoma cell line (HepG2) (Marino et al., 2002, 2003; Moon et al., 2004), and the ERβ containing human colon adenocarcinoma cells (DLD1) (Fiorelli et al., 1999; Di Leo et al., 2001) were used as experimental models. Cells were routinely grown in air containing 5% CO_2 in modified, phenol red-free, DMEM (HeLa cells) or RPMI-1640 (HepG2 and DLD1 cells) media, containing 10% (v/v) charcoal-stripped fetal calf serum, L-glutamine (2 mM), gentamicin (0.1 mg/ml), and penicillin (100 U/ml). Cells were passaged every 2 days (HeLa and DLD1 cells) or every 4 days (HepG2 cells) and media changed every 2 days.

Plasmids and transfection procedures

The expression vectors for pCR3.1-β-galactosidase, human ERα (pSG5-HE0) (Marino et al., 2003), and human ERβ (pCNX2-ERβ) (Ogawa et al., 1998) have been used. Furthermore an empty vector, pCMV5, was used as control (Marino et al., 2001). Plasmids were purified for transfection using a plasmid preparation kit according to manufacturer's instructions. A luciferase dose response curve showed that the maximum effect was present when 1 μg of DNA was transfected in HeLa cells together with 1 μg of pCR3.1-β-galactosidase to normalize transfection efficiency (~55–65%). HeLa cells were grown to ~70% confluence, then transfected using Lipofectamine Reagent according to the manufacturer's instructions. Six hours after transfection the medium was changed and 24 h thereafter cells were stimulated with 10 nM E2.

Cell viability and cell cycle

HeLa cells were grown to ~70% confluence in 6-well plates, then transfected and, after 24 h, stimulated. At different times after treatment cells were harvested with trypsin and centrifuged. Cells were stained with trypan blue solution and counted in a hemocytometer (improved Neubauer chamber) in quadruplicate. For the cell cycle analysis, 10^6 cells were fixed with 1 ml ice-cold 70% ethanol and subsequently stained with 2 μg/ml DAPI/PBS solution. The fluorescence of DNA was measured with a DAKO Galaxy flow cytometer equipped with HBO mercury lamp and the percentage of cells present in sub-G1, G1, S, and G2/M phases was calculated using a FloMax© Software.

Electrophoresis and immunoblotting

Stimulated and un-stimulated cells were lysed as described (Marino et al., 1998). When indicated 1 μM ICI 182,780 or 10 μM U 0126 or 10 μM Ly 294002 or 5 μM SB 203580 were added to the medium 15 or 30 min, respectively, before agonist stimulation. Cells were solubilized in 0.125 M Tris-HCl (pH 6.8) containing 10% SDS (w/v), 1 mM phenylmethylsulfonyl fluoride, and 5 μg/ml leupeptin and boiled for 2 min. Proteins were quantified using the Bradford Protein Assay (Bradford, 1976). Twenty microgram solubilized proteins were resolved using SDS–PAGE at 100 V for 1 h. The proteins were then electrophoretically transferred to nitrocellulose for 45 min at 100 V at 4°C. The nitrocellulose was treated with 3% bovine serum albumin in 138 mM NaCl, 26.8 mM KCl, 25 mM Tris-HCl (pH 8.0), 0.05% Tween-20, 0.1% BSA, and then probed at 4°C overnight with either one of anti-ERα, anti-ERβ, anti-phospho-ERK, anti-phospho-AKT, anti-phospho-p38, anti-caspase-3, anti-Bcl-2, or anti-PARP antibodies. The nitrocellulose was stripped by Restore Western Blot Stripping Buffer (Pierce Chemical Company, Rockford, IL) for 10 min at room temperature and then probed with either anti-ERK, anti-AKT, or anti-p38 antibodies (1 μg/ml). Anti-actin antibody (1 μg/ml) was used to normalize the sample loading. Antibody reaction was visualized with chemiluminescence reagent for Western blot.

RESULTS

Divergent effects of E2 in inducing cell growth in the presence of ERα or ERβ

The level of exogenous ERα or ERβ was assessed in HeLa cells untrasfected (none) or transfected with either empty, ERα, or ERβ expression vectors. The Western blot analysis (Fig. 1a) confirmed the absence of ERs in both un-transfected and empty vector-transfected HeLa cells, whereas a unique band at 67 kDa (ERα-containing HeLa cells) or at 57 kDa (ERβ-containing HeLa cells) was detected. The time course of growth of HeLa cells transfected with empty plasmid or ERα or ERβ expression vectors was examined in the presence of E2 and in the presence of the ER inhibitor ICI 182,780. Figure 1b shows that the growth of empty plasmid-transfected HeLa cells was not affected by E2 or ICI 182,780 suggesting that the presence of ER is necessary for the hormone effects. On the other hand, E2 was mitogen for ERα-transiently transfected HeLa cells (Fig. 1c), whereas a decrease in growth was detected after E2 stimulation in ERβ-transfected HeLa cells with respect to unstimu-

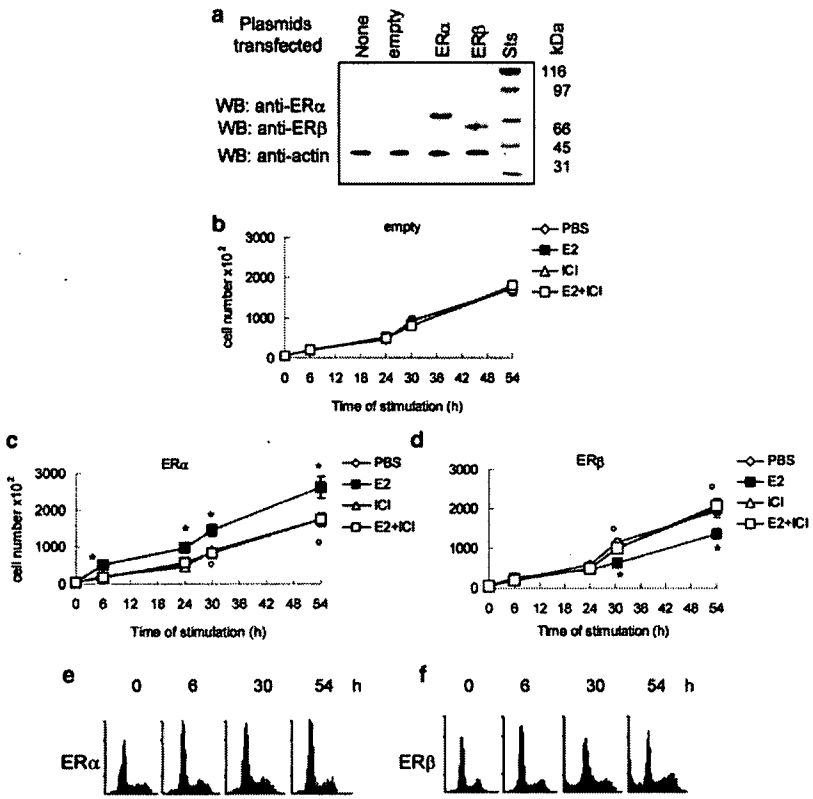

Fig. 1. Level of estrogen receptors (ERs) in transfected and un-transfected and time course of HeLa cell growth in the presence of 17β-estradiol (E2). Western blot analysis of ERα and ERβ levels were performed in un-transfected (none) or transfected HeLa cells with either empty, human ERα or human ERβ expression vectors (**part a**). HeLa cells transfected with empty (**part b**) or human ERα (**part c**) or human ERβ (**part d**) expression vectors were grown in DMEM in the presence of E2 (10 nM) and/or ICI 182,780 (ICI, 1 μM) counted at the indicated times. The data are the mean values ± SD of five independent experiments carried out in duplicate. $P < 0.001$, calculated with Student's *t*-test, compared with respective un-stimulated values (PBS) (*) or with E2-stimulated values (°). Flow cytometric analysis of the HeLa cells transfected with human ERα (**part e**) or human ERβ (**part f**) vectors after different time of E2-treatment compared with un-stimulated cells (0). The plots indicate cell cycle distribution present in sub-G1, G1, S, and G2/M phases, respectively. For details see the text.

lated ones (Fig. 1d). The cell pre-treatment with the ER inhibitor ICI 182,780 completely blocked the E2 effects both in ERα- and in ERβ-embedded HeLa cells. Further, we analyzed, by flow cytometry, the HeLa cell cycle distribution at different time after treatment. The typical plot of plasmid transfected-HeLa cell population is illustrated in Figure 1e and f (0 h). The first peak indicates the cell number in G1 phase of the cell cycle (50.0 ± 5.0%) followed by S phase (16.3 ± 3.2%), and by the peak of G2/M phase (19.8 ± 2.8%). Increasing the time of E2-stimulation (Fig. 1e; 6, 30, and 54 h), the number of cells in G1 phase of cell cycle increased reaching 65.4 ± 3.8% 54 h after the hormone administration to HeLa cells expressing ERα. On the contrary, when HeLa cells were endowed with ERβ (Fig. 1f; 6, 30, and 54 h), the number of cells in sub-G1 region increased reaching 9.5 ± 1.0% 54 h after the E2 stimulation thus suggesting the presence of DNA fragmentation.

Divergent effects of E2 in inducing an apoptotic cascade in the presence of ERα or ERβ

To determine whether the reported increase of cell population in the sub-G1 phase was truthfully related to the induction of an apoptotic cascade, we analyzed the cleavage of the caspase-3 proform (32-kDa band) which results in the production of the active subunit of the protease (17-kDa band). Caspase-3 proform was expressed in HeLa cells transfected with empty or ERα or ERβ expression vectors (Fig. 2a). No cleavage of caspase-3 was induced by E2 in empty or ERα-containing HeLa cells whereas E2 induced the production of the active subunit in the presence of ERβ.

To confirm that the appearance in the 17-kDa band was associated with an increase in caspase-3 activity, we analyzed one of the known substrates of caspase-3, PARP. This 116-kDa, DNA repair enzyme, is cleaved by

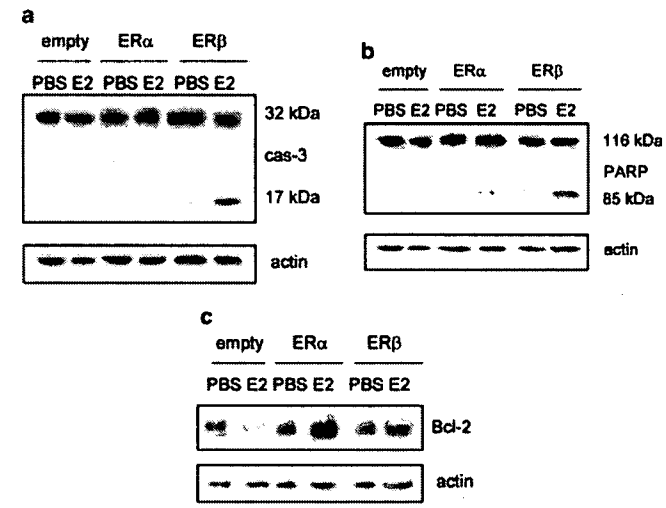

Fig. 2. Effect of E2 in the induction of pro-apoptotic proteins. Western blot analysis of caspase-3 (**part a**), PARP (**part b**) activation, and Bcl-2 (**part c**) levels were performed, as described in "Materials and Methods," on un-stimulated (PBS) and 24 h E2-treated (10 nM) HeLa cells transfected with human ERα, human ERβ, or empty expression vectors. The amounts of protein levels were normalized by comparison with actin expression. Typical blot of three independent experiments. For details see the text.

the caspase-3 producing the inactive 85-kDa fragment (Fig. 2b). By Western blot analysis, treatment of empty- and ERα-containing HeLa cells with E2 did not induce any conversion of PARP in the inactive form. On the contrary, the treatment of ERβ-transfected HeLa cells with E2 resulted in the conversion of PARP into the inactive 85-kDa fragment. These results were consistent with the idea that, in the presence of ERβ, E2 specifically induced an apoptotic cascade involving the caspase-3 activation and a downstream substrate like PARP. This was further confirmed by the expression of Bcl-2 level, the survival factor that can block both necrotic and apoptotic cell death (Dubal et al., 1999). Only the treatment of ERα-transfected HeLa cells with E2 markedly increased the amount of Bcl-2 (Fig. 2c).

Signal transduction pathways involved in the E2-induced apoptotic cascade

We previously reported that the rapid E2-induced activation of ERK/MAPK and PI3K/AKT pathways is sufficient and necessary for E2-induced cell cycle progression (i.e., DNA synthesis and the transcription of cyclin D_1 gene) (Marino et al., 2002, 2003). Then we asked if the inhibition of these rapid signals was involved in the E2–ERβ-induced apoptotic cascade.

No activation of signal transduction proteins was detected in cells transfected with empty vector and stimulated with E2 (data not shown). However, E2 increased ERK and AKT phosphorylation in HeLa cells transiently transfected with ERα (Fig. 3a). After reprobing the membranes using total ERK or AKT antibodies, to recognize the non-phosphorylated form of these proteins, the specific alteration of signaling proteins by E2 was confirmed to occur in the absence of changes in their expression levels (Fig. 3a). On the other hand, E2 failed to elicit any changes in the phosphorylation or expression level of ERK and AKT in cell expressing ERβ (Fig. 3a). Interestingly, a similar activation was observed in cancer cell lines which express endogenous ERα (HepG2) or ERβ (DLD1). In fact, E2 induced the rapid increase of ERK and AKT phosphorylation only in HepG2 cells (Fig. 3b) whereas it was ineffective in DLD1 cells (Fig. 3c). The level of endogenous ERα or ERβ was assessed in HepG2 and DLD1 cells. The Western blot analysis (Fig. 3d) confirmed the presence of a unique band at 67 kDa (HepG2 cells) or at 57 kDa (DLD1 cells) corresponding to ERα or ERβ, respectively.

Generally, the activation of PI3K/AKT and ERK/MAPK pathways causes cell survival in response to many mitogens and growth factors, whereas the activation of p38/MAPK has been associated with the regulation of apoptosis and differentiation processes (Ambrosino and Nebreda, 2001; Harper and LoGrasso, 2001; Talapatra and Thompson, 2001; Shimada et al., 2003; Porras et al., 2004). To verify this possibility, the effect of E2 on p38/MAPK activation was evaluated. A time course of E2-induced p38/MAPK phosphorylation in HeLa cells transfected with ERα or ERβ is shown in Figure 4a. A rapid and transient increase of p38/MAPK phosphorylation was detected from 15 to 30 min after E2 stimulation in ERα-transfected HeLa cells; whereas E2 induced a rapid (15 min) and persistent (24 h) increase of p38/MAPK phosphorylation in ERβ expressing HeLa cells. In the same way, E2 evoked a rapid (15 min) and transient activation of p38/MAPK in ERα-encoding HepG2 cells (Fig. 4b, upper part) and a rapid and persistent (24 h) phosphorylation of p38/MAPK in ERβ-containing DLD1 cells (Fig. 4b, lower part). Note that, the E2-induced p38/MAPK activation was prevented by the pure anti-ER ICI 182,780 in either cell lines (Fig. 4b). The same inhibitor completely

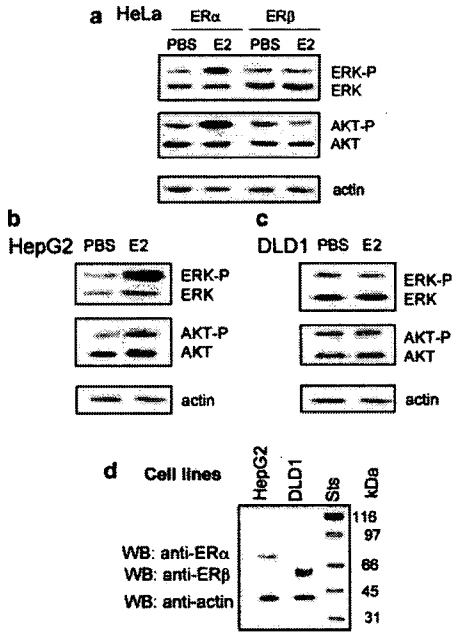

Fig. 3. Signal transduction pathways activated by E2. Western blot analysis of phosphorylated and un-phosphorylated ERK and AKT were performed, as described in "Materials and Methods," on un-stimulated (PBS) and 15 min E2-treated (10 nM) HeLa cells transfected with human ERα or human ERβ expression vectors (**part a**) or HepG2 cells (**part b**) or DLD1 cells (**part c**). Western blot analysis of ERα and ERβ levels were performed in HepG2 cells and DLD1 cells (**part d**). The amount of protein levels were normalized by comparison with actin expression. Typical blot of three independent experiments. For details see the text.

prevented the rapid (15 min) E2-induced p38/MAPK phosphorylation also in ER-transfected HeLa cells (Fig. 4c). Furthermore, the E2 inactive stereoisomer, 17α-estradiol, failed to induce p38/MAPK phosphorylation (Fig. 4c), whereas the E2 cell membrane impermeable, E2-BSA (Zheng et al., 1996; Marino et al., 2003), affected the p38/MAPK activation comparably to E2 (Fig. 4c). Altogether these data imply a membrane ER in the rapid and specific E2-induced activation of p38/MAPK signaling.

Cross-talk between proliferative and apoptotic signal transduction pathways and role of E2-induced p38/MAPK

The ability of E2 to induce p38/MAPK phosphorylation even in the presence of ERα was surprising and did not clarify the putative involvement of this kinase in the E2-induced apoptosis. Thus, we asked whether ERK/MAPK and PI3K/AKT cross-talk with p38/MAPK. None of the specific pathway inhibitors used (i.e., Ly 294002 and U 0126) prevented the E2-induced p38/MAPK phosphorylation in ERα-transfected HeLa cells (Fig. 5a) suggesting that the activation of this pathway was parallel and independent on ERK and AKT activation. On the contrary, the cell pre-treatment with the same inhibitors rescued the activation of the pro-apoptotic caspase-3 (Fig. 5b) as well as completely prevented E2-induced, anti-apoptotic, Bcl-2 accumulation (Fig. 5c). The same results were obtained in HepG2 cells (Fig. 5 d, e, and f) further indicating that E2–ERα-induced ERK and AKT activation negatively modulates the apoptotic signals. To direct evaluate the role of p38 in these effects in some experiments cells were pre-treated with the specific p38/MAPK inhibitor, SB 203580 (5 μM), before E2 stimulation. A block of p38/MAPK phosphorylation was evidenced while no effect was present on Bcl-2 levels in both cell lines considered. Note that, caspase-3 cleavage induced by E2 in the presence of U0126 was prevented by the pre-treatment of HepG2 cells with p38/MAPK inhibitor, SB 203580 (30 min) (Fig. 5g). However, the cell pretreatment with the signaling pathways inhibitors alone did not modify the p38/MAPK phosphorylation or caspase-3 and PARP cleavage.

Finally, the pre-treatment of ERβ-transfected HeLa cells with the specific p38/MAPK inhibitor, SB 203580, completely prevented the formation of the caspase-3 active fragment (Fig. 6a) and the cleavage of PARP (Fig. 6b) linking the p38/MAPK activation directly to the apoptosis. As expected, E2 induced p38/MAPK-dependent caspase-3 activation in ERβ-containing DLD1 cells (Fig. 6c) sustaining a pivotal role of the signaling activated by E2–ERβ complex (i.e., prolonged p38/MAPK phosphorylation) in inducing the apoptotic cascade.

DISCUSSION

E2 is known to support cell survival or induce cell death/apoptosis depending on the cell context (Song et al., 2001; Song and Santen, 2003). The mechanism(s) underling these opposite E2 effects could involve the classical/transcriptional mechanism of ER isoforms which, as ligand-dependent transcription factors, modulate the transcription of E2-induced target genes. In addition to this accepted model for the E2 action mechanism, emerging evidences indicated that rapid/non-genomic signaling molecules originating from the cell membrane are involved at least in E2–ERα-induced cell proliferation/survival (Castoria et al., 1999; Razandi et al., 1999, 2000a; Kousteni et al., 2001; Marino et al., 2001, 2002, 2003). These evidences prompted us to examine the non-genomic signaling mechanism(s) generated by the E2–ERβ complex and to compare the role(s) played by these rapid signals with those generated after E2–ERα binding. Although the different functions of ERα versus ERβ on cell proliferation/apoptosis balance has been suggested (Matthews and Gustafsson, 2003; Weihua et al., 2003), the contribution of signal transduction pathways generated by each isoform on these E2-induced cellular functions has not been yet clarified. Therefore, we chose the ER-devoid HeLa cells as experimental model. The transiently transfected HeLa cells allow us to discriminate the effect of each ER isoforms, without the mutual interference, in a E2-induced proliferation model (Marino et al., 2001, 2002). Furthermore, to avoid any dilemma due to the receptors over-expression, some experiments were performed in parallel in two different cancer cell lines which express endogenous ERα (HepG2) (Marino et al., 2001, 2002, 2003; Moon et al., 2004) or ERβ (DLD1) (Fiorelli et al., 1999; Di Leo et al., 2001).

In these experimental conditions, E2 induced different effects on cell growth or apoptosis in dependence on ER isoform present. While the E2–ERα complex activated multiple signal transduction pathways committed to

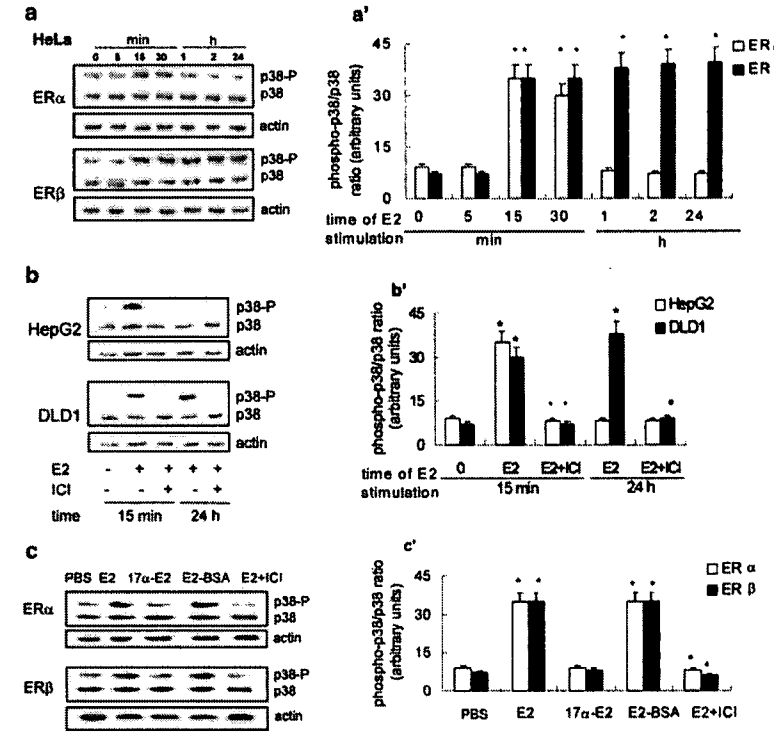

Fig. 4. Effect of E2 on p38/MAPK activation. Time course analysis of p38/MAPK phosphorylation was performed, as described in "Materials and Methods," on untreated (0, –) and E2-treated (10 nM) HeLa cells transfected with human ERα or human ERβ expression vectors (**parts a** and **a'**) or HepG2 or DLD1 cells (**parts b** and **b'**) at the indicated times. The amount of protein levels were normalized by comparison with actin expression. Parts (a) and (b) show the typical blot of three independent experiments; parts (a') and (b') show the data obtained by densitometric analysis, mean values ± SD. $P < 0.001$, calculated with Student's *t*-test, compared with respective un-stimulated (0, –) values (*) or with E2-stimulated values (°). For details see the text. Western blot analysis of p38/MAPK phosphorylation was performed, as described in "Materials and Methods," in un-stimulated (PBS) or 15 min E2- (10 nM) or 17α-estradiol- (17α-E2; 10 nM) or 17β-estradiol-BSA-(E2-BSA; 10 nM) treated HeLa cells transfected with human ERα or human ERβ expression vectors. In some experiments cells were pretreated with ICI 182,780 (ICI) (1 μM) before E2 stimulation. The amount of protein levels were normalized by comparison with actin expression. **Part (c)** shows the typical blot of three independent experiments; **part** (c') shows the data obtained by densitometric analysis, mean values ± SD. $P < 0.001$, calculated with Student's *t*-test, compared with respective un-stimulated control (PBS) values (*) or with E2-stimulated values (°). For details see the text.

both cell cycle progression and apoptotic cascade prevention, the E2–ERβ complex induced the rapid and persistent phosphorylation of p38/MAPK, which in turn, drove cells into the apoptotic cycle.

In the E2-stimulated ERα-containing HepG2 cells, we previously demonstrated that E2 enacted the rapid, non-genomic, and membrane starting signal transduction pathways which, in turn, worked cooperatively to achieve cell proliferation. In particular, E2-induced PKC-α was strongly related to DNA synthesis, but was not involved in cyclin D_1 transcription. On the contrary, E2-induced ERK/MAPK and PI3K/AKT pathways were strongly involved in both DNA synthesis and cyclin D_1 transcription (Marino et al., 2002, 2003). Present results clearly indicate, in well accordance with the literature (Razandi et al., 2000b; Kousteni et al., 2001), that these latter pathways have also a critical role in E2 action as a survival agent. While this work was in progress, Fernando and Wimalasena (2004) demonstrated that the prolonged activity of AKT was required to maintain the BAD phosphorylation decreasing its pro-apoptotic effect. In addition, we demonstrate that the E2-induced rapid activation of PI3K/AKT pathway is necessary to increase the level of the anti-apoptotic protein Bcl-2 and to avoid the cleavage of caspase-3 and the induction of apoptotic cascade. Beside AKT-mediated signaling, E2 can also signal through ERK/MAPK pathway. This pathway precedes and modulates AKT phosphorylation (Marino et al., 2003). In fact, the pre-treatment of HepG2 cells with U 0126 (ERK/MAPK inhibitor) rapidly increased the levels of the tumor-suppressor, PTEN, impairing the E2-induced AKT phosphorylation (Marino et al., 2003).

Work of the last years has established that expression and function of component of death machinery are under control of signaling pathways (see Rapp et al., 2004 and literature therein). ERK/MAPK as well as PI3K/AKT cascades cooperate in cellular protection. ERK/MAPK

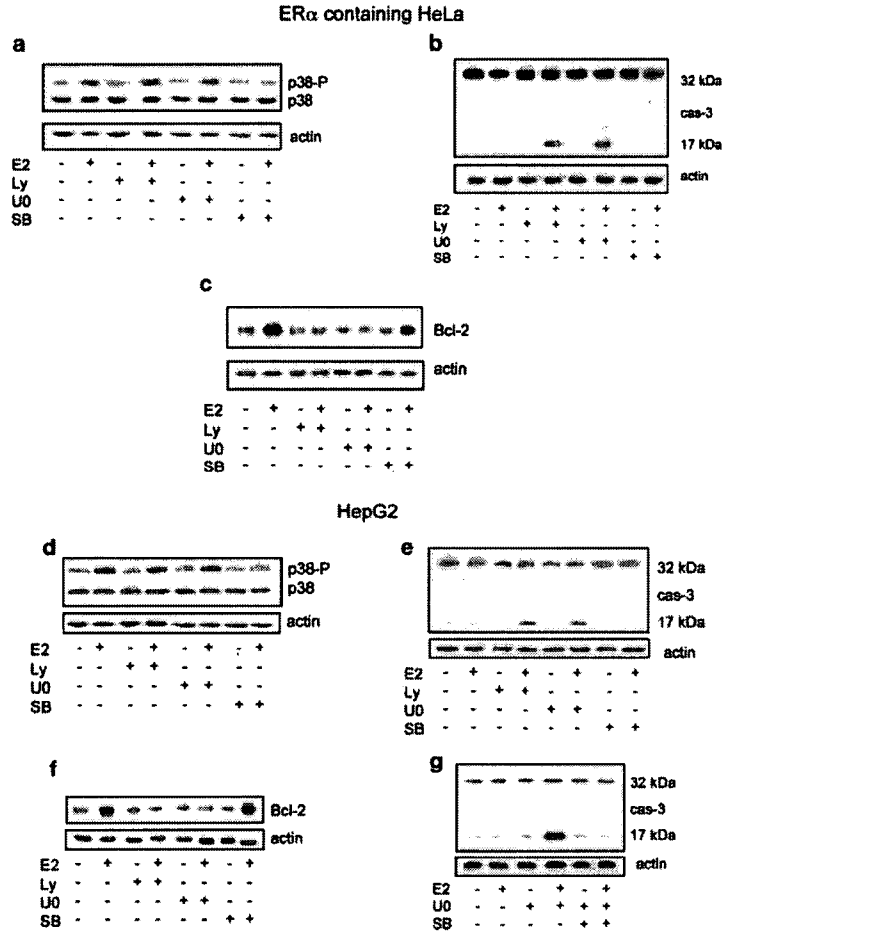

Fig. 5. Cross-talk among E2-induced ERK/MAPK, PI3K/AKT and p38/MAPK activation. Western blot analysis of p38/MAPK (**parts a** and **d**), caspase-3 (**parts b**, **e**, and **g**), and Bcl-2 (**parts c** and **f**) were performed, as described in "Materials and Methods," on un-stimulated (−) or E2-treated (10 nM) (15 min for p38 phosphorylation, 24 h for caspase-3 and Bcl-2 detection) HeLa cells transfected with human ERα expression vector or HepG2 cells. When indicated 10 μM U 0126, Ly 294002 (15 min) or 5 μM SB 203580 (30 min) (ERK/MAPK, PI3K/AKT, and p38/MAPK pathway inhibitors, respectively) were added before E2 administration. The amount of protein levels were normalized by comparison with actin expression. Typical blot of three independent experiments. For details see the text.

control cell survival by targeting Bcl-2 to the mitochondria membranes (Tamura et al., 2004) and together with PI3K/AKT may up-regulate the expression of Bcl-2 (Rapp et al., 2004). Furthermore a direct role of PI3K/AKT in caspase-3 inhibition has been recently reported after polyamine depletion (Zhang et al., 2004). Bcl-2 overexpression, in turn, decreases intracellular Ca^{++} level which can activate p38/MAPK and caspase cascades (Song et al., 2004). Our results, for the first time, show that steroid hormones may regulate this pathway. In fact, the ERK/MAPK and the PI3K/AKT pathways, rapidly activated by the E2–ERα complex, cooperatively enhance the expression of the anti-apoptotic protein (Bcl-2), block the parallel activation of the p38/MAPK, reduce the pro-apoptotic caspase-3 activation, and promote the G1/S transition via the enhancement of cyclin D_1 expression (Marino et al., 2002, 2003; present data).

One of the main findings in this study is the different signal generated by the E2–ERβ complex. There is 96% amino acid identity between the DNA-binding region (C domain) of ERα and ERβ, but in the ligand-binding region (E domain) the homology is only 53% (Kuiper et al., 1998; Matthews and Gustafsson, 2003). As the E domain of ERα is sufficient to elicit non-genomic actions (Marino et al., 2002; Razandi et al., 2002; Acconcia et al.,

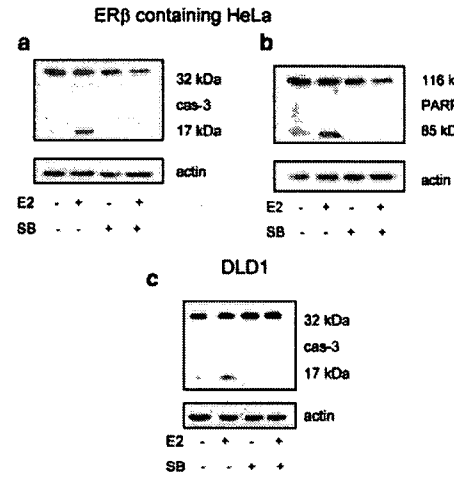

Fig. 6. Involvement of p38/MAPK in pro-apoptotic cascade activation. Western blot analysis of caspase-3 (**parts a** and **c**) and PARP (**part b**) activation were performed, as described in "Materials and Methods," on un-stimulated or 24 h 17β-estradiol-treated (E2; 10 nM) HeLa cells transfected with human ERβ expression vector or in DLD1 cells. When indicated 5 μM SB 203580 (p38/MAPK cascade inhibitor) was added 30 min before E2 administration. The amount of protein levels were normalized by comparison with actin expression. Typical blot of three independent experiments. For details see the text.

2004), it is most likely that different sets of signal transduction proteins may be activated by ERα and ERβ upon E2 binding. Besides these differences the two receptors display a different tissue localization and a different role in proliferation. For example, E2–ERα is a proliferative factor in the uterus, and the uterus of ERβ null mice is hypersensitive to the proliferative action of E2; the co-expression of both ER isoforms is rare during the proliferative phase of mammary gland cells typical of pregnancy, whereas more than 90% of ERβ-expressing mammary gland cells do not proliferate (Weihua et al., 2003); ERβ is abundantly expressed in normal colonic mucosa, but declines in colon adenocarcinoma paralleling the tumor's dedifferentiation (Konstantinopoulos et al., 2003); a progressive decline of ERβ expression has been found in multistage mammary carcinogenesis (Roger et al., 2001) and prostate cancer (Horvath et al., 2001). Very recently it has been reported that the induction of ERβ expression reduces the growth of exponentially proliferating breast cancer cells with a parallel decrease in components of the cell cycle associated with proliferation, namely cyclin D_1, cyclin E, Cdc25A, $p45^{Kip2}$ and an increase in the Cdk inhibitor $p27^{Kip1}$ (Matthews and Gustafsson, 2003; Paruthiyil et al., 2004; Strom et al., 2004). Our data amplify these evidences by adding the ability of ERβ isoform to rapidly induce the persistent membrane starting activation of p38/MAPK without any interference on the survival proliferative pathways, thus impairing the cell cycle components activation.

However, we were surprised to find that the E2–ERα complex increased p38/MAPK phosphorylation. Recently, Lee and Bai (2002) reported that in ERα-expressing endometrial cells, E2 activates the p38/MAPK pathway, which in turn mediates the ERα phosphorylation on threonine-311, promoting the receptor nuclear localization and interaction with specific receptor coactivators. In line with this result the E2-induced p38/MAPK phosphorylation plays a multifunctional role in cellular E2-induced effects. As discussed above, the contemporary increase of Bcl-2 levels, mediated by ERK/MAPK and PI3K/AKT pathways, may decrease the Ca^{++} levels impairing the prolonged p38/MAPK activation (Song et al., 2004).

Ample evidence indicates that the p38/MAPK pathway serves an important role in stress and immune response (Han et al., 1994). Furthermore, p38/MAPK pathway has been associated with a significant slowing in cell proliferation (Han et al., 1994; Badger et al., 1996) and with the regulation of the apoptosis (Kang et al., 2003). In particular p38/MAPK can sensitize cells to apoptosis through the positive regulation of Fas/CD-95 and Bax expression which, in turn, activate caspase cascades (Porras et al., 2004). The E2 capacity in activating p38/MAPK has been reported in a few articles and linked to the preservation of form of ERα- and ERβ-containing vascular endothelial cells (Razandi et al., 2000a), or their migration and proliferation (Geraldes et al., 2003), or even their apoptosis (Mori-Abe et al., 2003). Zhang and Shapiro (2000) reported the ability of E2 to induce p38/MAPK phosphorylation and cell apoptosis in a clone of ERα stably transfected HeLa cells (HeLa-ER5), unresponsive to the E2 proliferative stimuli. The reason for these disparities is not clear but could be related to the divergences in the experimental models, colture condition, E2 treatment period, proliferative capacity, or cell line variability. The E2 stimulation of two cell lines containing endogenous (DLD1) or transfected (HeLa) ERβ demonstrates the ability of human ERβ to drive cancer cells to apoptosis via p38/MAPK-cascade.

In conclusion, besides its role as negative modulator of ERα activities, our findings indicate that ERβ directs the anti-proliferative effects of E2 sustaining the tumor suppressor functions of ERβ. Therefore, the expression of ERs could account for the E2-dependent modulation of cell proliferation. In particular, E2 promotes cell survival through ERα-non-genomic signaling and cell death through ERβ-non-genomic signaling. Thus, the E2 opposite effects in cells co-expressing ERα and ERβ could depend on the balance between the signals originated by each isoform. However, the appearance of new and different signals in the presence of either receptors can not be excluded and it is currently under active investigation in our laboratory.

ACKNOWLEDGMENTS

The generous gift of DLD1 cells from Dr. Aldo Cavallini (Biochemistry Laboratory, I.R.C.C.S.S. de Bellis, Scientific Institute for Digestive Diseases, Via della Resistenza, I-70013 Castellana Grotte, Bari, Italy) is acknowledged. The editorial assistance of Mr. Peter De Muro is also acknowledged. This work was supported by grants from FIRB 2001 and 2004 University "Roma Tre" to Maria Marino.

LITERATURE CITED

Acconcia F, Ascenzi P, Fabozzi G, Visca P, Marino M. 2004. S-palmitoylation modulates human estrogen receptor-alpha functions. Biochem Biophys Res Commun 6:878–883.

Ambrosino C, Nebreda AR. 2001. Cell cycle regulation by p38 MAP kinases. Biol Cell 93:47–51.

Badger AM, Bradbeer JN, Votta B, Lee JC, Adams JL, Griswold DE. 1996. Pharmacological profile of SB 203580, a selective inhibitor of cytokine suppressive binding protein/p38 kinase, in animal models of arthritis, bone resorption, endotoxin shock and immune function. J Pharmacol Exp Ther 279:1453–1461.